Optimal Flow for Multi-Carrier Energy System at Community Level

Huo, Da

Award date:
2018

Awarding institution:
University of Bath

Optimal Flow for Multi-Carrier Energy System at Community Level

By
Da Huo

Thesis submitted for the degree of

Doctor of Philosophy

in

Department of Electronic and Electrical Engineering

University of Bath

September 2018

Signature …… Date ……

Contents

Contents i

Abstract vi

Acknowledgements viii

List of Figures ix

List of Tables xi

List of Abbreviations xii

Chapter 1 Introduction 1

1.1 Overview 2

1.1.1 Global Climate Change and Renewable Generations 2

1.1.2 Transition of Electrical Power Systems 4

1.1.3 Integration of multiple energy carriers 5

1.2 Research Motivation 8

1.3 Problem Statement 9

1.3.1 Complexity of the optimisation problem 9

1.3.2 Improper Modelling of Uncertainty 10

1.3.3 Neglect of Correlations between Renewable Generations 10

1.4 Objectives and Contributions 10

1.5 Thesis Layout 12

Chapter 2 Review of Energy Hub Optimisation 14

2.1 Energy Hub Modelling 15

2.1.1 Energy Hub Elements 16

2.1.2 Energy Hub Modelling 18

2.1.3 Transmission Network Modelling for Residential Houses 19

2.1.4 Electricity Network Modelling 20

2.1.5 Gas Network Modelling 20
2.2 Optimisation for Steady-State Energy Hub System 21
2.2.1 Energy Hub Optimisation Problem Formulation 21
2.2.2 General Procedures of Energy Hub Optimisation 22
2.2.3 Optimisation methods 23
2.2.4 Optimisation Techniques in previous literature 23
2.2.5 Integrated energy hub optimisation with other smart grid applications 26
2.3 Optimisation for Energy Hub System with Uncertainty 28
2.3.1 Monte Carlo Simulation 30
2.3.2 Scenario-reduction methods 31
2.3.3 Chance-constrained programming 32
2.4 Chapter summary 33
Chapter 3 Optimal Operation of Interconnected Energy Hubs by Using Decomposed Hybrid Particle Swarm and Interior-Point Approach 34
Chapter Overview 35
Statement of Authorship 36
3.1 Abstract 37
3.2 Introduction 37
3.3 Energy Hub Optimization 40
3.3.1. Energy Hub Modelling 40
3.3.3. Energy Storage Modelling 43
3.3.4. Optimization Problem Description 44
3.4 Decomposed PSO 47
3.4.1. PSO 47
3.4.2. Decomposition Technique 48
3.5 Demonstration 50
3.5.1. Two-hub system 51

3.5.2. Three-hub system 55
3.6 Conclusion 61
3.7 Appendix 61
3.7.1 Calculation of Battery Lifetime Cost 61
3.8 Chapter Summary 62
Chapter 4 Chance-Constrained Optimization for Multi Energy Hub Systems in a Smart City 64
Chapter Overview 65
Statement of Authorship 66
4.1 Abstract 67
4.2 Introduction 67
4.3 Energy Hub System Modelling 70
4.3.1. Energy Hub 70
4.3.2. Electricity Networks 72
4.3.3. Gas Networks 73
4.4 Problem Formulation and Methodology 73
4.4.1. CCP Energy Hub Optimization Problem Formulation 74
4.4.2. Transforming Chance Constraints to Deterministic Constraints 76
4.4.3. Overall Methodology 78
4.5 EVPI and VSS Model 78
4.6 Case Study 79
4.6.1. Data Setup 79
4.6.2. Derivation of PDF and CDF Curves 81
4.6.3. Case 1-Gas Flows with Chance Constraints 82
4.6.4. Case 2-Power Flows with Chance Constraints 84
4.6.5. Comparison between the Two Cases 87
4.7 Conclusion 89

4.8 Chapter Summary....90

Chapter 5 Chance-Constrained Multi Energy System Optimisation with Correlated Wind Generation....91

Chapter Overview....92

Statement of Authorship....93

5.1 Abstract....94

5.2 Introduction....94

5.3 Energy Hub System Modelling....96

5.3.1. Energy Hub....96

5.3.2. Electricity Network Modelling....98

5.3.3. Gas Network Modelling....99

5.4 Demand Response and Renewable Correlation....100

5.4.1. Demand Response with Price Elasticity....100

5.4.2. Correlated Wind Generation....101

5.5 Problem Formulation and Methodology....102

5.5.1. CCP Optimisation Formulation....102

5.5.2. Cornish-Fisher Expansion....104

5.5.3. Overall Flowchart of the Methodology....105

5.6 Case Study....106

5.6.1. Data Setup....106

5.6.2. Case 1-Power Flow Restricted by Chance Constraints....108

5.6.3. Case 2-Gas Flow Restricted by Chance Constraints....112

5.7 Conclusion....113

5.8 Chapter Summary....114

Chapter 6 Optimisation for Interconnected Energy Hub System with Combined Ground Source Heat Pump and Borehole Thermal Storage....115

Chapter Overview....116

Statement of Authorship 117
6.1 Abstract 118
6.2 Introduction 118
6.3 Modelling 121
6.3.1. Micro-CHP 122
6.3.2. Ground Source Heat Pump 122
6.3.3. Borehole 123
6.3.4. Energy Hub Model 126
6.4 Problem formulation and methodology 127
6.4.1. Optimisation problem formulation 127
6.4.2. Decomposed PSO 129
6.5 Case studies and results 131
6.5.1. System setup 131
6.5.2. Convergence analysis 132
6.5.3. Results and analysis 133
6.6 Conclusions and future work 135
6.7 Chapter Summary 136
Chapter 7 Conclusion 137
Chapter 8 Future Work 142
Publications 146
Reference 148

Abstract

Nowadays, the power system is transferring towards a smarter, cleaner, and more efficient system, which introduces challenges including the uncertainty in renewable generation, complication in customer behaviour, and applications in using the emerging technologies. In order to meet the challenges of the transition of the power system, the concept of energy hub is proposed to efficiently meet the increasing energy demand with less carbon emission by coordinating different energy infrastructures including electricity, gas, and heat. As a powerful conceptualisation, the energy hub system can increase system flexibility, reliability, and profits by maximally exploiting the value in each energy carrier.

From the perspective of saving energy and reducing carbon emissions, the operations of domestic and community-level buildings are modelled as energy hubs in this thesis, because they consume 41% of total energy, indicating the huge potential of enhancing energy utilisation efficiency. However, the optimal operations of energy hub can be affected by the integration of smart grid technologies, uncertainty in renewable generation and power system, and robustness of the employed algorithm. Yet, traditional methods fail to find the global minimum in solving the complicated energy hub optimisation problem and are unable to completely model the randomness of uncertain parameters, such as the renewable generations and customer behaviour. Therefore, this thesis contributes to these in two main ways: i) innovatively optimise the energy hub that is capable to reach a near-global solution, effectively incorporate the smart grid technologies and energy management with the energy hub optimisation; ii) explicitly model the impact of uncertainty on energy hub optimal operations.

Regarding the optimisation for interconnected energy hubs, which is generally formulated as a non-convex multi-period problem, this thesis proposes a decomposed approach of applying the hybridised Particle Swarm Optimisation with the interior-point method. The new approach overcomes the disadvantages of numerical methods and artificial intelligence algorithms that suffer from convergence only to a local minimum or prohibitive computation times respectively, thus it is capable of reaching a near-global solution, and fast enough for operating the energy hub system based on an online, receding time horizon implementation. The decomposed approach has been further applied to optimise the interconnected energy hub system considering the combined ground source heat pump and borehole thermal storage, which demonstrates high efficiency in supporting a community of residential houses.

Considering the uncertainty in the energy hub system, this thesis investigates the stochastic energy hub optimisation with two pieces of work. The first work innovatively proposes to employ the chance-constrained programming to optimise the energy hub, the power and gas flows between hubs are restricted by the chance constraints due to the fact that the temporary overloading is tolerable. The Cornish Fisher Expansion method is applied to transfer the chance constraints into deterministic constraints, and hence the deterministic optimisation approach is utilised to resolve the problem. Compared with the traditional methods, the proposed approach better captures the stochastic nature of uncertainties and avoids expensive computational costs of scenario generating methods. Additionally, correlations may exist among renewable generation. Hence, to model the effect of uncertainty with better accuracy, the second piece of work extends the research by considering the correlation between geographically close wind farms, and reflects customer response to varying energy prices and energy hub states. Chance-constrained programming is employed to resolve the problem.

All works are investigated on the interconnected energy hub system. Test system demonstrations prove the advantages of the proposed approaches in optimising energy hub system with better performance, and better captures the randomness of uncertainty, thus benefits both the system operators and customers with enhanced network security, less energy infrastructure cost and carbon emissions.

Acknowledgements

First and foremost, I would like to express my respectful gratitude to my supervisors, Dr. Chenghong Gu and Dr. Simon Le Blond, for the patience and consistent support they have shown me.

I would like to take this opportunity to thank my colleagues, Dr. Francis Robinson, Prof. Furong Li, Dr. Kang Ma, Miss Wei Wei, Dr. Yue Xiang, Dr. Dongmin Yu, Dr. Huiming Zhang for their willingness to share knowledge with me and provide me useful resources.

I would also like to thank all my colleagues and friends in the University of Bath, including Miss Yuwei Xu, Mr. Minghao Xu, Dr. Zhongjian Liu, Dr. Cheng Wang, Mr. Xiaohe Yan, Mr. Yuankai Bian, Mr. Hantao Wang, Dr. Ran Li, Mr. Xinhe Yang, Miss Wangwei Kong, Dr. Heng Shi, Dr. Martin Fullekrug, Mr. Zhuangzhuang Dai. I am sincerely grateful for their support over years.

Last but not least, I would like to express my ultimate gratitude to my beloved parents, who give me endless support and encouragement.

List of Figures

Fig. 1-1. Target of reducing carbon emission of the UK 2
Fig. 1-2.Electricity mix of the UK in 2014 and 2030 3
Fig. 1-3.Typical energy hub 6
Fig. 1-4.Energy management system with the utilisation of energy hub 7
Fig. 2-1.General energy hub model 18
Fig. 2-2.PDF curve of the wind speed at Cardiff observation station. 29
Fig. 3-1. An example of energy hub model 41
Fig. 3-2. Two-hub system with energy sharing available between hubs. 41
Fig. 3-3.Boiler efficiency against cyclic input energy normalized by steady-state input energy 42
Fig. 3-4.The working flow of the decomposition technique 49
Fig. 3-5.The time-of-use tariffs against 24 hours. 51
Fig. 3-6.The battery operations against 24 hours. 54
Fig. 3-7.Three-hub system with energy sharing available between hubs. 55
Fig. 3-8.The variant tariffs of electricity against 24 hours. 56
Fig. 3-9.Convergence behaviours of conventional PSO and decomposition technique 56
Fig. 3-10.The optimized battery operations by applying conventional PSO and decomposition technique. 57
Fig. 3-11.Battery state of charge over 24 time steps derived from the optimization with the battery lifetime cost considered 58
Fig. 3-12.Battery state of charge over 24 time steps derived from the optimization without considering the battery lifetime cost 59
Fig. 3-14. Computation time against different amount of particles 60
Fig. 3-13. Optimization results against different amount of particles 60
Fig. 4-1.Single energy hub 72
Fig. 4-2.The three-hub interconnected system. 75
Fig. 4-3. PDF and CDF curves of renewable energies inputs at step 9 80
Fig. 4-4.Flowchart of obtaining PDF and CDF curves from CCP 81
Fig. 4-5.The convergence of CCP implementing on the 3-hub system 82
Fig. 4-6.Case 1-CDF curve of the optimized total cost 83
Fig. 4-7.Case 1-CDF curve of the total gas injection at time step 9 84
Fig. 4-8.Case 2-CDF curve of the total gas injection at time step 9 84

Fig. 4-9.Case 2-CDF curve of the optimized total cost 85
Fig. 4-10.Optimal operations of hub 1 over 24 hours 86
Fig. 4-11.Dispatch factors under different chance constraints probability 86
Fig. 4-12.PDF diagrams of the optimized total cost with the probability of chance constraints higher than 80% derived from the two cases 88
Fig. 4-13.CDF curves of Maximum energy level for two cases 89
Fig. 5-1.A single energy hub 98
Fig. 5-2.Power outputs from wind turbines at farm 1 and 2 101
Fig. 5-3.The two-hub interconnected system. 102
Fig. 5-4.Flowchart of CCP-based energy hub optimisation 106
Fig. 5-5.PDF of wind speed and power generation derived at wind farm 1 at time step 9 107
Fig. 5-6.Electricity price over 24 hours. 107
Fig. 5-7.CDF curves of optimised total cost. 109
Fig. 5-8.CDF curves of the active power input to hub 2 at time step 9. 109
Fig. 5-9.Electricity demand of hub 1 over 24 hours 110
Fig. 5-10.Electrical demand of hub 2 over 24 hours. 110
Fig. 5-11.Optimal operations of hub 2 over 24 hours 111
Fig. 5-12.CDF curves of optimised total cost. 112
Fig. 5-13.CDF curves of the active power input to hub 2 at time step 9. 113
Fig. 6-1.Eleven interconnected energy hubs system 121
Fig. 6-2.Single FE borehole model cross section view 124
Fig. 6-3.Variation of borehole wall temperature with constant heat flux output 125
Fig. 6-4.Comparison of FE model and transfer function 126
Fig. 6-5.Example of single energy hub 126
Fig. 6-6.Working flow of the decomposed technique of applying PSO 130
Fig. 6-7. Energy consumptions of hub 1 over 24 hours 131
Fig. 6-8.Variant electricity prices against time 131
Fig. 6-9.Convergence behavior for the decomposed PSO applying to Case 3 133
Fig. 6-10.CoP for GSHP over 24 hours for each case 133
Fig. 6-11.Total electricity injection to 11-hub system over 24 hours for each case 135

List of Tables

Table 2-1.REVIEW OF ENERGY HUB OPTIMISATION PROBLEMS 22
Table 2-2.DIFFERENT TYPES OF DR SCHEMES 26
Table 3-1.THE OPTIMAL OPERATIONS FOR BATTERY.....52
Table 3-2.OPTIMIZATION RESULTS FOR 2-HUB SYSTEM.....53
Table 4-1.ENERGY HUB SYSTEM PARAMETERS AND CONSTRAINTS 80
Table 5-1.ENERGY HUB SYSTEM PARAMETERS AND CONSTRAINTS 108
Table 6-1.GSHP COP CALCULATION.....123
Table 6-2.BOREHOLE PARAMETERS.....124
Table 6-3. PARAMETERS FOR ELEVEN HUBS.....132
Table 6-4.ENERGY COST FOR EACH CASE.....133

List of Abbreviations

Chance-Constrained Programming	CCP
Cumulative Distribution Function	CDF
Cornish-Fisher Expansion	CF
Combined Heat and Power plant	CHP
Coefficient of Performance	CoP
Distributed Energy Resources	DER
Distributed Generation	DG
Distributed Multi-Energy Generation	DMG
Demand Response	DR
Demand Side Management	DSM
Energy Storage Systems	ESS
Electric Vehicle	EV
Expected Value of Perfect Information	EVPI
Finite Element	FE
Gas Furnace	GF
Ground Source Heat Pump	GSHP
Information Communications Technology	ICT

Monte Carlo Simulation	MCS
Mixed Integer Linear Programming	MILP
Probability Density Function	PDF
Particle Swarm Optimisation	PSO
Peer-to-Peer	P2P
Renewable Generations	RG
Renewable Heat Incentive	RHI
Real-Time-Pricing	RTP
State of Charge	SOC
Two-Point Estimate Method	2PEM
Time-of-use	TOU
Value of the Stochastic Solution	VSS
Vehicle-to-Grid	V2G
Wait-and-See solution	WS
Wind Turbine	WT

Chapter 1

Introduction

This chapter introduces the background, motivation, objectives, and contributions of the research. The structure of the thesis is also outlined.

1.1 Overview

1.1.1 Global Climate Change and Renewable Generations

The changing of global climate has become a disturbing issue to mankind over the last century. Fossil energies including coal, natural gas, and oil are largely utilised to generate 84% of global total energy, the gases generated along with the combustion of fossil energies have significantly polluted the environment [1]. According to the report of the Intergovernmental Panel on Climate Change in 2007 [2], the mean temperature of the global surface has increased by $0.74℃ \pm 0.18℃$ over the past 50 years. Climate scientists suggest that the greenhouse gas emissions, most of which is carbon dioxide (CO_2), should achieve an immediate reduction of approximately 60% to 80% in total by 2100 to restrict the global temperature rising of 2℃ [3]. In 2009, most countries attended the Copenhagen conference, and committed to mitigating the climate change by achieving the low-carbon society [4, 5].

The UK government plans to reduce the carbon emissions by approximately 80% before 2050 compared with the 1990 baseline [6]. In order to achieve this goal, the UK government issued the white paper 'The UK Low Carbon Transition Plan-National Strategy for Climate and Energy' [7] in 2009 to specifically illustrate the government policy of reducing carbon emission from individuals, communities to businesses. The carbon emission is aimed to be reduced according to the trajectories from 2010 to 2050 as indicated in Fig. 1-1. Therefore, the energy system in 2050 will be significantly changed compared with the current energy system. Instead of substantially applying the

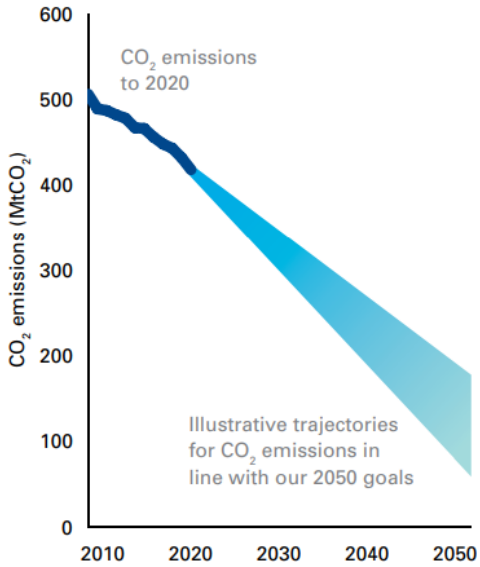

Fig. 1-1. Target of reducing carbon emission of the UK

fossil energy, the renewable energy such as solar, wind, hydro, geothermal and bio energies are foreseen to be the main source of supplying the loads; some environmental friendly power stations such as combined heat and power plant and nuclear power station will be largely used in the future; and vehicles will be supplied by clean energies of electricity/hydrogen/biogas.

Fig. 1-2 presents the mix of different energies to supply the electricity demand in 2014, and the predicted mix in 2030 [8]. As seen, fossil energy of coal and oil was the major source to supply the electricity demand in 2014, which accounts for 30% of the total. However, it is predicted to be excluded in the 2030 supply mix. The ratio of using renewable energy including solar and wind relative to the total is significantly enhanced from 11% to 50%.

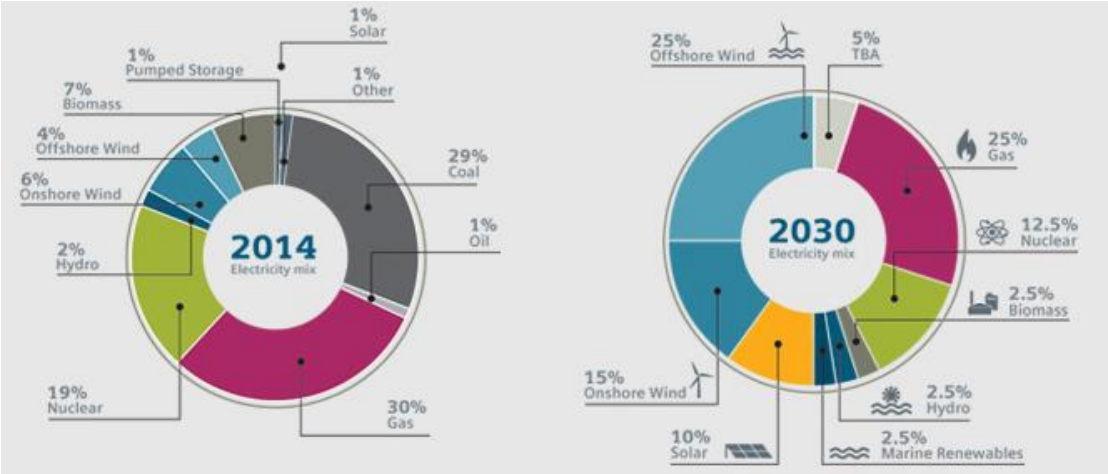

Fig. 1-2.Electricity mix of the UK in 2014 and 2030

The key targets to be delivered involving the application of renewable energies are summarised as follows: i) 40% electricity is generated from low carbon sources by 2020, where the power generated from renewables take up to 30% of total; ii) reducing the carbon emission from new cars by 40% against 2007 baseline, where 10% of energies applied in transportation is from renewable sources.

On the other hand, there are some standalone areas in practice, where the main power grid is difficult to be extended to such areas because building the transmission corridors is expensive and the system could be unreliable. However, renewable energies such as wind and solar are generally abundant in these areas. Hence the environmental friendly island micro-grid is established based on the renewable generations [5, 9] to support loads of the standalone area, meanwhile, the energy utilisation efficiency and quality are improved.

In conclusion, the power system benefits from the renewable generations by decreasing the carbon emissions and supporting standalone areas.

1.1.2 Transition of Electrical Power Systems

The power system nowadays is transforming towards a smarter, cleaner, and more efficient energy system, the changing environment and challenges are summarised in terms of the following aspects [10]:

- The renewable generations (RG) are increasingly invested and utilised to reduce the carbon emission and mitigate the pollution to the environment. However, the stochastic nature could potentially threaten the safety of the power system and thus require stable generation support.
- Energy Storage Systems (ESS) provides a feasible solution to integrate RG, it can also shave peak loads and provide reserves. Hence it is foreseen to be largely applied in the future power system.
- The application of Electric Vehicle (EV) is encouraged by the government due to its environmentally friendly characteristics. The Vehicle-to-Grid (V2G) scheme can bring further flexibility and reserves to the power system. However, the load of residential and community-level buildings will be significantly increased due to the increasing application of EV and other novel technologies such as heat pump, which complicates the load uncertainty.
- Consumers' environmental awareness is increased, and they are more active to participate in different energy management schemes to reduce the energy cost or use energies more efficiently, such as the demand response scheme. Additionally, consumers are investing in Distributed Energy Resources (DER) such as RG, concepts such as Peer-to-Peer (P2P) energy trading can be established among them. Together with other emerging technologies such as ESS and EV, the participation of consumers brings further flexibility to demand side energy management, however, complicates the load pattern.
- The transition of electrical energy markets is also ongoing due to the highly increasing energy demands, and the fast growth of distributed generations (DG) [1]. Specifically, DG consumes various energies such as fossil, wind, and gas from DER to generate power [11]. The electricity generated by DG has accounted for less than

10% to total electricity consumption in the UK in 2006 [12]. Comparatively, DG generated 50% of the total electricity in Denmark in 2006 [13].

In order to extend the application of DG to wider areas such as district heating and commercial buildings, the concept of distributed multi-energy generation (DMG) is proposed in [5, 14, 15]. DMG system contains a series of technologies to manage the cooperation between various energy infrastructures, which produces higher efficiency compared with conventional DG. However, the increasing of DG and DMG challenges the balancing and frequency regulation for transmission grid and brings new problems such as reverse power flows and congestion issues for distribution grid.

- The emerging technologies such as Information and Communications Technology (ICT) and smart meter improve the functions of communication and metering in the power system. Based on these technologies, the paradigms of smart grids and smart cities can be formulated to optimise and control the micro-girds, and thus facilitate the evolution of the power system.

Consequently, the transition of modern electrical power system maximise the system flexibility, profits, and mitigate the environment pollution by introducing advanced technology and operating mechanism based on smart grid technologies. However, the system uncertainty is increased, and the coupling between the emerging technologies brings further challenges. Therefore, robust and efficient energy management approaches should be developed to address these issues.

1.1.3 Integration of multiple energy carriers

As mentioned in the previous section, micro-grids have received increasing attention towards the decentralisation of energy systems led by restructuring the monopolistic frameworks of liberalized markets [16] and the deployment of renewable energy. Decentralized production has brought new technical challenges, such as balancing supply and demand within the micro-grid without compromising on safety or security of supply. Whether controlling the operation of micro-grid or managing access of renewable energy to the network, an energy management system is necessary to maintain system stability and reliability. Different energy infrastructures such as electricity, gas, and district heat work separately in the traditional energy system [17]. Nowadays, the co- and tri-generation enables the high efficiency of utilising various

energy carriers and increases system flexibility by means of exploiting every available energy carrier. Analysing the system from an integrated view has been proposed by Geidl as the Energy Hub concept [18], which couples multiple energy carriers and achieves the functions of input, output, converting, and storing [16].

With the combination of different energy carriers, the energy hub system is more flexible and reliable since the redundant pathways through the hub increase energy security and offer the possibility of operational optimisation when there is more than one way of supplying the loads [19]. The innovation of combining different energy infrastructures as an integrated system reveals great opportunities and improvements. A typical energy hub model is shown in Fig. 1-3 as an example. This energy hub consumes energy carriers including electricity, natural gas, and district heat, which are converted and/or stored within the hub. Specifically, the combined heat and power system (CHP) consumes natural gas to simultaneously generate power and heat [20]; the gas furnace (GF) combusts gas to provide heat; the battery and water tank are regarded as energy storage, the energy costs can thus be reduced by storing power and heat at time steps when the energies prices are low, and discharge at other time steps when the prices are high. Additionally, the energy storage system (ESS) can buffer the stochastic renewable generations by storing the excessive power generations, and discharging when the renewable generations are inferior to the expected value.

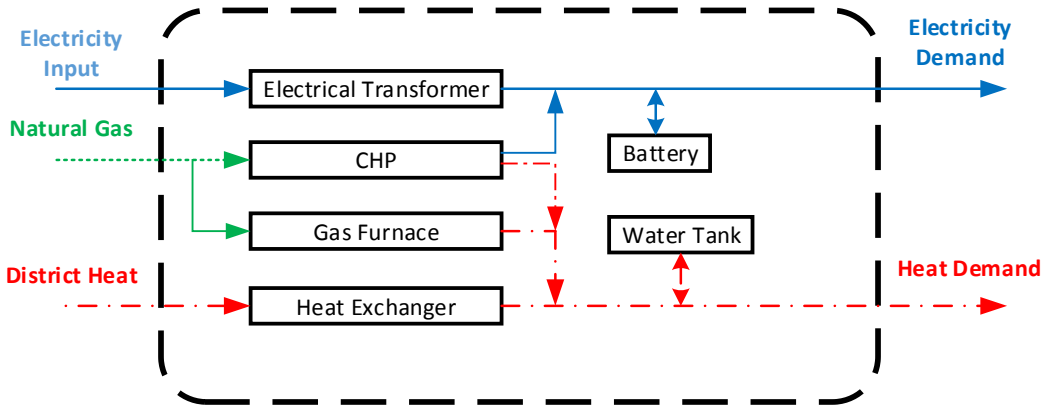

Fig. 1-3.Typical energy hub

The system reliability is increased since the consumers' demand does not depend on a single energy infrastructure. Additionally, the system becomes more flexible which leads to further advantages. For instance, during the peak load period, the electricity load could be satisfied by accordingly applying the CHP instead of buying expensive electricity from the grid, the battery storage can also discharge to economically meet the electricity load. The optimal energy management achieves the possibility of

lowering the energy cost or carbon emissions. The energy hubs can be applied to model multiple scales of the energy system, Fig. 1-4 [21] presents an energy management and control system with energy hubs.

In practice, residential houses, communities, industrial factories, and agriculture buildings could be regarded as the multi-carrier energy hubs with energy demand, conversion, and storage functionalities [22]. As shown in Fig. 1-4, a central controller is normally employed to control the operations of each hub based on the collected information such as forecasted renewable generations and loads, the optimal objectives can thus be achieved.

From the prospective of economically operating the energy system, the energy costs could be further reduced by interconnecting heterogeneous energy carriers at a community level, since the local renewable generations and pooled energy storage systems can be better leveraged without suffering the energy loss through large distance transmission. Additionally, the energy redundancy in each energy hub can be maximally utilised with the achievement of energy interconnection between hubs, which systematically achieves the system optimisation [23].

By considering the energy transformation within the energy hub system and safety operations, optimising the interconnected energy hub system could be formulated as

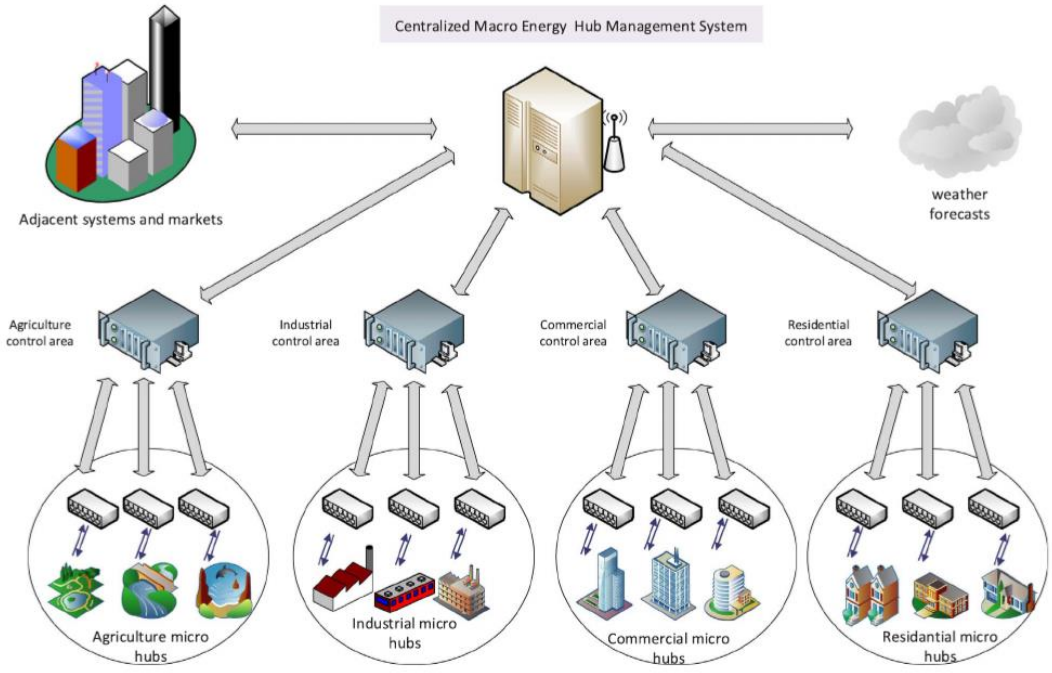

Fig. 1-4.Energy management system with the utilisation of energy hub

solving a non-convex multi-period problem. Moreover, the problem is transferred to a stochastic problem if uncertain variables are considered such as loads and renewable generations.

1.2 Research Motivation

Under the new circumstance of facilitating the update of the power system, coordination between multiple energy carriers, and the increasing adoption of renewable energies, the concept of energy hub is proposed to achieve the above functions. Multiple energy converters and energy storage system can be equipped within an energy hub, the energy demand of energy hub system can thus be satisfied by accordingly adjusting the utilisation of different energy carriers to achieve the corresponding optimisation objective, and hence increase the system flexibility. The system reliability is also improved because a specific energy demand can be satisfied by consuming various energies or supplied by using energy storage system. The energy hub system is well fitted to the modern power system by meeting the requirements of high reliability and flexibility, and the capability of adapting renewable generations.

The energy hub approach can be applied to any scales of energy system [24]. Domestic and community-level buildings consume 41% of total energy, and it is higher than the consumption in industries and transportation [25], which indicates the great potential of energy saving by employing an efficient energy hub approach. As illustrated in the previous section, the energy system can be further optimised by interconnecting energy hubs with the consideration of energy transmission networks. Moreover, by considering the constraints from energy transmission networks, the operation of an energy hub system is more related to operating the realistic smart city. Therefore, this thesis investigates the optimisation of an interconnected energy hub system which operates at residential and community level.

Renewable generations are generally incorporated into residential or community level buildings to lower energy cost and reduce carbon emissions. However, the renewable generations are generally stochastic and difficult to be predicted, the overestimation of renewables could cause the system operational cost to be extremely high, and the system security constraints may be violated when the impact of renewable generation is underestimated. Therefore, appropriate modelling for uncertain variables is a significant requirement when operating the energy system. Traditional methods applied

in energy hub optimisation to analyse uncertainty could suffer from an expensive computational cost or fail to fully capture the stochastic nature of uncertain variables, hence the development of an improved stochastic approach is an interesting research objective to safely operate the interconnect energy hubs under uncertainty.

1.3 Problem Statement

The optimisation of interconnected energy hub system has been investigated by many researchers, yet there are still challenges and difficulties in solving the optimisation problem. Three major issues are summarised as follows:

1.3.1 Complexity of the optimisation problem

When the renewable generations are excluded in the system or considered to be perfectly forecasted, the optimisation for energy hub system yields a deterministic problem. A typical energy hub system contains an energy storage system [26]. Regarding the variations of energy carriers prices, the energy storage system may charge during the low-tariff period, and discharge during the high-tariff period in order to low system costs. Therefore, the energy hub operations at current time step may affect the operations at other time steps and hence a multi-period optimisation is necessary. Additionally, distributed generators and converters within the energy hub system generally operate with non-constant efficiency, which can be formulated as a quadratic function in terms of the input energy [27]. As illustrated above, the deterministic optimisation problem can be formulated as a non-convex multi-period problem. A local minimum can be found by applying numerical methods, however, the global minimum is not guaranteed.

Additionally, to achieve a further reduction of energy costs or fitting the system with different technologies, the energy hub optimisation is incorporated with other system planning and operating techniques such as demand response [28] and optimal power flow [29]. Some energy storage systems such as inter-seasonal borehole systems have raised attention in recent years due to their high efficiency. Combining a borehole system with energy hub optimisation yields further energy saving, but complicates the system configuration and the optimisation problem.

1.3.2 Improper Modelling of Uncertainty

In order to optimally operate the energy hub system under the realistic circumstances, the uncertainty factors such as load and renewable generations should be appropriately modelled. The system security is threatened when uncertainties are underestimated, and it costs too much if uncertainties are overestimated [30]. The Monte Carlo method has been widely applied in energy hub optimisation to model uncertainty with an abundant number of scenarios [31-33], and the optimisation results are derived from each scenario. However, the optimisation suffers from a huge computational burden due to a large number of scenarios. Some scenario reduction methods or techniques such as 2 point estimate method are proposed to reduce the number of scenarios [34-38]. However, the stochastic nature of uncertain variables may not be completely reflected with a certain number of scenarios.

1.3.3 Neglect of Correlations between Renewable Generations

Correlations could exist between various uncertainties. For example, the wind speeds in some geographically closed areas are similar to each other, hence the stochastic power generations from the wind turbines at these areas are dependent on each other. However, the renewable generations are simplified as independent in previous researches. Thus the influence of uncertainty on the energy system fails to be well considered.

Additionally, considering the reactions of customers in response to energy hub optimisation and variant tariffs can further reduce the energy cost, because the customers can participate in the optimisation to reschedule their loads to cooperate with the energy hub optimisation. However, the integrated optimisation has not been investigated with the consideration of correlated uncertainties, and hence the optimisation results may be inaccurate.

1.4 Objectives and Contributions

In this thesis, the optimisation for interconnected energy hubs is investigated by combining them with other smart grid technologies. Further improvements have been made to better incorporate the uncertain renewable generations within the energy hub optimisation. The main objectives and contributions are summarised as follows:

- To investigate the optimal operations of interconnected energy hubs with other smart grid methods, where the problem is potentially formulated as a non-convex problem, new optimisation approached should be developed to improve the solution towards the global minimum.

  In doing so, a decomposed approach of applying Particle Swarm Optimisation hybridised with interior point method is proposed to optimise the steady-state energy hub system with the consideration of extending the battery lifetime. This approach overcomes the disadvantages of numerical methods and artificial intelligence algorithms that suffer from convergence only to a local minimum or prohibitive computation times, respectively.
- To accurately represent the stochastic nature of renewable generations and investigate the effects of the uncertainties on operating the interconnected energy hubs, appropriate stochastic programming approach should be applied to carry out the optimisation problem and analyse the results.

  In doing so, the chance-constrained programming is proposed to incorporate into the optimisation of interconnected energy hubs in a smart city, where the energy flows between adjacent hubs are innovatively restricted by chance constraints, thus permitting the temporary overloading acceptable on real energy networks. This novelty not only ensures system security but also helps reduce or defer network investment. The random nature of uncertain renewable generations could be better reflected by using chance-constrained programming compared with scenario generation methods.
- To better reflect the dependency between various renewable generations and customer interaction in optimising energy hub systems, new approaches should be developed to establish the relationships between uncertain renewable generations and monitor the effects of customer interaction within the optimisation scheme of energy hubs.

  In doing so, the correlations between geographically close wind farms are considered by establishing their relations using historical data. In addition, demand response is incorporated into the model to further increase the flexibility of energy hub systems and customers' benefits. The optimisation problem is modelled by optimally scheduling the demand and operating the energy hub system over a whole time horizon to achieve the minimum energy cost.

- To examine the applications of other efficient or low-carbon-emission equipment within the interconnected energy hubs, and explore the benefits to customers, the optimal operations of such a combined system should be investigated.

  In doing so, the high-performance combined borehole and ground source heat pump system is incorporated into a community of residential energy hubs to support the thermal loads for one day, and the combined system produces zero carbon emission at the residential level. Unlike the traditional Finite Element model to simulate borehole system for inter-seasonal operation, this work proposes an equivalent transfer function to model the performance of the borehole system, since the error is negligible for 24-hour operations.

1.5 Thesis Layout

The rest of the thesis is organised as follows:

Chapter two explicitly reviews the modelling for the interconnected energy hub system, and the optimisation approaches developed in the previous literature. The optimisation approaches are reviewed in terms of two aspects: optimisation under steady state and stochastic programming with the consideration of uncertainties. The challenges to current optimisation techniques are summarised, and the potential approaches to address these challenges are presented. Additionally, the combination of interconnected energy hubs with other smart grid operating approaches is reviewed.

Chapter three considers the battery lifetime cost in the optimisation to better utilise the battery from the long term run. It proposes a novel decomposed optimisation approach by applying Particle Swarm Optimisation to solve the complicated non-convex energy hub optimisation problem. The optimisation approach decouples the complicated optimization problem into sub-problems, namely the scheduling of storage and other elements in the energy hub system, and separately solves these by PSO and the numerical method ‘interior-point’.

Chapter four proposes the optimisation for stochastic energy hub system by using chance-constrained programming. The power and gas flows between adjacent hubs are restricted by chance constraints, which follows the fact that the temporary overloading in the energy system is allowable. Cornish-Fisher Expansion is utilised to incorporate the chance constraints into the optimization, which transforms the stochastic problem

into a deterministic problem. The interior-point method is then applied to resolve the developed model.

Chapter five follows chapter four to take consideration of the correlations between geographically closed renewable generations. It proposes to utilise the Pearson correlation to represent the relationship between wind farms' generations based on historical data. In addition, demand response is incorporated into the model to further increase the flexibility of energy hub systems and customers' benefits. The optimisation problem is modelled by optimally scheduling the demand and operating the energy hub system over a whole time horizon to achieve the minimum energy cost.

Chapter six proposes to apply the high performance of combined borehole heat storage with ground source heat pump (GSHP) to support the heat load of a community of residential users. The overall flexibility and energy cost is reduced by investigating the application of the combined system within the interconnected energy hub system. The borehole Finite Element (FE) model and an equivalent borehole transfer function are proposed and respectively applied to the optimisation to analyse the variation of GSHP performance over the entire optimisation time horizon of 24 hours.

Chapter seven concludes the main findings of the thesis and the major contributions.

Chapter eight presents some potential research topics in future work.

Chapter 2

Review of Energy Hub Optimisation

This chapter reviews the modelling of energy hub system, together with the related optimisation techniques under steady-state and with uncertainty.

2.1 Energy Hub Modelling

Energy hub is developed as an efficient and promising approach to optimally manage the multi-carrier system [1, 2]. The utilisation of energy hub benefits the optimal management of DER, smart grid, and facilitates the demand side energy management. Proposed by Geidl [3], energy hub is defined as the framework to consume, convert, store, and transmit various energies to meet the energy demands. The energy hub can be potentially applied to model the multi-carrier system and related interconnected systems, any scales of multi-energy systems can be optimally managed by using the energy hub concept [4].

By applying the energy hub approach, the redundancy in each energy carrier is fully exploited to achieve the optimisation objective, meanwhile, the system flexibility and reliability are increased. Many countries are encouraging the utilisation of energy hub at the demand side, the efforts are reviewed as follows [5]:

- **The United Kingdom**

The UK government has highly supported the research in integrating electricity and natural gas system [6]. In 2015, the project 'Energy Systems Catapult' was jointly sponsored by Department of Energy and Climate Change in the UK and Innovate UK to investigate the operations of the multi-carrier system to meet various demands of energy users in Birmingham.

- **Germany**

In 2008, Germany Federal Ministry proposed the 'E-Energy project' to design the future multi-carrier system, which enables the communication between energy systems and home appliances based on the concept of Information Communications Technology (ICT). The project is established in order to enhance the reliability and efficiency of energy users. By carrying out this project, the employment of distributed energy has been enhanced to take up to 50% in Germany by 2015.

- **The United States**

The National Science Foundation in the US proposed the concept of future renewable electric energy delivery and management (FREEDM) system in 2008 [7], enabling the future residential consumers to flexibly manage the utilisation of distributed renewable

energy and distributed energy storage devices. The energy hub optimisation is well developed and applied to schedule the use of home appliances.

- **China**

The Chinese government has considered the efficient utilisation of renewable and sustainable energy as an important national strategy. The initiative of 'Internet + smart energy' is proposed in 2015 to consider the integration of various energy infrastructures of electricity, natural gas, and thermal energy to establish the energy internet. The Chinese government has supported and issues several projects to facilitate the implementation of this initiative.

One project is implemented in a high-tech industry park in Jiaxing City to design an active distribution network (ADN) to coordinate the operations of solar PV and energy storage system to meet local energy demands. Additionally, the reliability of the ADN is improved, and thus ensures the security of the operating distribution power system.

Another representative multi-carrier management is implemented based on Shanghai Tower, which integrates electricity, gas, and thermal to meet the demands of the tower with the joint application of air source heat pump, ground source heat pump, CHP, gas furnace, and ice storage system. By optimally scheduling the internal energy consumption and shaving peak loads with the energy hub optimisation, the energy utilisation efficiency is increased by 22%.

2.1.1 Energy Hub Elements

- **Resources**

Energy hub integrates various energy carriers, typically includes electricity, natural gas, district heating, and renewable energy sources (RES) to meet customers' multiple demands such as power and thermal [8].

DERs are generally located near the energy hub system, using DERs can effectively reduce the energy loss through the energy transmission and distribution processes, and hence increase the energy utilising efficiency. Therefore, DER has become the main generation system to supply power to the energy hub by using the technologies of gas turbines, renewable generations, etc. [9]. Nowadays, the fossil energy is still the major source to generate power. However, RES such as solar, wind, and biomass will be largely applied in future DER, due to their environmental-friendly characteristics.

- **Conversion**

Energy hub can be regarded as the block between producers and consumers. It applies various energies by means of energy converters to meet the consumers' loads. On one hand, the direct connections are generally contained within the energy hub. For example, the electricity from the grid and district heating can be directly transmitted through the energy hub without conversion to meet the electricity and thermal loads. On the other hand, the energy converters are essential for energy hub to transform the input energies to other forms of energies to meet the demands.

Most of the converters convert one type of energy into another type of energy. Previous literature has investigated the energy hub system including mostly gas furnaces, heat pumps, fuel cells, transformers, heat exchangers, and renewable generations such as solar panels and wind turbines. Specifically, gas furnaces combust natural gas to generate heat; heat pumps are driven by electricity to provide cooling or heating depending on customer's needs; RES could be applied to produce several energies. For instance, solar energy is capable of producing power and heat, wind power can be transformed to power, and geothermal energy can be transferred to serve the heat demands by means of ground source heat pumps.

The combined heat and power (CHP) plants are increasingly applied and analysed in the energy hub system recently, the installed units of CHP in the US has risen from the number of 640 in 1980 to 5541 in 2014 [10]. CHP is a typical co-generation plant that simultaneously generates power and heat with the consumption of natural gas, it improves the overall efficiency of using conventional power plants to generate power and heat from 60% to 90%, meanwhile reduce the carbon emissions by 30% [11-13].

The energy hub system benefits from the cooperation with various converters to meet the energy demands, the system reliability is increased because a single energy demand can be met upon converting various energies, the profits are also maximised by accordingly adjusting the use of different energy carriers against the changing energy tariffs.

- **Energy storage system**

The energy storage system (ESS) provides the additional reserve and flexible solution, and hence it is included in the energy hub system. The mostly applied ESS in energy hubs are the power and heat storage, they store the excessive energy at one time step,

and release the energy when required. The advantages of using ESS can be summarised as [14-16]: i) The ESS can be applied to facilitate the integration of renewable generations with the energy hubs, it mitigates the fluctuation of RES by storing the excessive energy output, and discharging to supply the load when the RES is in shortage, the ESS, therefore, maintains the reliability between the supply and demand sides; ii) Similarly, the ESS can be applied to mitigate the uncertainty from consumers' loads; iii) The ESS can participate in some optimisation schemes of smart grid, such as peak shaving, and energy management of storing energy in low-tariff periods, and discharging in peak-tariff period to reduce the energy cost.

2.1.2 Energy Hub Modelling

The optimisation for energy hub system is carried out by mathematically minimising the value of the objective function, hence the expressions of energy hub models are illustrated in this section in order to formulate the optimisation problem. A general modelling of a single energy hub is depicted in Fig. 2-1, where multiple inputs and outputs are contained.

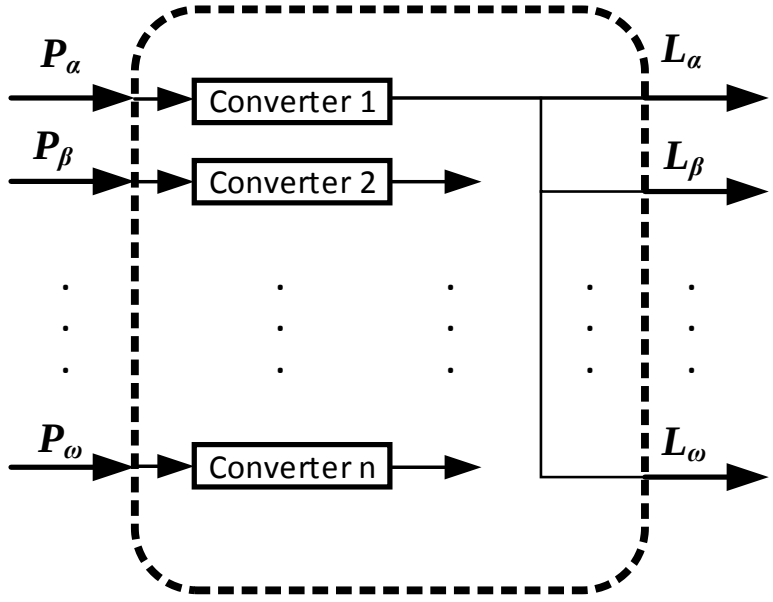

Fig. 2-1.General energy hub model

As seen, a series of converters are included in the energy hub to interactively transform the input energies (P_α, P_β... P_ω) to outputs (L_α, L_β... L_ω), and α to ω represents different energy carriers. The relations between energy hub outputs and inputs can be denoted by the form of a matrix:

$$\begin{bmatrix} L_\alpha \\ \vdots \\ L_\omega \end{bmatrix} = \begin{bmatrix} c_{\alpha\alpha} & \cdots & c_{\omega\alpha} \\ \vdots & \ddots & \vdots \\ c_{\alpha\omega} & \cdots & c_{\omega\omega} \end{bmatrix} \begin{bmatrix} P_\alpha \\ \vdots \\ P_\omega \end{bmatrix} \tag{2-1}$$

The middle matrix is defined as the coupling matrix (*C*), which indicates the power mapping from inputs to outputs.

As indicated in the previous section, the ESS is generally equipped within the energy hub system. Assuming the energy exchange between the ESS and energy hub system is denoted as M_h, the stored energy in ESS E_h at time step *t* is expressed as:

$$M_h(t) = \frac{1}{e_h}\left(E_h(t) - E_h(t-1) + E_h^{stb}\right) \tag{2-2}$$

Where E_h^{stb} represents the ESS standby loss at each time step, and e_h can be denoted as:

$$e_h = \begin{cases} e_h^+ & \text{if } M_h(t) \geq 0 \quad \text{(charging/standby)} \\ \frac{1}{e_h^-} & \text{else} \qquad\qquad\qquad\quad \text{(discharging)} \end{cases} \tag{2-3}$$

Where e_h^+ and e_h^- mean the charging efficiency and discharging efficiency. Therefore, when the ESS is charging, (2-2) and (2-3) indicate that the energy level of ESS at current time step *t* equals to the energy level at previous time step *(t-1)* plus the charging energy multiplied by the charging efficiency, minus the standby loss. It also makes sense for the case when the ESS is discharging.

2.1.3 Transmission Network Modelling for Residential Houses

This thesis mainly studies the optimisation for interconnected energy hubs, hence the mathematical models of different energy carriers' transmission networks are also presented in this section. Regarding the energy hub system where each residential house represents an energy hub, the energy transmissions between houses can be simply formulated by the nodal conservation law as shown in (2-4). It is because that the distance between the residential houses is generally close, and the optimisation for residential houses is carried out for 24 hours in this thesis, one hour or less time is regarded as a time step, the energy loss in the transmission at such short time period is negligible.

$$E_m = \sum_{n=1}^{N} E_{mn} \tag{2-4}$$

(2-4) indicates that the energy injected to node *m* E_m is equal to the sum of the energy flows along branch *m* to *n* E_{mn}. *N* represents the number of nodes.

2.1.4 Electricity Network Modelling

This thesis also investigates the optimisation for community level buildings such as universities and hospitals, where each of them is regarded as an energy hub, and the electrical loads of each hub generally contain both active and reactive loads. Hence the complex power transmission network should be considered to be equipped within the energy hub system. Additionally, the loads of community level buildings are effectively higher than the residential houses, the number of energy demands is therefore higher. Energy transmission system such as gas network needs to be appropriately modelled by considering both the upstream and downstream pressures within the pipelines to enable a certain amount of gas to be successfully transmitted to each building. In this thesis, the complex power and gas are considered to be transferred between interconnected hubs. The related mathematical models are presented as follows [2, 3, 17].

The nodal complex power balance at node m is established in (2-5), where S_m is the complex power injected to the node, S_{mn} is the complex power flow from node m to n. N is the number of the nodes in the power network.

$$S_m = \sum_{n=1}^{N} S_{mn} \tag{2-5}$$

The complex power flow S_{mn} is expressed in (2-6) in terms of the transmission line parameters and complex bus voltage at bus m (V_m) and n (V_n).

$$S_{mn} = \frac{|V_m|^2}{\tilde{Z}_{mn}^*} - \frac{V_m V_n^*}{Z_{mn}^*} \tag{2-6}$$

All the lines between buses are assumed to be equivalent to a π-circuit in this thesis, hence $\tilde{Z}_{mn}$ can be expressed in (2-7) in terms of the series impedance Z_{mn} and shunt admittance Y_{mn}.

$$\tilde{Z}_{mn} = \left(\frac{1}{Z_{mn}} + \frac{Y_{mn}}{2}\right)^{-1} \tag{2-7}$$

2.1.5 Gas Network Modelling

Similar to the electricity network, the modelling of the gas network also follows the nodal conservation law [2, 3, 17]. The nodal gas flow balance is formulated in (2-8).

$$Q_m = \sum_{n=1}^{N} Q_{mn} \tag{2-8}$$

Q_m represents the gas injection to node m, N represents the total number of nodes. Q_{mn} quantifies the gas flow between node m and n, which can be expressed by the upstream pressure p_m and downstream pressure p_n within the pipeline as shown in (2-9).

$$Q_{mn} = k_{mn} sn_{mn} \sqrt{sn_{mn}(p_m^2 - p_n^2)} \tag{2-9a}$$

$$sn_{mn} = \begin{cases} +1, & \text{if } p_m \geq p_n \\ -1, & \text{else} \end{cases} \tag{2-9b}$$

Where k_{mn} indicates the physical properties of the pipeline.
The compressor is also needed in transmitting gas, and the gas consumed by the compressor is formulated in (2-10).

$$Q_{com} = k_{com} Q_{mn}(p_m - p_k) \tag{2-10}$$

As seen, k_{com} indicates the physical properties of the compressor, the suction and discharge pressures at the two sides of the compressor are represented by p_m and p_k respectively. The gas flow rate Q_{mn} can be utilised to quantify the gas power flow between node m and n as shown in (2-11), where GHV means the gross heating value of gas.

$$P_{mn} = GHV \cdot Q_{mn} \tag{2-11}$$

2.2 Optimisation for Steady-State Energy Hub System

2.2.1 Energy Hub Optimisation Problem Formulation

The energy hub system exploits the value of each available energy carrier to flexibly achieve the optimisation goal, it is mathematically resolved by finding the minimum of the objective function. The general optimisation problem formulation is shown in (2-12).

$$\text{Minmise objective function } \mathcal{F}(x) \tag{2-12}$$

$$\text{Subject to } \begin{cases} g(x) = 0 \\ h(x) < 0 \end{cases}$$

The optimisation is implemented by determining the control vector x to realise the minimum value of the objective function $\mathcal{F}$, meanwhile satisfies the equality constraints g and inequality constraints h. In solving the energy management problem of using energy hub, the control vector generally contains the operations of the hub elements at each time step, such as the energy input to each converter and the energy exchange between the ESS with the system. The objective function $\mathcal{F}$ can be defined as the energy

costs, carbon emission, or other factors depending on the needs of the system operator. The equality constraints are built according to the conservation law in the energy hub system, such as the energy transformation within each hub and the energy transmission between hubs. The inequality constraints are established by considering the safety issues. For example, the energy input each converter should be within a boundary to ensure the converter is safely operated.

Table 2-1.REVIEW OF ENERGY HUB OPTIMISATION PROBLEMS

Optimisation objectives	
Energy costs	[2, 6, 17-21]
Multi-objective containing energy costs, energy consumption, carbon emission costs, peak load charges, etc.	[22-24]
Constraints	
Operational restrictions of energy hub components and transmission networks	[2, 6, 17-21, 23, 24]
Residential house devices' operational constraints	[22, 23]
Restriction of consumers' comfort (e.g. room temperature)	[18, 23, 24]
Weather restrictions (e.g. humidity, carbon emission level)	[24]
Industrial process limitations	[22]
Controllable components	
Residential house appliances	[23]
Energy hub components	[2, 6, 17-22, 24]

The energy hub optimisation problems investigated in previous literature are shown in Table 2-1 in terms of different optimisation objectives, constraints, and control variables.

2.2.2 General Procedures of Energy Hub Optimisation

The optimisation for energy hub system is carried out by formulating the optimisation as a mathematical problem based on the energy hub system parameters, the algorithm is then applied to solve the problem to derive the optimal operations of the energy hub system. The specific steps to carry out an optimisation is indicated as follows:

1) For the time horizon that the energy hub to be optimised, the energy loads such as electricity and heat loads, and energy prices are normally simulated and forecasted by using historic data;
2) Forecast the renewable generations over the time horizon, a specific value of generations at each time step is obtained if the optimisation is carried out for the steady-state energy hub system;
3) Model the cost functions of all energy generations;
4) Model the objective function to be optimised, and the equality and inequality constraints for the optimisation.
5) Apply an appropriate optimisation technique to optimise the model.

2.2.3 Optimisation methods

- Linear optimisation: The energy hub optimisation problem is formulated linearly, where the hub elements are simply modelled and the coupling matrix is invariant at all of the time steps. The problem can thus be resolved by applying Linear Programming or Mixed Integer Linear Programming methods. Some conventional methods such as Newton-Raphson method can also be employed [25].
- Non-linear optimisation (convex case): If the energy hub optimisation problem is established as a non-linear and convex problem, numerical methods such as interior-point method are capable of solving the problem, and a global minimum can be reached.
- Non-convex optimisation: The optimisation problem is formulated as a non-convex problem if the hub elements are modelled explicitly or the complex transmission network is considered. The local minimum can be found by applying the numerical method, however, the global minimum is not ensured. Some artificial intelligence algorithms such as genetic algorithm can be utilised to solve the problem to reach a result closer to the global minimum. However, a trade-off between computational burden and optimisation performance need to be made.

2.2.4 Optimisation Techniques in previous literature

The optimal operation of an energy hub system enables the effective utilisation of the elements within the system to minimise energy use, monetary cost or carbon emissions, or some weighted combination of these objectives. Different technologies and

algorithms have been applied to the multi-hub problem depending on the complexity of the optimisation problem as follows:

- **Linear optimisation**

Reference [23] proposes novel mathematical models for the appliances in a residential house, together with the solar PV and energy storage/generation systems. The operations of the residential house are optimally scheduled by using the energy hub optimisation considering end users preferences. A multi-objective function is established and formulated by the combinations of weighted objectives, which contain the energy costs, energy consumption, carbon emission costs, and peak load charges. The optimisation problem is linearly formulated, and Mixed Integer Linear Programming (MILP) is employed to resolve the problem. This research contributes to the energy hub optimisation at the residential level. However, the components within the energy hub system are simply formulated with constant efficiency, which may defer with the realistic operations of the converters and storages.

The MILP method has also been applied in [26], where the authors model the energy hub components with the linear formulation, and approximate the complex power and gas transmission network as in [2, 27] to the linear formulation. The authors have demonstrated that the optimisation results produce high accuracy with fast computation, nevertheless, errors may still appear due to the simplification.

- **Non-linear convex optimisation**

Recent researches study the integration of energy hub optimisation with demand side management (DSM) to further maximise the system flexibility and profits. The DSM is implemented for the demand side of the energy system regarding the behavioural and technological changes. The typical DSM scheme is the demand response, which will be reviewed in section 2.2.5. The optimisation approaches applied in the integrated energy hub with DSM are reviewed as follows:

Reference [28] introduces the "smart energy hub" system which uses a cloud computing platform to enable customers with must run loads to participate in a demand side management program. An integrated demand side management is proposed in [29] and [30], where a group of energy hubs is incorporated to respond to the scheme, and the interactions between hubs are formulated as a non-cooperative game, the existence of the unique Nash equilibrium is proved. The interactions between energy hubs are

investigated in a competitive electricity market in [31], where the performance of an energy management system under different energy pricing schemes for a group of 10 hubs is studied.

The optimisation problems in the above literature are formulated as a convex problem, which is resolved by using the method of exact line search is applied, and the global minimum can be confirmed. However, most energy hub optimisation problems are formulated as a non-convex problem, the proposed optimisation techniques in the papers can only reach a local minimum when solving the non-convex problem. Additionally, the ESS is not considered in the energy hub system, which simplifies the problem.

- **Non-convex optimisation**

The optimisation for energy hub system is generally expressed as a non-convex problem because the complex electricity power and gas power transmission are considered as the equality constraints. Different optimisation approaches are developed in literature and presented as follows:

Paper [18] proposes a general modelling technique for both the economic dispatch of energy hub and optimal power flow between multiple hubs, a decomposed solution is presented by applying the multi-agent genetic algorithm (MAGA) to optimise the modelled framework of interconnected energy hubs.

Paper [32] investigates the optimal energy flow problem within the context of an interconnected energy hub system, where the electricity, gas, and district heating networks are considered. The paper also models the converters with non-constant efficiency and adopts the quadratic function derived from the converters' power-efficiency curve to represent the efficiency. A modified approach of using teaching-learning optimisation is proposed to solve the optimisation problem.

The above two papers innovatively resolve the optimisation for interconnected energy hubs. However, the ESS is not considered in the energy hubs, and hence the flexibility and profits of the system are reduced.

Model predictive control (MPC) is employed in [27] and [17] to optimally manage the operations of three interconnected energy hubs. Specifically, [27] investigates the effects on energy hub optimisation with different prediction horizon and energy storage

characteristics. Although numerical methods are applied within the MPC scheme, so a global minimum cannot be guaranteed in the solution.

2.2.5 Integrated energy hub optimisation with other smart grid applications

- **Demand response**

To facilitate power system stability by shaving peak load and reducing energy costs, the demand response (DR) scheme has been employed to encourage customers to re-allocate energy usage in response to variant energy carrier prices [21, 33, 34]. The DR scheme has been widely applied worldwide, especially in the United States, Europe and China [35]. The typical demand response programs can be classified into price-based DR and incentive-based DR, which are illustrated in Table 2-2 [35].

This thesis mainly studies the integration of price-based DR to energy hub optimisation.

Table 2-2.DIFFERENT TYPES OF DR SCHEMES

Priced-based DR	Incentive-based DR
Time-of-use (TOU): the TOU rate indicates the electricity tariff variations over 24 hours, where each hour is normally regarded as a time step. The TOU rate represents the unit price of the power to customers, it is extensively adopted for residential and industrial customers.	Direct Load Control (DLC): The DLC scheme is specifically designed for residential or small-industrial customers. The retailers or energy provides could directly terminate the use of some appliances of the customer with short notice. The DLC is operated to eliminate the system contingencies and maintain reliability.
Real-Time-Pricing (RTP): the RTP represents the varying hourly electricity tariff caused by the change from the wholesale market. It is normally known in advance within the DR scheme before one day or one hour.	Interruptible/Curtailable Service (I/C): The I/C is designed for large industries or commercial buildings. It provides discount or incentives to customers to reduce load during fault condition.
Critical Peak Pricing (CPP): CPP is designed to define the high-price periods in advance, and it is only implemented for short period in case of extremely high demand or system faults which last long.	Demand Bidding/Buyback: the consumers would propose the prices, that they are willing to amend their loads, to the utility companies; the program also suggest the consumers of the amount of loads they would amend according to the price given by utility companies.
	Other schemes include Emergency DR, Capacity Market Programs, etc.

From the perspective of operating energy hub systems, energy demand could be satisfied by accordingly increasing the utilisation of cheaper energy carrier to reduce energy costs. For example, instead of inputting relatively expensive electricity from the grid to meet energy hub electrical demand, the Combined Heat and Power (CHP) can be switched on to consume gas to produce electricity and heat. Therefore, combining DR with the energy hub can bring further profits by responding to energy prices and optimising the cooperation of various energy carriers. The integrated DR with energy hub optimisation is proposed in [33, 36] to benefit both the customers and energy utility companies in real-time pricing scheme.

As illustrated in [34], the house appliances are firstly classified into four categories including deferrable appliances, thermal appliance, curtailable appliances, and critical appliances. The demand response is then implemented depending on the characteristics of different appliances to reschedule the loads. Instead of classifying different appliances, this thesis investigates the integration of energy hub with general demand response scheme, where the demands are categorised into elastic and inelastic demands. The definitions of these terms are introduced as follows:

Customer demand generally changes in response to the variation of energy carrier prices, defined as elastic demand [37]. Conversely, the demand not affected by the variations of energy prices is defined as inelastic demand. The sensitivity of demand in relation to energy price change is quantified by price elasticity, defined as [38, 39]:

$$L = a \cdot P^{\varepsilon} \tag{2-13}$$

Where L is load, P is energy price, and ε represents the price elasticity. a is a coefficient, which could be formulated by a given reference load L_{ref} and price P_{ref}. Specifically, L_{ref} indicates the customers' load before implementing the demand response scheme, and L is the new load. The reference price P_{ref} is input by customers. The price elasticity over the entire simulation time horizon is assumed to be constant.

Traditional demand response considering elastic demand is carried out by optimally determining the demand allocation over entire simulation time in response to energy prices.

- **Combination of borehole and ground source heat pump system**

In 2014, the Renewable Heat Incentive (RHI) was launched in the UK to increase the installation of low carbon technologies [40]. Heat pumps have lower carbon emissions than the conventional heating methods such as a boiler. Ground source heat pumps (GSHP) are widely used since they have higher and more stable coefficient of performance (CoP) over other heat pump types, due to ground temperatures remaining constant through the whole year [41]. Additionally, the efficiency of the heat pump is depending on the heat source temperature and indoor temperature. The application of the borehole storage can significantly increase the GSHP performance since the thermal storage provides a high temperature source, raising the GSHP coefficient of performance (CoP).

Borehole thermal storage uses the ground as a heat source and storage medium. High temperature fluid flows through the borehole pipes and stores the heat energy into the surrounding ground and this process is done by heat transfer [42]. After the fluid dumps the heat into the borehole, the temperature settles down in the borehole wall area and when the heat is needed from the borehole, the fluid extracts the heat from borehole wall and provide high temperature source.

The high efficiency of the combined borehole and GSHP indicates great energy saving for community-level buildings, the incorporation of the system to energy hub suggests further cost minimisation and potentially increase the flexibility to satisfy multiple energy demands.

2.3 Optimisation for Energy Hub System with Uncertainty

In reality, uncertainties always present in power systems operation or energy management problem. According to [43], uncertainties can be categorised as follows:

i) Uncertainty is measured mathematically, which represents the difference between the estimated values and true values, indicating the errors in observation or calculation.

ii) Uncertainty from sources, including transmission capacity, generation availability, load requirements, unplanned outages, market rules, fuel price, energy price, market forces, weather and other interruption, etc.

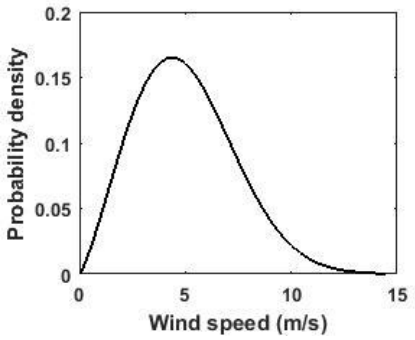

Fig. 2-2.PDF curve of the wind speed at Cardiff observation station.

Uncertainty can be expressed by the probability density function (PDF). For example, the PDF curve of the wind speed from 9.00 AM to 10.00 AM at an observation station in Cardiff is shown in Fig. 2-2, which is derived by fitting historical data in the period between 9.00 AM to 10.00 AM over one year [44]. As seen, the possible wind speeds vary between 0 and 13 m/s, and the highest probability is 0.16 when the wind speed is approximately 5 m/s. If a wind turbine is located at this stations and accessed to the power system, the uncertain power output led by the uncertain wind speeds could significantly affect the power system operations, because the overestimate of uncertainty could cause the system to cost too much, and an underestimate of uncertain factors might threaten the secure operation of the power system.

Therefore, in solving the energy management or power system operating problems with the consideration of uncertain factors, an appropriate modelling approach should be implemented for uncertainties. Various approaches have been developed to model the uncertainty, which are summarised as follows [45]:

i) Probabilistic approach: The PDF of the uncertain variables are assumed to be known, which can be derived by fitting historical data of the uncertain variables. Stochastic programming methods such as Monte Carlo simulation are applied to solve the probabilistic problem.

ii) Possibilistic approach: It is also referred to as the fuzzy approach, which assigns a membership function to model the uncertain variables.

iii) Robust optimisation: It is applied to provide optimal robust solutions based on the uncertain data forecasted within the confidence intervals. It should be noted that the solutions are also optimal to the worst-case scenario of the uncertain variables.

Some other approaches are proposed by the combinations of the above approaches. This thesis proposes to apply the probabilistic approach to resolve energy hub optimisation problem with uncertainty. The methods developed in solving probabilistic energy hub optimisation are reviewed in this section.

2.3.1 Monte Carlo Simulation

The scenario methods are widely applied to represent the uncertain variables by scenarios, and each of them corresponds with a probability. In applying the scenarios methods, the characteristics of uncertain variables including distributions, moments, and cumulants are firstly derived from their historical data, different scenarios are then generated based on the uncertain variable characteristics. The stochastic programming is carried out by repeatedly solving the deterministic problem for the energy hub problem, where each scenario is regarded as the input value of the uncertain variable. The final optimisation results are derived from the results from each deterministic programming.

Monte Carlo Simulation (MCS) is the most common and fundamental method to generate scenarios according to the distribution of uncertain variables, and it has been broadly utilised in solving energy hub problem with uncertainty.

Paper [46] proposes a valuating method for integrated demand side management with the energy hub optimisation, where the stochastic energy prices are modelled through the MCS. The stochastic model allows the valuation to be carried out by flexibly exploiting the elements of energy conversion, energy storage, and demand side energy management, while the uncertain prices are explicitly considered.

A hierarchical control scheme is proposed in [20] to optimally manage the operations of the greenhouses with the application of energy hub optimisation. The MCS is employed to simulate the uncertain factors of RTP and weather parameters including outdoor temperature, humidity, wind speed, and solar irradiation. The energy cost of the greenhouses is accordingly optimised with the consideration of stochastic weather, electricity price, while the climate change from the greenhouses is controlled.

The advantage of using the MCS is that a large number of scenarios is generated to represent the uncertain variables, and their stochastic nature is explicitly expressed by the scenarios, hence allows comparatively accurate results when solving the

probabilistic problem. However, the large number of scenarios also greatly increase the computational burden.

2.3.2 Scenario-reduction methods

Some scenario-reduction methods are developed to limit the number of scenarios to mitigate the computational burden.

Paper [47] proposes to solve the energy hub planning problem with the consideration of random wind power generation, demands, and availability of components. The MCS is firstly applied to generate massive scenarios for the uncertain variables, a scenario-based approximation method provided by GAMS is then applied to reduce the number of scenarios. The optimisation problem is resolved based on the limited number of scenarios.

Paper [24] classifies the dependencies among various energy carriers into internal dependency and external dependency. Internal dependency represents the possible changes of energy supply by considering how to optimally utilise the converters and energy storage, which is controlled by the system operators, and the external dependency refers to the operations of consuming the energy depending on the consumers' preferences. The integrated demand response with energy hub is implemented by modelling the uncertainties of internal and external dependencies. A scenario reduction method based on roulette wheel mechanism is utilised to model the uncertainties in optimising the probabilistic energy hubs.

In addition to the scenario reduction methods, some other methods such as the two-point estimate method (2PEM) and point estimate method (PEM) are developed to generate a limited number of scenarios to simulate the uncertainty.

In [48], the PEM is employed to model the wind power generation in solving the probabilistic energy hub optimisation problem. Compared with the MCS, the PEM is more efficient and requires less computational cost.

Paper [49] proposes the home energy management within the context of an energy hub, the uncertain solar power generation is considered and modelled by the 2PEM method. The 2PEM generates 2 concentration points at each time step, and hence 48 scenarios are derived for 24 time steps' energy management. The probabilistic energy

management is carried out by considering home appliances, plug-in hybrid electric vehicle, storages, and typical energy converters such as CHP.

An improved 2PEM is utilised in [21] to model the uncertainties from load and energy prices during optimally scheduling the energy hub operations. The improved approach referred to as the 2m+1 PEM generates 97 scenarios for 24 time steps' optimisation. It is demonstrated that the 2m+1 PEM performs better in solving probabilistic energy hub problems compared with 2PEM and MCS.

The limited number of scenarios can be applied to efficiently model the uncertainty and solved with energy hub optimisation. However, the reduced number of scenarios may fail to fully capture the stochastic nature of uncertain factors.

2.3.3 Chance-constrained programming

In contrast to scenario-based methods, chance-constrained programming (CCP) is a consistently robust and reliable approach to resolve uncertainty [50]. Each chance constraint is modelled by a boundary, the acceptable probability of constraint violation. The CCP optimization is then resolved to meet both normal constraints and chance constraints. Whilst the stochastic nature of uncertain elements can cause occasional system overloading, investment to meet these rare stress events could be prohibitively expensive. The CCP has not been applied to energy hub optimisation. However, CCP has been applied to power system operating problems, including demand response, optimal power flow, and unit commitment in [51], [52], and [53].

The chance-constrained optimisation problem is defined as follows [50]:

$$\min \quad f(x,u,\xi) \tag{2-14}$$

$$s.t. \begin{cases} g(x,u,\xi)=0 \\ h(x,u,\xi)\le 0 \\ Pr_i(y_i(u,\xi)\le y_i^{SP}, i=1,\dots,I)\ge \alpha \end{cases}$$

Where x, u, and ξ respectively indicate the state variables, control variables, and uncertain variables; f, g, and h represent the objective function, equality constraints, and inequality constraints. Pr denotes the probability measure of chance constraints, and y_i^{SP} is the specific boundary to limit the constraints, α is the pre-defined probability level, a higher value of α implies a stronger desire to hold the constraints. i indicates the number of chance constraints.

By defining a probability level for the chance constraints, solving the CCP means to optimise the problem *f* with equality constraints *g*, inequality constraints *h* and chance constraints satisfied, under the condition that the values of uncertainty variables ξ are randomly distributed according to their distributions.

In solving the CCP problem, the non-convex CCP problem is converted into a convex problem and linear programming is applied in [54]. The back-mapping approach is utilized in [50, 52], where the probability of chance constraints is derived by mapping them back to the uncertainty variables' distributions. Non-linear programming is then applied to solve the optimization problem. A sample average approximation method is developed in [55] to resolve chance-constrained problems.

2.4 Chapter summary

This chapter firstly presents an overview of energy hub in terms of definition, modelling, and mathematical formulation.

It then reviews the energy hub optimisation under steady state and with the consideration of uncertainty. Different optimisation approaches are developed for energy hub system, and the joint-optimisation of energy hubs with other smart grid operating methods, such as demand response, is introduced.

The main limitations of existing methods of optimising steady-state energy hub are: the optimisations fail to be proved to converge to a local minimum when the optimisation problem is formulated as a complicated non-convex problem. The limitations to stochastic programming in optimising energy hub with uncertainty are: i) Monte Carlo Simulation requires many computational efforts in solving a large number of scenarios; ii) with the application of scenario-reduction methods, the limited number might fail to reflect the stochastic nature of uncertain variables.

Chapter 3

Optimal Operation of Interconnected Energy Hubs by Using Decomposed Hybrid Particle Swarm and Interior-Point Approach

This chapter proposes Particle Swarm Optimization (PSO) hybridised with a numerical method, referred to collectively as the decomposition technique to optimise the operations of interconnected energy hubs under steady state.

Chapter Overview

As illustrated in section 2.2.4, the interconnected energy hub optimisation problem can be expressed in a simplified form of linear problem or non-linear convex problem. However, the problem is frequently formulated as a non-convex problem due to the inclusion of complex power and gas network, and the problem is considered as a multi-period problem if the ESS is considered within the system.

Previous literature have utilised the numerical methods to solve the optimisation problem. However, only local minimum can be reached, and the global minimum is not guaranteed. Some researches propose to employ the artificial intelligence algorithms such as genetic algorithm to optimise the problem, and hence to reach the global minimum. Nevertheless, ESS is not considered in these researches, the system flexibility is reduced, and the problem is simplified, hence the robustness of the optimisation techniques is not proved to be capable of solving general interconnected energy hubs optimisation problem.

Therefore, to address the deficiency in previous researches, this chapter explicitly formulates the energy hub optimisation under steady state by a non-convex and multi-period problem. This chapter assumes the renewable power generations, energy hub loads, and energy prices to be perfectly known, the energy hubs are considered to be interconnected with electricity and heat transmission networks. In order to practically simulate the energy hub operations, some of the energy converters are simulated with non-constant efficiency based on real-time operational data. The batteries are considered as the ESS to be equipped within the energy hubs. To better utilise the ESS from the long run, the battery lifetime cost is also considered together with the system energy costs as the objective function to avoid unnecessary degradation.

More importantly, this chapter proposes a novel optimisation technique to optimise the steady-state interconnected energy hub problem. A decomposed approach of utilising particle swarm optimisation (PSO) hybridised with interior-point method is innovatively developed to resolve the non-convex and highly-constrained optimisation problem. It is demonstrated that the optimisation technique performs better in terms of convergence and computational speed compared with the traditional PSO. The contributions of the chapter can be summarised as follows:

i) The decomposed technique of applying PSO hybridised with interior-point is demonstrated to be capable of solving non-convex multi-period energy hub optimisation problem.

ii) A group of residential house is formulated as a system of interconnected energy hubs, the batteries within the system are better utilised by including the battery lifetime cost in the objective function.

iii) The performance of the decomposed PSO is proved to be better compared with the conventional PSO by solving the same 3-hub problem.

Statement of Authorship

This declaration concerns the article entitled:			
Optimal Operation of Interconnected Energy Hubs by Using Decomposed Hybrid Particle Swarm and Interior-Point Approach			
Publication status: Published			
Publication details (reference)	D. Huo, S. Le Blond, C. Gu, W. Wei, and D. Yu, "Optimal operation of interconnected energy hubs by using decomposed hybrid particle swarm and interior-point approach," International Journal of Electrical Power & Energy Systems, vol. 95, no. Supplement C, pp. 36-46, 2018/02/01/ 2018.		
Candidate's contribution to the paper	The candidate proposed the idea of the paper, he designed the methodology, and predominantly executed the coding to derive the experimental results. Other authors helped the candidate with the design of case studies, format of the paper, and improvement of academic writing. The percentage of the candidate did compared with the whole work is indicated as follows: Formulation of ideas: 100% Design of methodology: 90% Simulation work: 90% Presentation of data in journal format: 80%		
Statement from candidate	This paper reports on original research I conducted during the period of my Higher Degree by Research candidature.		
Signed	Da Huo	Date	27/07/2018

3.1 Abstract

The Energy Hub has become an important concept for formally optimizing multi-carrier energy infrastructure to increase system flexibility and efficiency. The existence of energy storage within energy hubs enables the dynamic coordination of energy supply and demand against varying energy tariffs and local renewable generation to save energy cost. The battery lifetime cost may be included in the optimization objective function to better utilize battery for long term use. However, the operational optimization of an interconnected energy hub system with battery lifetime considered presents a highly constrained, multi-period, non-convex problem. This paper proposes Particle Swarm Optimization (PSO) hybridised with a numerical method, referred to collectively as the decomposition technique. It decouples the complicated optimization problem into sub-problems, namely the scheduling of storage and other elements in the energy hub system, and separately solves these by PSO and the numerical method 'interior-point'. This approach thus overcomes the disadvantages of numerical methods and artificial intelligence algorithms that suffer from convergence only to a local minimum or prohibitive computation times, respectively. The new approach is applied to an example two-hub system and a three-hub system over a time horizon of 24 hours. It is also applied to a large eleven-hub system to test the performance of the approach and discuss the potential applications. The results demonstrate that the method is capable of achieving very near the global minimum, verified by an analytical approach, and is fast enough to allow an online, receding time horizon implementation.

3.2 Introduction

Energy hub modelling relates to the utilization of co-generation or tri-generation, which increases system flexibility by means of exploiting every available energy carrier, such as electricity, gas, and heat [1, 2]. A typical energy hub contains multiple energy carriers, which achieves the function of importing, exporting, converting, and storing energy [3, 4]. The energy hub approach takes advantage of existing infrastructures as much as possible and can be applied to various sizes of the energy system. Domestic buildings are modelled in this paper, which consume approximately 40% of society's total energy [5] but an individual domestic load profile is fairly stochastic such that it cannot always be met with onsite generation. Interconnecting heterogeneous energy infrastructure at local level can best leverage renewable generation and pooled storage without suffering large distance transmission losses and enable self-sufficient energy communities.

The optimal operation of an energy hub system enables the effective utilization of the elements within the system to minimise energy use, monetary cost or emissions, or some weighted combination of these objectives. Different algorithms have been applied to the multi-hub optimization problem. Reference [6] presents a decomposed solution of a multi-agent genetic algorithm to optimize the power and gas flow between energy hubs. Papers [7] and [8] employ model predictive control (MPC) to optimally control the operation of three interconnected energy hubs, although numerical methods are applied within the MPC scheme, so a global minimum cannot be guaranteed in the solution. In [9] and [10], a grid of 10 hubs is modelled, where the energy transfer between hubs is formulated as a non-cooperative game. The existence of the unique Nash equilibrium is proved. References [11, 12] propose an integrated demand response program and simulate the scheme on a smart grid of six energy hubs. The integrated demand response problem is formulated as an ordinal potential game and the Nash equilibrium is proven to be unique. Reference [13] investigates the performance of an energy management system under different energy pricing schemes for a group of 10 hubs. Reference [14] introduces the "smart energy hub" system which uses a cloud computing platform to enable customers with must run loads to participate in a demand side management program. Reference [15] investigates the optimization performance between deterministic and stochastic approaches applied to multi-period optimization for a 3-hub system over a mixed industrial and residential area. Reference [16] generates a novel mathematical model for storage, general appliances, and other renewable components in residential houses. Mixed integer linear programming (MILP) is applied to optimize the control for residential energy hubs considering end-user preferences.

References [9] to [15] propose the optimization for multi-hubs. However, storage is not considered when the problem is formulated as a non-convex problem in [9] to [12]. In reference [13], the storage is modelled in the energy hub optimization, but the problem is formulated as a convex problem. The optimal operation of multiple hubs with energy storage and interconnection available between hubs has hitherto been formulated as a highly constrained, non-linear multi-period optimization. However, the lifetime of the battery system suffers as its utilization increases, an aspect which has not been addressed in previous energy hub literature. In this paper, the battery lifetime cost is calculated and included in the objective function based on the method proposed by [17].

Therefore, the optimization problem is formulated as a non-convex, multi-period problem.

Numerical algorithms such as MILP provide fast computation times, but perform poorly when solving non-convex problems, because the solver can easily fall into local minima. Alternatively, particle swarm optimization (PSO) and related optimization approaches have been applied to optimize the operation of power systems due to their straightforward implementation and high efficiency [18]. For example, multi-pass iteration PSO was applied to the optimal scheduling of a battery coupled with wind turbine generators [19]. Co-evolutionary PSO was applied to smart home operation strategies [20]. A hybrid algorithm combining PSO and a bacterial foraging algorithm was proposed and applied to the optimal scheduling of an active distribution network [21].

Despite high robustness and accuracy compared with other algorithms [19], PSO has never been applied to solve energy hub optimization problems. However, conventional PSO is not suitable for solving highly-constrained non-linear problems with a large number of variables where the feasible region is narrow in hundreds of dimensions, meaning the time spent on finding feasible particles is considerable. Thus, improvement to conventional PSO is required in order to fully harness its potential for multi-hub optimization. This paper proposes a decomposed solution by applying a novel hybrid PSO and numerical optimization by combining conventional PSO with the 'interior point' method. Each particle in the PSO routine represents the storage operations over the whole optimization time horizon (24 hours in this paper). Based on the storage operation, the 'interior-point' algorithm is applied to optimize the operations of other elements in the system of energy hubs over 24 hours. The resulting energy cost over the full 24 hour time horizon is formulated as the fitness score. All particles then are updated based on the conventional PSO routine until the optimization completes. The decomposition technique is demonstrated to be capable of optimizing multi-energy hubs efficiently, and the storage operation obtained from the decomposition technique is benchmarked to be very close to the theoretical optimal strategy of storage. Additionally, the decomposed PSO yields better optimization results with less computation compared with the conventional PSO. The approach is applied to two energy hub systems to illustrate its effectiveness. The main contributions of this paper are illustrated as follows:

i) A decomposition technique of applying particle swarm optimization is proposed in this paper, and it is capable of solving the non-convex multi-period optimization problem. The decomposition technique is validated by a simple two-hub system for which the theoretical minimum can be derived empirically.

ii) A group of residential houses is simulated as an interconnected energy hub system, an optimization problem is expressed to minimize the total cost of the energy hub system over 24 hours. With the battery lifetime cost considered in the optimization, the problem is formulated as a non-convex problem. The decomposed PSO approach is applied to optimally solve the problem. The optimization results indicate that the battery SOC varies between 60% and 90% to avoid unnecessary degradation of the battery lifetime for three residential hubs.

iii) The performance of the decomposed PSO approach is compared with the conventional PSO being applied to solve a same three-hub problem. The decomposition technique achieves a 58% greater energy saving for three-hub optimization with 98% saving of computation time comparing with the conventional PSO.

This paper is organized in six sections. Section II illustrates the general optimization problems for multi-energy hubs which the energy interconnection is enabled between hubs. An explicit description of the decomposition technique applying PSO is presented in section III. Section IV presents the case studies and related results. Section V concludes the paper.

3.3 Energy Hub Optimization

3.3.1. Energy Hub Modelling

A typical energy hub model that enables energy sharing between hubs is shown in Fig. 3-1. It consumes various input resources including electricity from grid (P_{ele}), solar energy (P_{so}), and gas (P_{gas}) to meet the electricity load (L_{ele}) and thermal load (L_{th}). The energy flow between hubs is denoted by E_{rh} and H_{rh} , which indicate the power and heat exchange with other hubs. The mathematical formulation between hub inputs and outputs under steady state operation is shown in (3-1).

$$\begin{bmatrix} L_{ele}(t) \\ L_{th}(t) + H_{rh}(t) \end{bmatrix} =$$

$$\begin{bmatrix} \eta_{PV} \cdot \big(1 - v_1(t)\big) & 1 - v_1(t) & v_2(t) \cdot \eta_e \\ \eta_{PV} \cdot v_1(t) \cdot CoP & v_1(t) \cdot CoP & v_2(t) \cdot \eta_{th} + \eta_{bo} \cdot \big(1 - v_2(t)\big) \end{bmatrix} \times$$

$$\begin{bmatrix} P_{so}(t) \\ P_{ele}(t) + E_{sh}(t) - E_{hs}(t) + E_{rh}(t) \\ P_{gas}(t) \end{bmatrix} \tag{3-1}$$

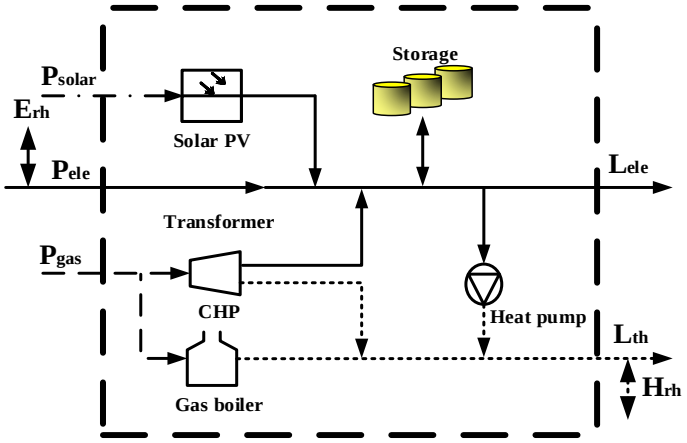

Fig. 3-2. An example of energy hub model

The first matrix on the right hand side is the coupling matrix C, which defines the relationship between inputs P and outputs L. The parameter t within the brackets indicates that these variables are time dependent. Since the problem is considered in a discretized time domain, they are fixed in each time step. The coefficient v is the dispatch factor between 1 and 0 which generally denotes the portion of the energy injected to a certain converter. For the example energy hub model, v_1 is the portion of electricity injected to heat pump over total electricity input. v_2 indicates the percentage of gas input to CHP over total gas input. Parameters η_{so} and η_{bo} express the efficiency of the Solar PV and boiler respectively. η_e and η_{th} represents the electric efficiency and thermal efficiency of CHP respectively. E_{sh} and E_{hs} indicate the charging and discharging energy.

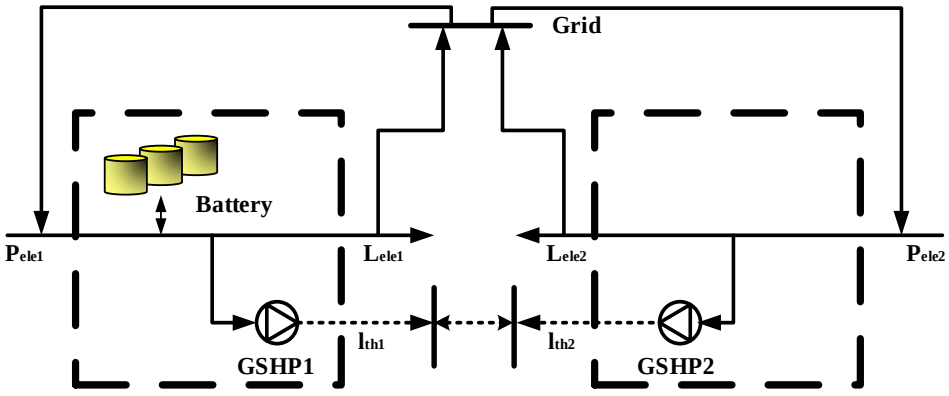

Fig. 3-1. Two-hub system with energy sharing available between hubs.

The assumptions for modelling the energy hub system are as follows:

Assumption 1: The energy hub system modelled enables electricity and heat sharing between hubs. The electrical interconnection between hubs is the electricity exchange with the grid. For example, in Fig. 3-2 electricity transfer from hub 1 to hub 2 is achieved by injecting electricity to grid from hub 1, and extracting the same amount of electricity from grid to hub 2. For heat transfer, a district heat network must be installed between the hubs.

3.3.2. Converters Modelling

The most common residential heating in the UK, a gas boiler, is modelled within the energy hub. The efficiency of a gas boiler can be formulated as a nonlinear expression in terms of the input energy $P_{gas}(t)$.

Assumption 2: the efficiency of the boiler simulated in this paper is non-constant, and the characteristics of the cyclic fuel utilization efficiency with respect to cyclic input energy normalized by steady-state input energy is derived based on Reference [22]. The data points and approximated curve are shown in Fig. 3-3.

The boiler efficiency varying with the input energy can, therefore, be represented by the approximated curve. The expression of boiler efficiency η_{bo} is shown in (3-2):

$$\eta_{bo}(t) = 0.8218646 - \frac{0.01686}{P^{*}_{gas}(t)} \tag{3-2}$$

Where $P_{gas}{}^{*}(t)$ is the value of instant gas input at time step t normalized by steady-

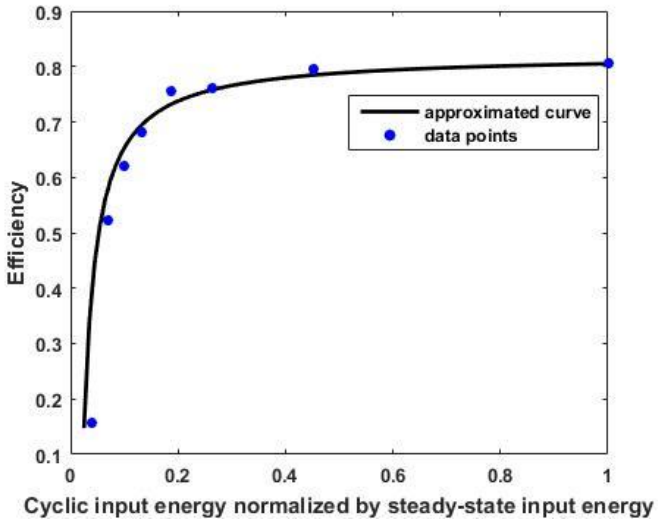

Fig. 3-3.Boiler efficiency against cyclic input energy normalized by steady-state input energy

state input. It should be noted that the value of $P_{gas}{}^{*}(t)$ is within the boundary of 0 to 1.

In addition, the ground source heat pump (GSHP) is selected in this paper due to its high efficiency and potential to decarbonise heat, and its increasing uptake in some European countries, America and Japan [23]. The efficiency of the heat pump is described as the Coefficient of Performance (CoP) and is expressed in (3-3):

$$Heat\ output = CoP \cdot P_{HP}(t) \tag{3-3}$$

Where P_{HP} is the power input to the GSHP.

Assumption 3: the CoP of GSHP is set to be constant over the whole time horizon.

Micro-combined heat and power (micro-CHP) reduces electricity utilization from the grid and increases energy efficiency by simultaneously generating power and heat [24]. Hence it is modelled in this paper.

Assumption 4: The micro-CHP simulated in this paper is assumed to be steady-state with constant electric efficiency and thermal efficiency, the values of 0.33 and 0.57 are respectively adopted to simulate the efficiencies. The ramp rate constraint e_{ramp} to restrict the micro-CHP power output is considered and given by (3-4), e_p is the power output of the micro-CHP.

$$-e_{ramp} \leq e_p(t-1) - e_p(t) \leq e_{ramp} \tag{3-4}$$

3.3.3. Energy Storage Modelling

The lead-acid battery is employed as the energy storage within the energy hubs in this work. The battery is considered to be a simple buffering device. Since the electrical energy within the storage at the current time step is equal to the electricity at last time step plus the charging energy or minus the discharging energy, and minus the standby loss. The i_{th} battery's energy level $E_i(t)$ is mathematically expressed in (3-5).

$$E_i(t) = E_i(t-1) + E_{stb,i}(t) + E_{hs,i}(t) \cdot \eta_{char} - E_{sh,i}(t)/\eta_{dis} \tag{3-5}$$

$E(t-1)$ represents the energy within the storage in the previous time step. E_{stb} is the standby loss, E_{sh} and E_{hs} indicate the charging and discharging energy. η_{char} and η_{dis}

are charging efficiency and discharging efficiency respectively. Since the battery can only charge, discharge, or on standby at any time step, constraint (3-6) is considered in the optimization problem.

$$E_{hs,i}(t) \cdot E_{sh,i}(t) = 0 \tag{3-6}$$

In addition, the characteristic of battery lifetime is considered since the operation of the battery at different states of charge (SOC) result in different losses. The lifetime drops quicker when operating the battery during low SOCs compared to high SOCs [25]. To maximize the benefits of battery utilisation from the prospective of long term operation, the battery lifetime cost penalty is calculated and added to the objective function. Reference [17] suggests the method of calculating battery lifetime cost $C_{bl}(t)$ and it is illustrated in Appendix.

Assumption 5: During the process of optimization, the initial state of charge of each battery is set to be 70%, and to consistently utilize the batteries for the next day, the state of charge at the final time step needs to be reverted to above 70%. The SOC of the three batteries is assumed to be limited between 0 and 100%.

3.3.4. Optimization Problem Description

The objective is to minimize the system cost including the energy cost and battery lifetime cost over a time horizon of 24 hours. With the knowledge of electricity load, heat load, energy carrier price and solar energy generation, the objective is to control the energy hub operation at each time step to achieve a holistic 24 hour optimization. The system operation vector contains energy injected into each hub, the dispatch factor within each hub, the energy exchange between hubs, and the charging/discharging energy of energy storage at each time step. The control vector $u(t)$ is expressed in (3-7):

$$u(t) = \left[P_{ele,i}(t), P_{gas,i}(t), E_{ij}(t), H_{ij}(t), E_{sh}(t), v_i(t)\right], \forall i, \forall t \tag{3-7}$$

For a system containing Ω number of interconnected energy hubs, the optimization problem may be formulated as equations (3-8a) to (3-8o), the variables used in problem (3-8) are defined thusly:

Subscripts i and j denote the hub index.$P_{ele}(t)$ and $P_{gas}(t)$ represent the electricity and

gas input to energy hub at time step t. $v_i(t)$ denotes the dispatch factor at time step t. The electricity and heat exchange between hubs are denoted as $E_{ij}(t)$ and $H_{ij}(t)$, which means the energy flow direction is from hub *i* to hub *j* at time step t. The flow direction is reversed when the value of $E_{ij}(t)$ and $H_{ij}(t)$ are negative. $SOC(t)$ is the battery state of charge. $E_s(t)$ represents the energy stored in the battery at time step t, which has to be limited within the battery capacity. $E_{sh}(t)$ and $E_{hs}(t)$ are the charging and discharging power from the battery. Π(t) denotes the energy price. $P_{HP}(t)$ and $P_{Bo}(t)$ are the energy injection to heat pump and boiler respectively. N is the number of total time steps. $e_p(t)$ represents the electricity output of Micro-CHP, and $e_{ramp}(t)$ is the Micro-CHP ramp rate at time step t.

The optimization problem is described by (3-8a) – (3-8o):

Minimize

$$\sum_{t=1}^{N}\left[\sum_{i=1}^{\Omega}[P_{ele,i}(t)\times\Pi_{ele}(t)+P_{gas,i}(t)\times\Pi_{gas}(t)+C_{bl,i}(t)]\right] \quad (3\text{-}8a)$$

Subject to

$$L_i(t)=C_i(t)\cdot P_i(t),\forall i,\forall t \quad (3\text{-}8b)$$

$$0\le v_i(t)\le 1\ \forall i,\forall t \quad (3\text{-}8c)$$

Electricity

$$P_{ele,i,min}(t)\le P_{ele,i}(t)\le P_{ele,i,max}(t),\forall i,\forall t \quad (3\text{-}8d)$$

$$E_{ij,min}(t)\le E_{ij}(t)\le E_{ij,max}(t),\forall i,\forall t \quad (3\text{-}8e)$$

Heat

$$H_{ij,min}(t)\le H_{ij}(t)\le H_{ij,max}(t),\forall i,\forall t \quad (3\text{-}8f)$$

Battery

$$SOC_{i,min}(t)\le SOC_i(t)\le SOC_{i,max}(t),\forall i,\forall t \quad (3\text{-}8g)$$

$$0\le E_{sh,i}(t)\le E_{sh,i,max}(t),\forall i,\forall t \quad (3\text{-}8h)$$

$$0 \leq E_{hs,i}(t) \leq E_{hs,i,max}(t), \forall i, \forall t \quad \text{(3-8i)}$$

$$E_{sh,i}(t) \cdot E_{hs,i}(t) = 0, \forall i, \forall t \quad \text{(3-8j)}$$

Micro-CHP

$$e_{p,i,min}(t) \leq e_{p,i}(t) \leq e_{p,i,max}(t), \forall i, \forall t \quad \text{(3-8k)}$$

$$e_{ramp}(t) \leq e_{p,i}(t) - e_{p,i}(t-1) \leq e_{ramp}(t), \forall i, \forall t \quad \text{(3-8l)}$$

Gas

$$P_{gas,i,min}(t) \leq P_{gas,i}(t) \leq P_{gas,max}(t), \forall i, \forall t \quad \text{(3-8m)}$$

GSHP

$$P_{HP,i,min}(t) \leq P_{HP,i}(t) \leq P_{HP,i,max}(t), \forall i, \forall t \quad \text{(3-8n)}$$

Boiler

$$P_{Bo,i,min}(t) \leq P_{Bo,i}(t) \leq P_{Bo,i,max}(t), \quad \forall i, \forall t \quad \text{(3-8o)}$$

As indicated by (3-8), the optimization is carried out considering the security constraints. (3-8b) indicates the coupling constraints between hub inputs and outputs to reflect equations (3-2) (3-3) and (3-5). (3-8b) is the transformation of (3-1) which reflects the mathematical transformation between energy hub input and output. (3-8d) and (3-8m) refer to the minimum and maximum energy input to a single hub. (3-8e) and (3-8f) suggest the adjustment of energy transmission limitation between hubs. (3-8g) indicates the limitation of energy level within batteries. (3-8h) and (3-8i) indicate the limitation of charging energy and discharging energy at each time step. (3-8j) avoids simultaneously charging and discharging the battery. (3-8k), (3-8n), and (3-8o) represent the minimum and maximum energy injection to micro-CHP, GSHP, and boiler respectively. (3-8l) limits the ramp rate for micro-CHP electric output.

Whilst solving the energy hub optimization problem, the control variables mentioned in (3-7) at each time step must satisfy all constraints illustrated above. Therefore, the multi-hub problem is necessarily a multi-period optimization containing a large number of variables and constraints. For instance, the 3-hub scenario investigated in this paper

contains 504 variables and 480 constraints. Clearly, the optimization problem becomes more complicated as the number of hubs increases. Additionally, it was concluded by graphing the functions associated with the battery lifetime cost ((3-A1) to (3-A6) in the Appendix) that these fail to satisfy the definition of a convex problem. Therefore, the optimization problem is a non-convex problem.

3.4 Decomposed PSO

3.4.1. PSO

Particle swarm optimization was proposed based on the behaviour of flocking birds or schools of fish [26]. Each particle describes a solution to a problem that can be quantitatively measured by its performance. At each iteration of the optimization, the particles trend towards the global minimum based on two factors, the best performance of any particle ever achieved P_i^g and the best position P_i^k of particle *i*. The PSO working mechanism is illustrated by means of mathematical formulations in (3-9) and (3-10):

The position X of a particle i at iteration $k+1$ is

$$X_i^{k+1} = X_i^k + V_i^{k+1} \tag{3-9}$$

V_i^{k+1} indicates the new velocity for particle i at $k+1$ iteration. It is derived as:

$$V_i^{k+1} = \omega V_i^k + c_1 r_1 \left(P_i^k - X_i^k\right) + c_2 r_2 \left(P_i^g - X_i^k\right) \tag{3-10}$$

r_1 and r_2 represent two random numbers between 0 and 1. c_1 and c_2 are the cognitive parameter and social parameter, the two weighting factors that model the confidence of the current particle in itself and in the swarm [27]. Parameter ω is the inertia weight, a coefficient applied to particle velocity, which influences the PSO convergence behaviour by increasing the distance the particle will travel from its previous position.

At the beginning of the optimization, the PSO algorithm firstly generates a population of particles randomly over the search space, where the position of each particle represents a solution. The particles are evaluated by applying the solution to the problem to obtain a fitness score for each particle. P_i^g and P_i^k can therefore be found. All particles are updated using (3-9) and (3-10) at each iteration, with this process

repeated until the stopping criteria is met.

When conventional PSO is used on highly constrained and non-convex optimization problems, the particles tend to fall into infeasible regions during initialization and updating. This problem can be solved by utilizing the sequential quadratic programming (SQP) algorithm [28]. The SQP algorithm solves an optimization problem by seeking the Karush-Kuhn-Tucker first order optimally condition, which can find a local minimum near the starting point. In other words, the position of an infeasible particle is taken as the starting point and then by utilizing the SQP algorithm, a feasible particle can be found nearby that replaces the infeasible one.

3.4.2. Decomposition Technique

The multi-energy hub optimization is a multi-period problem with many variables. Since the main purposes of storage are to time-shift renewably generated energy to meet loads and arbitrage against varying tariffs, its operational management must, therefore, consider the energy price, renewable generation, and converter working status to schedule its operational state in each time step, i.e. charging, discharging or on standby. The operation of storage in the current time step will influence the operation in other time steps and thus a multi-period optimization approach is necessary. The complexity of the problem requires significant computation time and may compromise optimization accuracy. However, if the optimal operation of the complex time-dependent device (such as storage) is known in advance, other control variables in (3-7) can then be obtained by applying numerical methods in each time step.

The stochastic nature of PSO is capable of solving non-convex problems with non-continuous search spaces, whilst the numerical function 'interior-point' can handle non-linear constrained problems with acceptable performance and computation time, so the decomposition technique here harnesses advantages of both methods. In general, during the generating and updating of all particles, only the control information of every battery is included in each particle (i.e. charging and discharging energy). For the optimization of a three-hub system containing three batteries over 24 time steps, there are totally 144 variables included in each particle. Whilst the operations of remaining elements in the energy hub system are derived using the interior point method based on the information in each particle, and the fitness score of each particle can therefore be

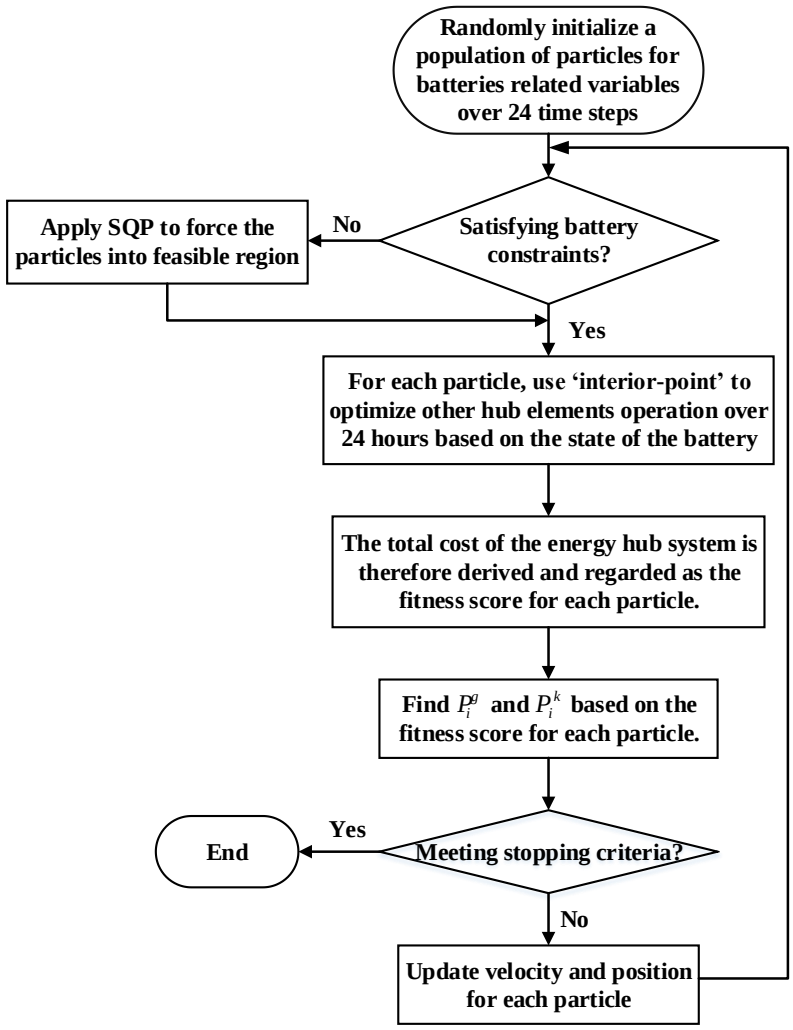

Fig. 3-4.The working flow of the decomposition technique

calculated. The procedure is shown in Fig. 3-4 and can be described thusly:

1) Randomly initialize a population of particles, where the position of each particle denotes the solution of two variables over 24 hours: charging energy and discharging energy. The variables should be generated within the boundary set by the optimization, including the maximum charging/discharging energy, minimum and maximum battery capacity or SOC as indicated in (8h), (8i) and (8g). The magnitude of charging power at each step multiplied by discharging power should be equal to zero, meaning the battery can only either be charging, discharging, or on standby. This is achieved by applying SQP algorithm to find a feasible point satisfying above conditions near the initial point.

2) For each time step, the charging and discharging energy can be regarded as the extra output and input for energy hub system without a battery. Therefore, the operations of the battery between each time step can be decoupled from each other.

3) The 'interior-point' method is then applied to optimize the operation over the whole time period based on electricity load, heat load, renewable energy generation, extra input, and extra output. The optimized total system cost over 24 time steps is then derived. Meanwhile, the battery lifetime cost related to the battery working status over 24 time steps is calculated. The fitness score of each particle is thus the total operational cost from both battery operation and optimized overall hub management.

4) Find P_i^g and P_i^k, see if the best particle satisfies the stopping criteria. If the stopping criteria is met, then the solution of the best particle is the final solution to the optimization. If not, update the velocities and positions for particles based on (9) and (10).

5) Repeat steps 2 to 4 until the stopping criteria is met.

The decomposition technique decouples the optimization for batteries and other hub elements. The optimal operations of batteries are derived based on the PSO, the optimization for other hub elements is obtained by applying the interior-point method. The efficiency of the algorithm is increased, and the computation time is therefore reduced.

The decomposed-PSO algorithm is achieved based on modification of the open source PSO MATLAB routine developed by ETH Zurich [28]. The decomposed method is illustrated in terms of the optimization for the two-hub system in next section.

3.5 Demonstration

This section applies the novel PSO algorithm to two multi energy-hub systems across two use scenarios. The first part introduces a two-hub system, which is simple enough such that a theoretical minimum may be analytically calculated for benchmarking the performance of the PSO algorithm. The second part investigates a three-hub system with converters and batteries illustrated in section II. The potential application of the decomposition technique is discussed based on the computation speed and operation results in the third part.

3.5.1. Two-hub system

To demonstrate the effectiveness of the decomposed-optimization in finding the global minimum, a 2-hub system optimization problem is proposed and investigated. The battery lifetime cost is excluded in the problem, hence the theoretical minimum can be derived analytically, and the performance of the decomposition technique can be evaluated. The 2-hub system with energy sharing is shown in Fig. 3-2.

Each of the two hubs represents a residential house. The load and generation profile is assumed to be a winter day in the UK based on [29] and [30]. A battery is equipped in hub 1, with charging efficiency and discharging efficiency assumed to be 95%, and standby losses assumed to be negligible (justified because the self-discharge rate on diurnal timescales is very small). The battery minimum and maximum capacities are 4 kWh and 17.376 kWh. To verify that the redundant energy within each hub is adequately utilized by the energy sharing between hubs, the different performance of converters is assumed in each hub. A ground source heat pump with CoP of 3.0 and another heat pump with CoP of 4.2 are included in hub 1 and hub 2 respectively. Time-of-use electricity tariffs (derived from [31]) are assumed, in this case shown in Fig. 3-5. The optimization problem statements refer to (3-8).

1) Validation

The benchmark approach to calculate the global minimum of the two-hub system over 24 hours is shown in this section. The total energy cost, *TC*, for the two hubs is given in (3-11).

$$TC = \sum_{t=1}^{24}\left[P_{ele,1}(t) + P_{ele,2}(t) + E_{sh}(t)\right] \cdot \Pi_{ele}(t) \tag{3-11}$$

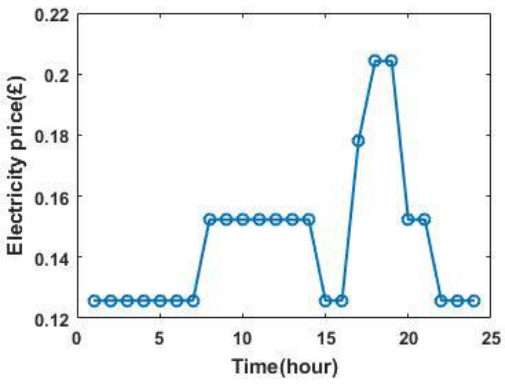

Fig. 3-5.The time-of-use tariffs against 24 hours.

$P_{ele,1}(t)$ and $P_{ele,2}(t)$ indicate the electricity consumption including the power input to the heat pump and electricity load of hub 1 and hub 2 respectively. $E_{sh}(t)$ represents the electricity exchange between hubs and energy storage. The optimization strategy is as follows: the consumed electricity is utilized to support the ground source heat pump to generate heat, and meet the electricity load. According to equation (3-3), the electricity requirement for heat can be reduced by exploiting the high CoP of heat pumps. Since heat between hubs is transferable, the heat pump in hub 2 (CoP of 4.2) is applied to support the heat load for two hubs at each time step.

In addition to selecting high performance heating converters, storage can also be utilized to reduce energy cost. Based on achieving the objective of reducing the energy cost for the whole system, the operation of the battery should follow the broad strategy of charging during low tariffs and discharging during high tariffs. The battery needs to be fully charged during periods 1-7 since the electricity prices at these times are lowest. For periods 17-19, the prices are the highest, hence the storage needs to discharge within the maximum discharging power. The price from 15-16 is the lowest, hence some energy could be charged during 8-14 and recharge during 15-16 only if the remaining power at the end of 16 is capable of meeting the demand during 17-19. After considering the maximum discharging/charging power (3kW), the battery operation at each time step can be derived and indicated in table 3-1. Based on the operation of storage and heat pump, the total energy cost, *TC*, can be calculated as £6.73 from (3-11).

Table 3-1.THE OPTIMAL OPERATIONS FOR BATTERY

Period	Charging energy(kWh)	Discharging energy(kWh)	Battery state of charge(kWh)
1-7	14.08	0	17.376
8-14	0	6	11.376
15-16	6	0	17.076
17	0	2.646	14.429
18-19	0	5.78	8.649
20-21	0	4.6494	4
22-24	0	0	4

2) First scenario

The 2-hub system optimization problem is solved by the decomposed PSO method on

Matlab, which is running on a 3.40 GHz Intel i5 quad core desktop with 8 GB of RAM. The procedures of implementing decomposed PSO is illustrated as follows:

1) A group of particles is generated, each particle contains each battery's charging and discharging energy over 24 time steps, which is randomly generated within the boundary set by optimization. Hence there are totally 48 variables contained in one particle. The charging and discharging energy in first three steps in the first particle is shown for example: 2.65 and 0.21, 1.24 and 0.11, 2.15, 0.02.

2) The SQP method is then applied to find a feasible point near the randomly generated point based on the battery constraints, in this case a feasible point indicates that the battery has to be either charging, discharging, or standby. The 6 variables in procedure 1 turns to be: 2.71 and 0, 1.21 and 0, 2.10 and 0.

3) The battery scheduling is then abstracted from the individual time step optimization, in that the charging and discharging power of the battery at each time step are regarded as extra energy exported/imported from/to the hub. Given the battery information and the constraints within the energy hub system, the 'interior-point' method is applied to optimally decide the variables over 24 time steps, such as the value of energy carrier injection to the hub, dispatch factor, etc. The total energy cost over whole time horizon can therefore be calculated, and regarded as the fitness score of the related particle.

4) The speed of each particle is generated based on equation (10), the PSO keeps updating particles' positions and speeds until the stopping criteria is met.

The optimization results of total energy cost over 24 hours are shown in table 3-2 over a range of different particle population sizes.

Table 3-2.OPTIMIZATION RESULTS FOR 2-HUB SYSTEM

Particle population	Optimization results(£)	Computation time(s)
10	6.783	106
20	6.776	250
30	6.737	271
40	6.733	260
50	6.752	419

As shown from table 3-2, the performance of the algorithm improves when the particle population increases. However, the optimization results do not consistently increase with increasing particle population due to the stochastic nature of PSO. The best result is £6.73, which demonstrates that the algorithm is capable of reaching very close to the global minimum for a highly-constrained, non-linear problem.

For comparison, when the storage is not present and energy sharing is unavailable between hubs, the energy demand for each hub can only be met with its own converters, and the total minimum energy cost is calculated as £7.84. When storage is not equipped with the system and energy sharing is available between hubs, the optimization problem is transformed to an optimal flow problem at each time step. The optimization can be solved by applying the 'interior-point' method, and the theoretical minimum energy cost is derived as £7.32. Compared with the 2-hub system without energy sharing and storage, the optimization achieves an energy cost saving of 14.14%.

To demonstrate the accuracy of decomposed-PSO, the optimal operation of the battery at each time step derived from a 30 particle optimization is compared with the battery operation derived from the benchmark approach, and is shown in Fig. 3-6. It can be observed that the optimized battery operations derived from the decomposition technique closely approximate to the operations obtained from the benchmark theoretical minimum.

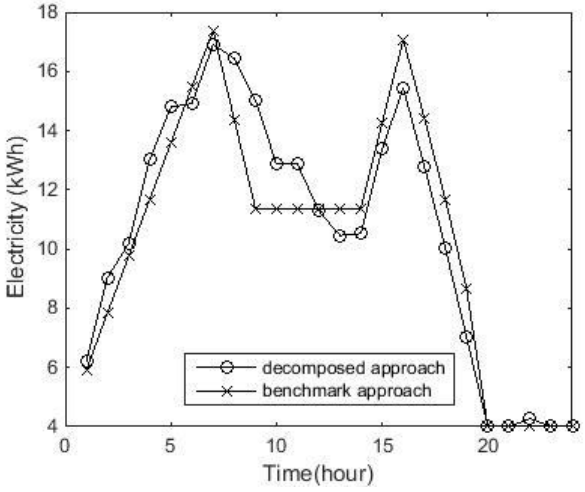

Fig. 3-6.The battery operations against 24 hours.

3.5.2. Three-hub system

A three-hub system is presented and shown in Fig. 3-7. The three hubs respectively contain a battery with sizes of 5.3 kWh, 10.5 kWh and 21 kWh, the related battery parameters can be found in [25]. Different heating converters including GSHP, micro-CHP, and gas boiler are equipped in the three hubs. The CoP of GSHP is selected as 4, the constraint parameters of micro-CHP are adopted from [24, 32], where the electric efficiency is 0.33, the thermal efficiency is 0.57, the ramp rate is 0.06 kW/min. The efficiency of the gas boiler is non-linear against the gas input, and is illustrated in section II. The electricity load $L_{ele}(t)$ and heat load $L_{th}(t)$ for each hub are satisfied by optimally scheduling the utilization of all heating converters and batteries.

The gas price is assumed to be constant at £0.03 per kWh over all 24 time steps. The electricity price is varied every hour in this case to reflect the time-of-use electricity tariffs all retailers will likely adopt in the near future. The variant electricity price against 24 hours is derived from [31] and shown in Fig. 3-8, with average half hourly tariffs used to produce an hourly pricing granularity. (These energy costs are typical in the UK at time of writing, but future prices will clearly yield different overall costs than the results shown in this paper.) The same method of modelling electricity demand and

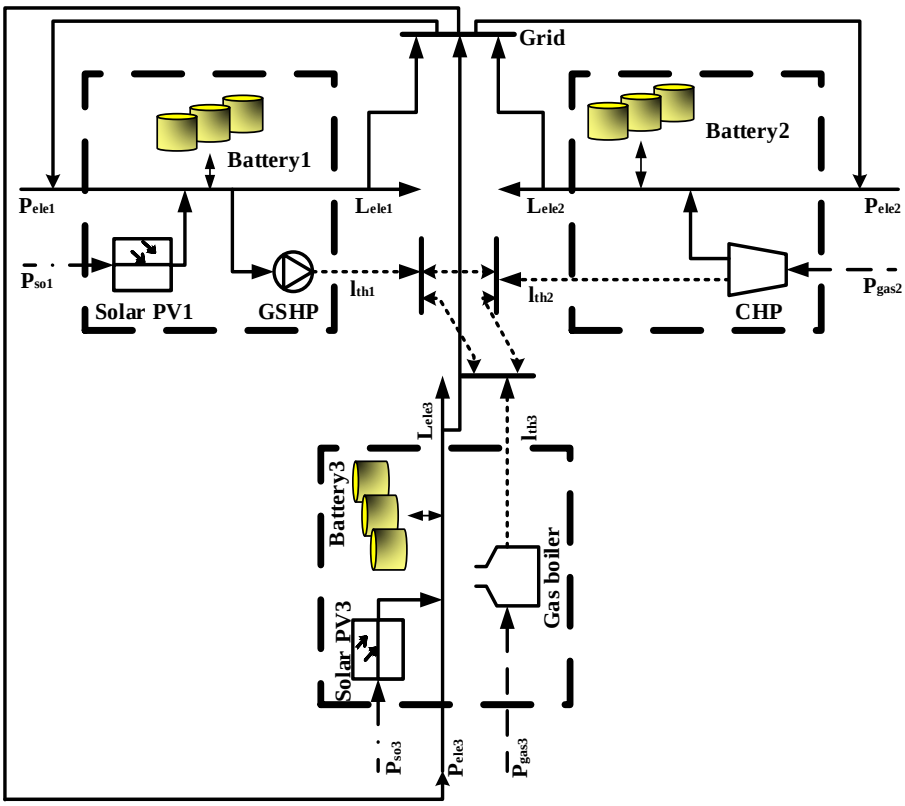

Fig. 3-7.Three-hub system with energy sharing available between hubs.

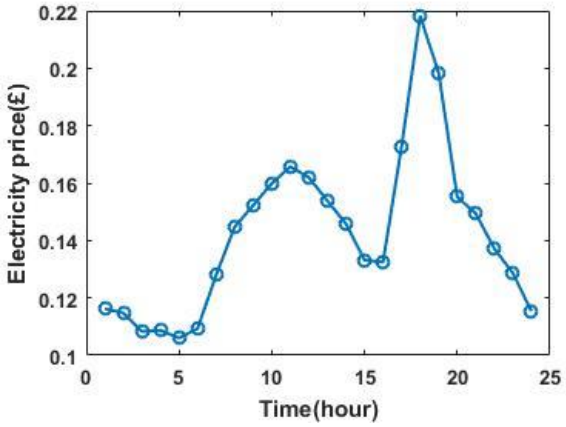

Fig. 3-8.The variant tariffs of electricity against 24 hours.

heat demand used in [31] is employed here. Additionally, the solar PV generations $P_{SO}(t)$ are simulated with the Photovoltaic Geographical Information System [33]. To demonstrate the superiority of the decomposition technique, the conventional PSO is applied to solve this optimization problem. The comparison between the decomposition technique and conventional PSO is illustrated by convergence behaviour and computation time.

1) Second Scenario

In this scenario, the performance between the conventional PSO and the decomposition technique in solving the optimization problem above is compared.

Since the time spent on conventional PSO increases massively with rising particle population size, a modest population of 10 particles was applied to both conventional PSO and decomposition technique to observe the convergence behaviour, and the

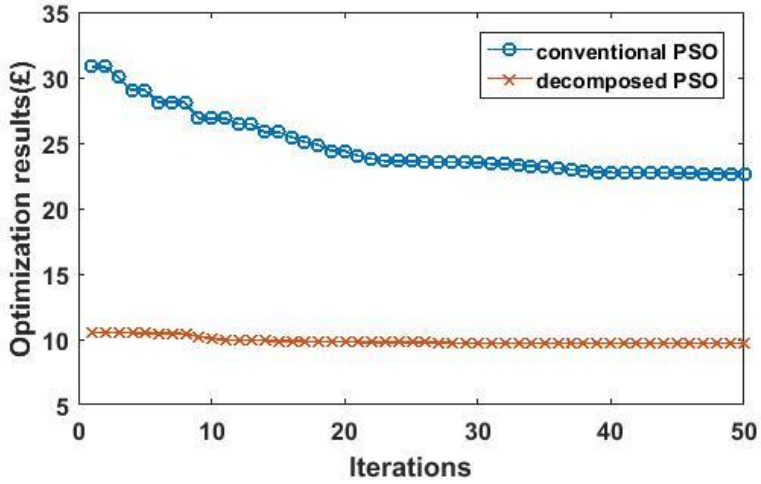

Fig. 3-9.Convergence behaviours of conventional PSO and decomposition technique

comparison is shown in Fig. 3-9. The blue circles and the orange crosses represent the performance of applying conventional PSO and the decomposition technique respectively.

As indicated in Fig. 3-9, the objective function value by applying decomposed PSO plateaus from between 15 and 20 iterations onwards, for conventional PSO, the objective function value trends to flat around 35 iterations. Under the conservative stall generations (50) and stall tolerance settings (£0.000001), the conventional PSO optimization converges at the 162nd iteration after 8970 s, and the optimization result is £22.61. The decomposition technique converges at 143rd iteration after 121 s, and achieves a much improved optimization result of £9.30.

The optimized battery operations for hub 2, derived from two optimization methods, are shown in Fig. 3-10 in terms of battery SOC. The pink circles and orange crosses represent the battery SOC at each time step optimized by conventional PSO and decomposed PSO, and the blue dotted line indicates the electricity price variation over 24 time steps. From the perspective of optimally exploiting the storage to save energy cost, both of the two methods achieve the optimization by charging storage during the low tariff period and recharging during the high tariff period. It could be concluded from Fig. 3-10 that the electricity tariff experiences two peak values over 24 time steps. The two peak values appear at step 11 and step 18. Both of the optimization methods indicate that the storage is discharging since the first peak electricity price from step 9 to 10. Nevertheless, the storage operation derived from the decomposition technique

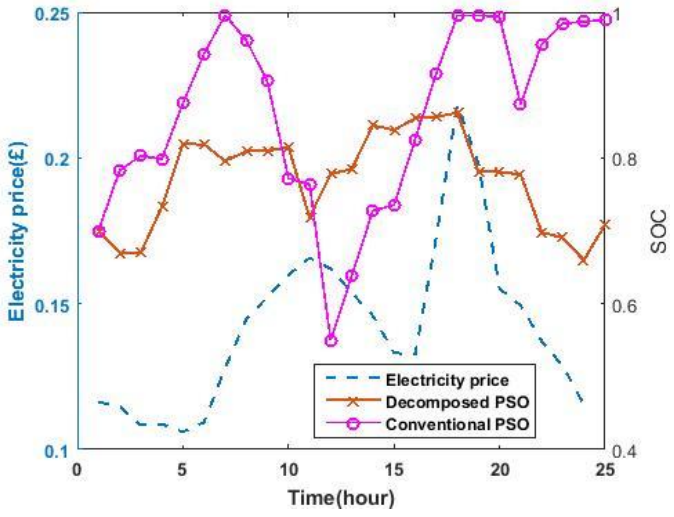

Fig. 3-10.The optimized battery operations by applying conventional PSO and decomposition technique.

discharges around the first peak electricity price from step 10 to 11, and then rapidly charges from step 11 to 18 to prepare for the second peak electricity price. With conventional PSO, the storage barely discharges at the first peak electricity price. Thus comparing with the conventional PSO, the decomposition technique can better optimize the storage operation and further reach the optimum. However, it could be derived from Fig. 3-10 that the battery scheduling operations derived from both optimization methods fail to fully discharge around the peak tariff period, which may lead to further cost saving. This is due to the low number of particles that degrades the performance of the optimization.

2) Impact of Battery Lifetime Cost

To investigate the influence of battery lifetime cost in the objective function on battery scheduling, the optimization is run when considering battery lifetime and compared to when the battery lifetime consideration is omitted. 30 to 50 particles used in decomposed PSO reach a result very close to the global minimum for the 3-hub optimization based on extensive experimentation. Hence 50 particles are applied in the optimization. The SOC of three batteries over 24 time steps when considering battery lifetime and compared with excluding the battery lifetime in the objective function are shown in Fig. 3-11 and Fig. 3-12 respectively. The green, blue, and red lines represent the variation of SOC of battery in hub 1, 2, and 3 over 24 hours respectively.

The total energy costs for these two optimizations are £9.0268 and £9.0070, the battery lifetime costs are £0.0331 and £0.0728. Clearly when omitting the battery lifetime cost

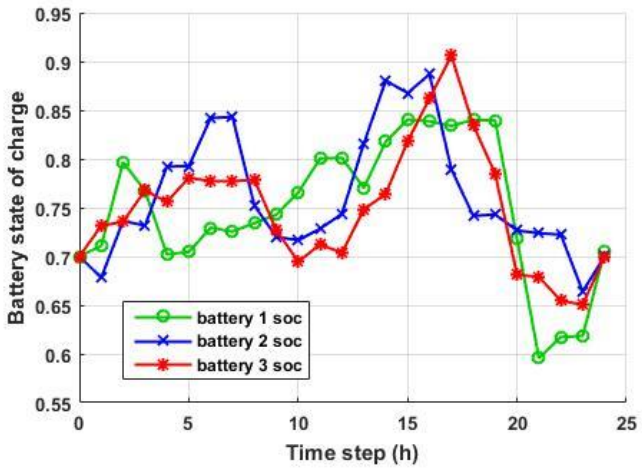

Fig. 3-11.Battery state of charge over 24 time steps derived from the optimization with the battery lifetime cost considered

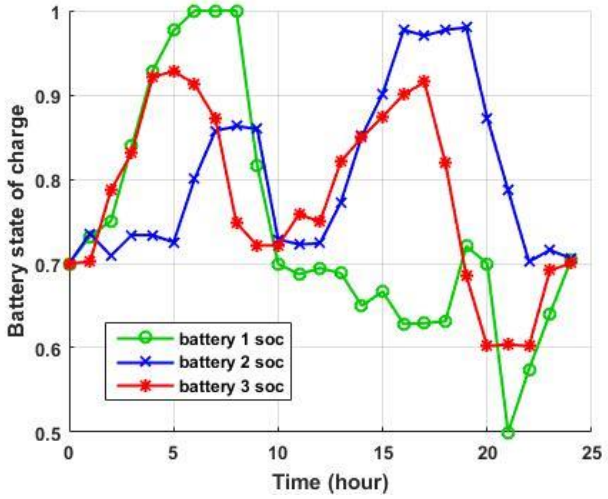

Fig. 3-12.Battery state of charge over 24 time steps derived from the optimization without considering the battery lifetime cost

the batteries are exploited to yield more energy saving. However, the battery lifetime cost is higher, and thus the system total cost is higher (sum of energy cost and battery lifetime cost) at £9.0798, compared to £9.0599 when battery lifetime is considered. When the battery lifetime is not optimized, the variation of SOC is broader, for example, the battery in hub 1 even varies between 50% and 100%. When the battery lifetime is considered in the objective function, the SOC of three batteries all varies from approximately 60% to 90%. It may be concluded from the calculation of battery lifetime cost that the cost increases when the battery is operated during lower SOCs. Hence the battery is better operated at high SOCs to avoid unnecessary degradation of battery lifetime.

3) Applications

The optimization problem uses a fixed time step of one hour. To allow an online, receding time horizon implementation, the optimization for scheduling the system of energy hubs must be completed within the time step. Therefore, the size of the system of energy hubs that the decomposition technique is capable of optimizing within one hour is investigated. With the same modelling method applied, a 5-hub system and an 11-hub system are simulated with the same level of complexity to the 3-hub system investigated in section V. The decomposition technique is applied with 30 particles to 3, 5, and 11 hub systems. The computation time for solving these three cases are 270 s, 779 s, and 1011 s respectively.

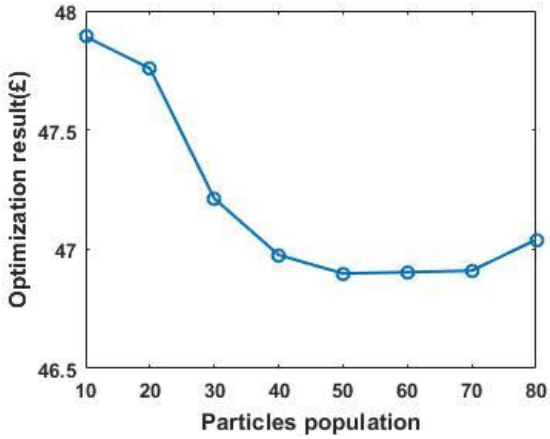

Fig. 3-14. Optimization results against different amount of particles

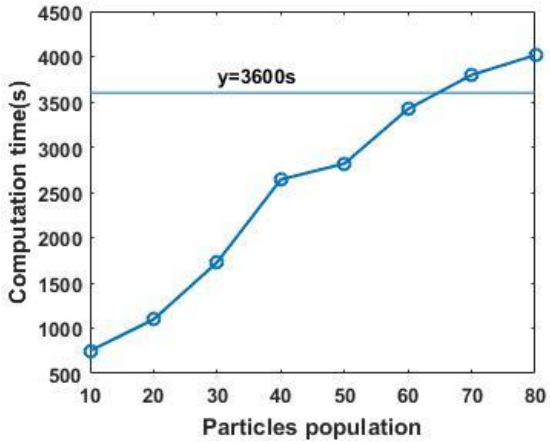

Fig. 3-13. Computation time against different amount of particles

The decomposition technique was tested with different numbers of particles, for the 11-hub system, and the optimization results and computation time are shown in Fig. 3-13 and Fig. 3-14 respectively. In Fig. 3-14 'y=3600 s' was drawn as a reference which indicates the time budget for a receding time horizon implementation with a time step of 1 hour.

It could be observed from Fig. 3-13 that the optimization results generally plateau at approximately £46.89 when the population of particles applied in PSO is 40. Increasing population size beyond this does not increase system benefit. In contrast, the computation time increases approximately linearly as the number of particles increases. The computation time of implementing PSO with 60 particles on this problem is 3421 s representing the best trade-off between computation time and performance for this particular system.

With a receding time horizon implementation, operations are calculated up to a certain time horizon, for which all load data is predicted in advance, but only the optimized operation for the next time step is implemented. In the next time step the time horizon is increased by one and the process is repeated. This makes the best use of load prediction data on the basis that the predicated data closer to the current time step is likely to be more accurate. On the other hand, a fixed time horizon approach may be used for larger multi-hub systems that are more computationally intensive to solve.

3.6 Conclusion

This paper presents a decomposed method that hybridises particle swarm optimization and the 'interior point' method to solve the optimal scheduling problem for a multi-energy hub system with the consideration of battery lifetime. For a 3 residential energy hub system, the utilization of battery varies from 60% to 90% to avoid unnecessary degradation of the battery lifetime, and the system thus benefits long term through increased battery lifetimes. The optimization demonstrably achieves very near the global minimum. This method can be applied in a receding time horizon approach for solving a practical system of size around 10 hubs, always leveraging the most up to date load prediction. For a larger system with more storage technologies, a fixed time horizon approach can be used, or the time step may be increased or the time horizon reduced. From the view of energy management, the storage operation is more accurate when the predicted horizon is longer and generally speaking, the time step smaller, necessitating a trade-off between optimization performance and computation time. Alternatively, the computation time could be shortened using high performance hardware or cloud computing.

3.7 Appendix

3.7.1 Calculation of Battery Lifetime Cost

The life loss of a battery $L_{loss}(t)$ over a certain time period *t* can be expressed as:

$$L_{loss}(t) = \frac{A_c(t)}{A_{total}} \tag{3-A1}$$

Where $A_c(t)$ is the effective cumulative Ah throughput during the use of battery and A_{total} is the total cumulative Ah throughput in the life cycle. The value of A_{total} is

selected as 390Q effective Ah over its lifetime [25], which Q Ah is the capacity of a battery. $A_c(t)$ is formulated in (3-A2).

$$A_c(t) = \lambda_{soc} \cdot A'_c(t) \tag{3-A2}$$

λ_{soc} is the effective weighting factor. The relation between λ_{soc} and battery state of charge (SOC) is estimated as a linear formulation based on [25] and expressed in (3-A3).

$$\lambda_{soc} = \begin{cases} -1.5 \cdot SOC + 2.05 & if\ SOC\ \geq 50\% \\ 1.3 & if\ SOC < 50\% \end{cases} \tag{3-A3}$$

$A'_c(t)$ indicates the actual Ah throughput. Assuming the SOC of the battery varies from a to b in a certain time period, $A'_c(t)$ and $A_c(t)$ can be expressed in terms of a and b shown in (3-A4) and (3-A5) respectively.

$$A'_c(t) = (a - b) \cdot Q \tag{3-A4}$$

$$A_c(t) = \begin{cases} \int_b^a \lambda_{soc} dsoc \cdot A'_c(t) & if\ a\ \geq b \\ 0 & if\ a < b \end{cases} \tag{3-A5}$$

The life loss cost $C_{bl}(t)$ is calculated with (3-A6).

$$C_{bl}(t) = L_{loss}(t) \cdot C_{init-bat} \tag{3-A6}$$

$C_{init-bat}$ represents the initial investment cost of battery, and it is assumed to be 0.534 £/Ah [34] multiply by the battery capacity. The life loss cost can thus be calculated with (3-A1) to (3-A6).

3.8 Chapter Summary

This chapter illustrates the mathematical formulation of the optimisation problem for energy hub system under steady state. It presents the mathematical formulations for energy hub system elements including energy converters, energy storages, and transmission networks. Moreover, it also considers the non-constant efficiency of some energy converters, hence allows a more practical optimal operations compared with previous researches where the converter efficiency is assumed to be constant. The battery lifetime cost accounts for the battery lifetime loss in each time's charging and discharging, and it is included in the objective function in order to utilise the battery for a long term use and avoid the unnecessary degradation.

Most importantly, a novel decomposed technique is proposed to optimise the interconnected energy hub system, which is formulated as a multi-period non-convex problem. The optimisation algorithm is hybridised by PSO and interior-point method, it decouples the complicated energy hub problem into sub-problem and separately resolved by PSO and interior-point method. The optimisation technique effectively improves the optimisation results and computational speed compared with the conventional PSO. Additionally, the method is demonstrated to be fast enough to allow an online, receding time horizon implementation.

Chapter 4

Chance-Constrained Optimization for Multi Energy Hub Systems in a Smart City

This chapter proposes to utilise chance-constrained programming to analyse and resolve the energy hub optimisation problem with uncertain renewable generation, the energy flows between adjacent hubs are innovatively restricted by chance constraints.

Chapter Overview

Chapter 3 presents the optimal energy management within the context of interconnected energy hub system. The optimisation is assumed to be carry out for steady-state operation, where the renewable power generations, loads, and energy prices are assumed to be perfectly known over the optimisation horizon. However, uncertainty always existed among them, the renewable power generations such as solar PV and wind turbine can be easily affected by the weather conditions, the energy hub loads are significantly dependent on the customer behaviour. The uncertain weather conditions and customer behaviour could lead to the mathematical difference between the forecast values and realistic values. The overestimate of uncertain variables causes prohibitively high operational cost, and the underestimate of uncertain variables can cause the violation of safety constraints, which potentially damages the power system. Therefore, appropriate modelling techniques should be employed to simulate the effects of uncertain variables to the energy management problem.

As illustrated in Section 2.3, probabilistic approaches have been applied in previous energy hub optimisation problem to simulate the uncertainties. Monte Carlo methods and other scenario generation methods are applied to generate scenarios for uncertain variables, the probabilistic energy hub optimisation problem can therefore be resolved by deterministically optimising each scenario and integrating the results. However, the probabilistic programming suffers from the huge computational burden due to the large number of scenarios generated by MCS, the scenario reduction methods can mitigate the computational burden, but may fail to completely reflect the stochastic nature of uncertain variables.

To address the above issues, this chapter proposes to apply chance-constrained programming to optimise the probabilistic interconnected energy hub system. Based on the fact that the temporary overloading is tolerable for real energy networks, the power and gas flows between adjacent hubs are restricted by chance constraints with a given probability level. Chance-constrained programming can then be solved by satisfying both the deterministic and chance constraints. In contrast to scenario-based methods, the effects of uncertain elements are reflected by chance constraints, and the stochastic characteristics of uncertainty can be fully considered. The contributions of this chapter are summarised as follows:

iv) Chance-constrained programming is applied to resolve the energy hub optimisation problem with uncertainty for the first time.

v) Cornish Fisher Expansion method is employed to mathematically convert chance constraints into deterministic constraints.

vi) The impact of chance constraints is extensively investigated, the results from chance-constrained programming are compared with the results from using deterministic approach and scenario-based method.

Statement of Authorship

<table>
<tr><th colspan="4">This declaration concerns the article entitled:</th></tr>
<tr><td colspan="4">Chance-Constrained Optimization for Multi Energy Hub Systems in a Smart City</td></tr>
<tr><td colspan="4">Publication status: Accepted</td></tr>
<tr><td>Publication details (reference)</td><td colspan="3">Huo, D., Gu, C., Ma, K., Wei, W., Xiang, Y. & Le Blond, S. “Chance-Constrained Optimization for Multi Energy Hub Systems in a Smart City” 21 Jul 2018 (Accepted/In press) In : IEEE Transactions on Industrial Electronics. 10 p.</td></tr>
<tr><td>Candidate’s contribution to the paper</td><td colspan="3">The candidate and the second author jointly proposed the idea of the paper, and they designed the methodology. The candidate executed all the coding to derive the experimental results. Other authors helped the candidate with the design of case studies, format of the paper, and improvement of academic writing. The percentage of the candidate did compared with the whole work is indicated as follows:
Formulation of ideas: 70%
Design of methodology: 80%
Simulation work: 90%
Presentation of data in journal format: 80%</td></tr>
<tr><td>Statement from candidate</td><td colspan="3">This paper reports on original research I conducted during the period of my Higher Degree by Research candidature.</td></tr>
<tr><td>Signed</td><td>Da Huo</td><td>Date</td><td>01/08/2018</td></tr>
</table>

4.1 Abstract

The Energy Hub is a powerful conceptualisation of how to acquire, convert, and distribute energy resources in the smart city. However, uncertainties such as intermittent renewable energy injection present challenges to energy hub optimization. This paper solves the optimal energy flow of adjacent energy hubs to minimize the energy costs by utilizing the flexibility of energy resources in a smart city with uncertain renewable generation. It innovatively models the power and gas flows between hubs using chance constraints, thus permitting the temporary overloading acceptable on real energy networks. This novelty not only ensures system security but also helps reduce or defer network investment. By restricting the probability of chance constraints over a specific level, the energy hub optimization is formulated as a multi-period stochastic problem with the total generation cost as the objective. Cornish-Fisher Expansion is utilized to incorporate the chance constraints into the optimization, which transforms the stochastic problem into a deterministic problem. The interior-point method is then applied to resolve the developed model. The proposed chance-constrained optimization is demonstrated on a 3-hub system and results extensively illustrate the impact of chance constraints on power and gas flows. This work can benefit energy hub operators by maximizing renewable energy penetration at the lowest cost in a smart city.

4.2 Introduction

A smart energy city enables flexible management of energy infrastructure to efficiently meet demand. Within a smart energy city, the energy hub concept can coordinate multiple energy carriers to optimally satisfy demand [1-5]. Energy hubs could increase energy system flexibility and exploit the unused capacity of various energy carriers. Energy hubs have been applied to many energy system planning and operation problems in smart energy cities, such as demand response [6], system operations [7], and optimal power flows [8]. Buildings or communities in the smart energy city can be treated as energy hubs [1, 9] and the energy flows between them can be optimally scheduled to minimize energy transportation and exploitation costs, minimizing the energy costs of a smart energy city. The optimal energy flow of energy hub involves optimizing electricity and other carriers, such as natural gas and heat, which can be formulated as a multi-period problem. In [10-13], the optimization for multi-carrier systems including adjustment of the energy flows between hubs is investigated.

In the aforementioned literature, the steady-state model of energy hub systems is utilized and optimization problems are all formulated as deterministic models. In reality, uncertainties always present in energy management, due to customer load and renewable energy. System thermal and voltage constraints may be temporarily violated if uncertain variables are underestimated, otherwise system operational cost will be prohibitively high when the impact of uncertain variables is overestimated [14]. Therefore, modelling and estimation of uncertain variables are important in optimizing energy hubs.

Uncertainty has been included in energy hub optimization in previous research. In [5, 15, 16], Monte Carlo simulation is applied to model the uncertain inputs but the optimization requires much computational effort due to the large number of scenarios. A scenario reduction method is applied to minimise the number of scenarios in [17, 18]. Other methods including two-point estimate method (2PEM), the point estimate method, and the improved 2PEM method have been applied in [19-21] respectively to model renewable generation in energy hub systems. The reality is that a certain number of scenarios may not completely represent the stochastic nature of uncertain variables, causing the results to be inaccurate.

In contrast to scenario-based methods, chance-constrained programming (CCP) is a consistently robust and reliable approach to resolve uncertainty [22]. Each chance constraint is modelled by a boundary, the acceptable probability of constraint violation. The CCP optimization is then resolved to meet both normal constraints and chance constraints. Whilst the stochastic nature of uncertain elements can cause occasional system overloading, investment to meet these rare stress events could be prohibitively expensive. However, in reality, some temporary overloading is tolerable in both gas and electricity networks, and CCP is, therefore, a promising approach to this problem. CCP has been applied to power system operating problems, including demand response, optimal power flow, and unit commitment [23], [24], and [25]. However, it has not been applied to the energy hub optimization problem.

This paper formulates a novel, chance-constrained approach to solve the optimal energy flows for multiple energy hubs with uncertain renewable generation. The uncertain elements of solar and wind generations are simulated by fitting historical data to specific distributions. The power and gas flows along branches between adjacent hubs are modelled as chance constraints at specific probability levels. The optimization thus

becomes a non-convex stochastic problem. In solving the CCP problem, the non-convex CCP problem is converted into a convex problem and linear programming is applied in [26]. The back-mapping approach is utilized in [22, 24], where the probability of chance constraints is derived by mapping them back to the uncertainty variables' distributions. Non-linear programming is then applied to solve the optimization problem. A sample average approximation method is developed in [27] to resolve chance-constrained problems.

This paper utilizes the Cornish-Fisher Expansion method to translate chance constraints into deterministic constraints so that deterministic programming can be applied. Because of its flexibility and robustness [1], the interior point method is thus used to solve the developed model. The CCP enables energy hub system reliability to be realized above a specific level with low costs by restricting the probability of the chance constraints over the predefined level. This work can benefit energy hub operators by maximizing renewable energy penetration at the lowest cost in a smart city.

The main contributions of the paper are as follows: i) compared with [24] where the load uncertainties are modelled as random inputs in multiple hub optimization, the uncertainty of renewable generation is considered in multi-hub optimization; ii) in contrast to only treating the power flows between buses as chance constraints [24], both power and gas flows between adjacent hubs are restricted by chance constraints; iii) the CCP is incorporated into the energy hub optimization, which can better model the uncertainty characteristics compared with the scenario generation methods in [17-21] and reduce the huge computational burden caused in [5, 15, 16]; iv) in contrast to the approaches in [22, 24, 26, 27] for solving CCP, the chance constraints are mathematically converted into deterministic constraints through Cornish Fisher Expansion, and thus the deterministic programming is applied to solve CCP; v) the impact of chance constraints on energy hub system optimization is extensively investigated; vi) the comparison between CCP and deterministic approaches is quantified by using the value of expected value of perfect information (EVPI) and value of the stochastic solution (VSS) .

The remainder of the paper is organised as follows: the mathematical formulations of the energy hub system with the power and gas network are illustrated in section II. The CCP problem formulation and the methodology of implementing the CCP for the system optimization are introduced in section III. Section IV introduces the concepts of

EVPI and VSS. Section V discusses different case studies and related results, and section VI concludes the paper.

4.3 Energy Hub System Modelling

The mathematical model of the energy hub system is illustrated in this section. The equality constraints are based on the law of energy conservation between hubs. The inequality constraints arise from safe operational limits such as maximum converter output and maximum power injection to a single hub.

4.3.1. Energy Hub

Both electricity and heat demand can be satisfied by adjusting different energy converters in hubs according to optimization objectives. The energy hub used in this paper is equipped with energy converters, namely Combined Heat and Power (CHP), Ground Source Heat Pump (GSHP), and Gas Furnace (GF). CHP simultaneously generates heat and power, GF combusts gas to generate heat. GSHP coverts power to heat by extracting heat from the ground, and it is widely used in Europe and American due to its high efficiency.

The relations between converter inputs and outputs for CHP, GSHP, and GF are shown in (4-1), (4-2), and (4-3) respectively. η_e and η_{gh} indicate the electric and thermal efficiency of CHP. The efficiency of GSHP is the coefficient of performance (COP). η_F is the efficiency of GF. P_{CHP}, P_{HP}, and P_{GF} represent the energy injection to CHP, GSHP, and GF. The electric output $P_{CHP,Eout}$ and heat output $P_{CHP,Hout}$ of CHP are quantified by (4-1a) and (4-1b), the outputs of GSHP $P_{HP,out}(t)$ and GF $P_{GF,out}(t)$ are calculated by (4-2) and (4-3).

$$P_{CHP,Eout}(t) = \eta_e \cdot P_{CHP}(t) \tag{4-1a}$$

$$P_{CHP,Hout}(t) = \eta_{th} \cdot P_{CHP}(t) \tag{4-1b}$$

$$P_{HP,out}(t) = COP \cdot P_{HP}(t) \tag{4-2}$$

$$P_{GF,out}(t) = \eta_F \cdot P_{GF}(t) \tag{4-3}$$

Heat storage is also considered to store excessive heat, which can be utilized later when the heat load is exorbitant. Heat storage is formulated in (4-4) [28], where M_h specifies the energy exchange between the hub and heat storage, E_h indicates the stored energy, and E_h^{stb} is the standby thermal loss through the water tank wall at the current time

interval. e_h^+ and e_h^- are the charging and discharging efficiency respectively. These variables are a function of t, denoting the time step within a discretized time domain.

$$M_h(t) = \frac{1}{e_h}\left(E_h(t) - E_h(t-1) + E_h^{stb}\right) \tag{4-4a}$$

$$e_h = \begin{cases} e_h^+ & \text{if } M_h(t) \geq 0 \quad \text{(charging/standby)} \\ \frac{1}{e_h^-} & \text{else} \qquad\qquad\qquad\quad \text{(discharging)} \end{cases} \tag{4-4b}$$

Because the storage charges when M_h is greater than 0, the above equation means: the stored energy at current time step *t* equals the stored energy at previous time step *(t-1)* plus the charging energy multiplied by the charging efficiency, minus the standby loss. This explanation also applies when the storage discharges.

Additionally, renewable generation including solar photovoltaics and wind generation cooperates with other hub elements to meet demand. The output of the solar photovoltaic system $P_{so,out}$ is quantified by multiplying solar irradiance $P_{so,in}$ with the efficiency η_{so}.

$$P_{so,out} = P_{so,in} \cdot \eta_{so} \tag{4-5}$$

The power output P_{wi} from wind turbines is expressed in terms of the wind speed v_w (m/s) as shown in (4-6) [29], where v_{ci}, v_{rs}, and v_{co} represents the cut-in, rated, and cut-out wind speed, P_{rated} indicates the rated power.

$$P_{wi} = \begin{cases} 0, & \text{if } 0 < v_w < v_{ci}, \text{or } v_w > v_{co} \\ P_{rated} \cdot \left(\frac{v_w - v_{ci}}{v_{rs} - v_{ci}}\right), & \text{if } v_{ci} \leq v_w \leq v_{rs} \\ P_{rated}, & \text{if } v_{rs} \leq v_w \leq v_{co} \end{cases} \tag{4-6}$$

The energy hub modelled represents a community such as a university or hospital in a smart energy city. The schematic diagram of a single energy hub is shown in Fig. 1.

As indicated in Fig. 4-1, the demand including electricity L_{ele} and heat L_{th} is satisfied by electricity input P_{ele}, gas input P_{gas}, energy exchange with the storage M_h, and renewable generation $P_{re,in}$. The energy hub system presents multiple inputs and outputs, hence the coupling between hub outputs (represented as *L*) and inputs (represented as *P*) is formulated with a matrix of converter efficiencies (representing as *C*). The mathematical transformation of the energy hub in Fig. 4-1 is formulated in (4-7).

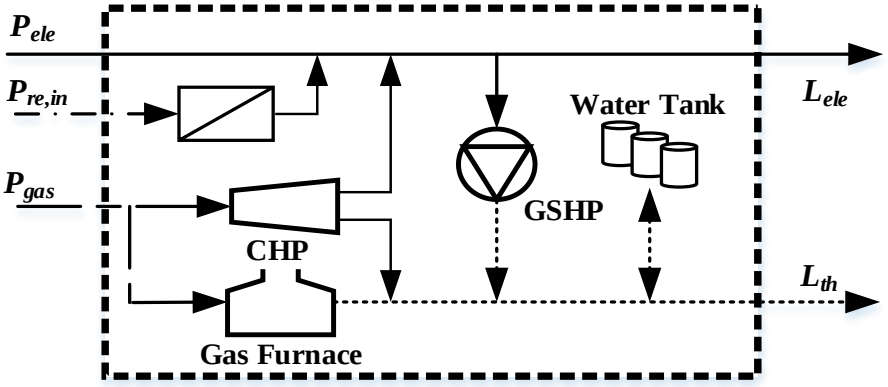

Fig. 4-1.Single energy hub

$$\begin{bmatrix} L_{ele}(t) \\ L_{th}(t) + M_h(t) \end{bmatrix} = \begin{bmatrix} 1 - v_e(t) & \eta_{re}(1 - v_e(t)) & v_g(t)\eta_e(1 - v_e(t)) \\ v_e(t)COP & v_e(t)\eta_{re}COP & v_g(t)(\eta_{th} + \eta_e v_e(t)COP) + \eta_F - v_g(t)\eta_F \end{bmatrix} \times \begin{bmatrix} P_{ele}(t) \\ P_{re,in}(t) \\ P_{gas}(t) \end{bmatrix} \quad (4\text{-}7)$$

As indicated in (4-7), v_e and v_g are the dispatch factors of electricity and gas. Specifically for this hub, v_e indicates the portion of electricity injection to GSHP relative to the total electricity input. Similarly, v_g is the proportion of gas injected to CHP relative to the total gas input.

4.3.2. Electricity Networks

The mathematical formulations of electricity networks are indicated as follows [8]. The complex nodal power balance for node *m* is in (4-8), where S_m is the complex power injected to node, S_{mn} is the complex power flow from node *m* to *n*, and *N* is the number of nodes in the power network.

$$S_m = \sum_{n=1}^{N} S_{mn} \quad (4\text{-}8)$$

The complex power flow S_{mn} is expressed in (4-9) in terms of the complex nodal voltage V_m and V_n, and the line parameters.

$$S_{mn} = \frac{|V_m|^2}{\tilde{Z}_{mn}^*} - \frac{V_m V_n^*}{Z_{mn}^*} \quad (4\text{-}9)$$

Assuming that the line between two nodes is represented by a π equivalent circuit, Z_{mn} and Y_{mn} respectively indicate the series impedance and shunt admittance. Therefore, $\tilde{Z}_{mn}$ is

$$\tilde{Z}_{mn} = \left(\frac{1}{Z_{mn}} + \frac{Y_{mn}}{2}\right)^{-1} \tag{4-10}$$

4.3.3. Gas Networks

The gas injection to each node follows the conservation law of nodal gas flow balance. The mathematical formulations of the gas network are illustrated as follows [8], where the nodal gas flow balance for node *m* is

$$Q_m = \sum_{n=1}^{N} Q_{mn} \tag{4-11}$$

Where Q_m indicates gas injection to node *m*. Q_{mn} in (4-12) represents the gas flow between nodes *m* and *n*, which is expressed in terms of the upstream pressure p_m, downstream pressure p_n and k_{mn} depend on the pipeline's physical properties.

$$Q_{mn} = k_{mn} sn_{mn} \sqrt{sn_{mn}(p_m^2 - p_n^2)} \tag{4-12a}$$

$$sn_{mn} = \begin{cases} +1, & \text{if } p_m \geq p_n \\ -1, & \text{else} \end{cases} \tag{4-12b}$$

The gas consumed by compressors Q_{com} is formulated as

$$Q_{com} = k_{com} Q_{mn}(p_m - p_k) \tag{4-13}$$

Where k_{com} characterizes the properties of the compressor, p_m and p_k indicate the suction and discharge pressures at the two sides of the compressor. Specifically, gas power flow P_{mn} can be quantified by gas flow rate Q_{mn} and the gross heating value of gas (represented as GHV) as shown in (4-14).

$$P_{mn} = GHV \cdot Q_{mn} \tag{4-14}$$

4.4 Problem Formulation and Methodology

In a systematic way, the optimal operation normally consists of the following steps [7, 8, 11-13]:

i) the electricity load, heat load, and energy prices are normally forecasted by using historic data;

ii) the energy output of different generation is forecast, where the key uncertainties are the renewable generation;
iii) model the cost functions of all energy generation;
iv) model the operation objective function, and equality and inequality constraints for the optimization;
v) find an appropriate optimization approach to solve the model.

However, traditional deterministic methods fail to provide a reliable optimal solution because the renewable generation is assumed to be accurately forecasted. Chance-constrained programming enables the optimization of the system with the distributions of uncertain variables explicitly represented. By defining a probability level for the chance constraints, solving the CCP means to optimize the system with safety constraints and chance constraints satisfied, under the condition that the values of uncertainty variables are randomly distributed according to their distributions.

The impact of uncertain renewable generation on the energy hub system is modelled by chance constraints and the formulation of the optimization is presented in this section. Additionally, this section introduces the concept of Cornish-Fisher Expansion to convert chance constraints into deterministic constraints. The steps of the CCP implementation are at the end of this section.

4.4.1. CCP Energy Hub Optimization Problem Formulation

A system of three interconnected energy hubs in Fig. 4-2 is to illustrate the problem formulation. The electricity and gas networks supported by G1, G2, and N are embedded in the system to satisfy electricity and heat demand. G1 and G2 are generation power outputs, and N is the gas injection to the energy hub system. As shown in Fig. 4-2, heating converters including CHP, GSHP, and GF are installed within each hub, and a water tank is also contained in each hub as heat storage. A solar photovoltaic system and a wind farm are installed at hubs 1 and 2 respectively.

The objective is to minimize the total system cost by optimally determining the power flow, gas flow, and the operation of each hub element over the whole operation time horizon with uncertain renewable. Meanwhile, the chance constraints on power and gas flows between adjacent hubs should be above the predefined probability level of confidence.

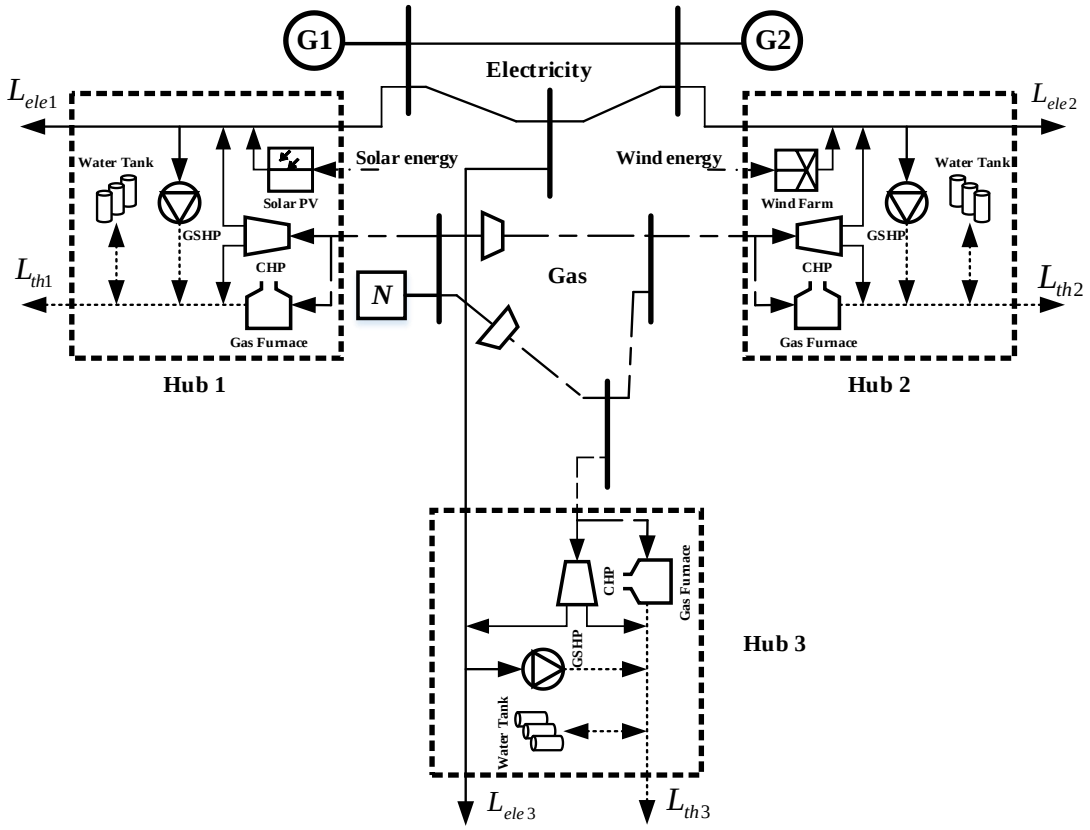

Fig. 4-2.The three-hub interconnected system.

The optimal solution is denoted as the control vector *u(t)*, which contains the power and gas injection to the network and each hub, the voltage and pressure at each bus, the pressure of compressor, the power and gas flows between adjacent hubs, the energy exchange with the heat storage in each hub, and the dispatch factors for each hub. All these variables at all time-steps are included in the control vector *u(t).*

$$u(t) = [P_{ele,i}(t), P_{gas,i}(t), V_i(t), P_{Gi}(t), P_N(t), S_{i,j}(t), p_i(t),$$

$$Q_{i,j}(t), p_{com,i}(t), Mh_i(t), Eh_i(t), v_{e,i}(t), v_{g,i}(t)] \ \forall t, \forall i \quad (4\text{-}15)$$

In (4-15), '*i*' is the index number related to hubs, buses, nodes, and compressors. The definitions of other variables are in previous sections. The total cost (*TC*) of the electricity and gas generation is the objective to be minimized in terms of a quadratic function over whole time horizon *T*. It should be noticed that sn_{mn} in (4-12a) and (4-12b) is a binary variable, but it is temporarily used to calculate the gas flow Q_{mn} in (4-15). Hence sn_{mn} is not mentioned in the decision variables. The stochastic programming problem is formulated in (4-16).

Objective:

$$\text{Min } TC = \sum_{t=1}^{T} \sum_{i \in \{G_1, G_2, N\}} (a_{i,t} + b_{i,t} P_{i,t} + c_{it} P_{i,t}^2) \quad (4\text{-}16a)$$

Subject to:

$$\begin{cases} \text{Equality constraints: } (4-1)-(4-14) \\ \text{Inequality constraints:} \\ 0 \le v_{e,i}(t) \le 1 \quad 0 \le v_{g,i}(t) \le 1 & (4-16b) \\ 0 \le P_{G,i}(t) \le P_{G,i,max}(t) \quad 0 \le P_N(t) \le P_{N,max}(t) & (4-16c) \\ 0 \le P_{ele,i}(t) \le P_{ele,i,max}(t) \quad 0 \le P_{gas,i}(t) \le P_{gas,i,max}(t) & (4-16d) \\ 0 \le p_i(t) \le p_{i,max}(t) \quad 0 \le V_i(t) \le V_{i,max}(t) & (4-16e) \\ M_{h,i,min}(t) \le M_{h,i}(t) \le M_{h,i,max}(t) & (4-16f) \\ E_{h,i,min}(t) \le E_{h,i}(t) \le E_{hi,max}(t) & (4-16g) \\ p_{com,i,min}(t) \le p_{com,i}(t) \le p_{com,i,max}(t) & (4-16h) \\ \text{Chance constraints:} \\ \Pr\{Q_{i,j}(t) \le Q_{i,j}^{max}\} \ge \alpha \quad \Pr\{S_{i,j}(t) \le S_{i,j}^{max}\} \ge \alpha & (4-16i) \end{cases}$$

The objective function in (4-16a) indicates the total cost on the network to be minimized over the whole time horizon, where a, b, and c represent the coefficient of generation cost. (4-16b) specifies the constraint on dispatch factors, which should be within the boundary between 0 and 1. (4-16c) indicates the constraint for total power and gas injection to the networks. (4-16d) reflects the minimum and maximum power and gas input to each hub. (4-16e) refers to the limitations of the pressure and voltage at each bus. (4-16f) denotes the limitation of heat energy exchange with the storage, the minimum and maximum heat energy that can be stored in the storage are defined in (4-16g). (4-16h) represents the limitation of compressor's pressure.

In addition to equality and inequality constraints, the chance constraints are also established with a confidence level of α. The power flows S_{ij} and gas flows Q_{ij} between adjacent hubs are constrained by chance constraints in this paper, and they are specified in (4-16i), where *Pr* means the probability of chance constraints.

Equation (4-16i) indicates that the problem is formulated as a stochastic problem. To transform the stochastic problem to a deterministic problem, the quantile of chance constraints is calculated by Cornish-Fisher Expansion to fit the optimization, and (4-16) is thus solvable with the interior-point method.

4.4.2. Transforming Chance Constraints to Deterministic Constraints

In order to incorporate chance constraints into the optimization, the probability level of chance constraints is transferred by quantile, which reflects the inverse function of a

stochastic variable's Cumulative Distribution Function (CDF). Because of the monotone relation between the quantile and its inverse CDF, (4-16i) could be expressed by (4-17).

$$q_{Q_{i,j}}(\alpha_i) \leq Q_{i,j,max} \qquad q_{S_{i,j}}(\alpha_i) \leq S_{i,j,max} \tag{4-17}$$

Where q is the quantile function formulated by the Cornish-Fisher Expansion with the utilization of cumulants. Five orders of cumulants are applied in this paper. The quantile function q in terms of probability level of α is indicated in (4-18) [30].

$$q(\alpha) = A(\alpha) + \frac{A^2(\alpha)-1}{6}\kappa_3 + \frac{A^3(\alpha)-3A(\alpha)}{24}\kappa_4 - \frac{A^3(\alpha)-5A(\alpha)}{36}\kappa_3^2 + \frac{A^4(\alpha)-6A^2(\alpha)+3}{120}\kappa_5 - \frac{A^4(\alpha)-5A^2(\alpha)+2}{24}\kappa_3\kappa_4 + \frac{12A^4(\alpha)-53A^2(\alpha)+17}{324}\kappa_3^2 \tag{4-18}$$

The symbol A in (4-18) indicates the quantile of standard normal distribution, κ_v represents the cumulants with order v. It should be noted that the quantile q and cumulants κ_v follow the form of standard measure. For a variable q with a mean value of μ and standard deviation of σ, the normalized form of the variable and the cumulants are denoted as $q^* = (q-\mu)/\sigma$ and $\kappa_v^* = \kappa_v/\sigma^v$ respectively.

In order to calculate the quantile, the chance constraints need to be expressed in terms of uncertainty variables and other variables. Taking the chance constraint Q_{12} restricting the gas flow between hub 1 and 2 as an example, at each time step they are expressed by the composition of control variables x and uncertainty variables ξ, derived from (4-1)-(4-14). The chance constraint of Q_{12} at time step t is

$$Q_{1,2}(t) = a_1\xi_{solar}(t) + a_2\xi_{wind}(t) + Co(t) \tag{4-19}$$

Where, ζ_{solar} and ζ_{wind} stand for the uncertainty inputs of solar and wind energy respectively, a_1 and a_2 represent the coefficient related to ζ_{solar} and ζ_{wind}. Hence the two uncertain inputs perform linear relations with the variable gas flow between hub 1 and 2. Because the uncertain inputs to the energy hub system are linearly related to the chance constraints (power and gas flow between hubs), it is straightforward to obtain the linear relation in (4-19) through (4-1) - (4-14). *Co(t)* represents the polynomials containing control variables x, and it is irrelevant to the calculation of quantile. The first part in (4-19) related to the uncertainty inputs is expanded by the Cornish-Fisher Expansion to convert it to a deterministic formulation [30]. Assuming the uncertainty is abbreviated as *Un(t)*, the cumulant for *Un(t)* with order v is formulated in

$$\kappa_{Un(t),v} = a_1^v \kappa_{\xi_{solar,v}}(t) + a_2^v \kappa_{\xi_{wind,v}}(t) \quad (4\text{-}20)$$

Where $\kappa_{\xi_{solar,v}}(t)$and $\kappa_{\xi_{wind,v}}(t)$represent the cumulants of variables $\xi_{solar}(t)$ and $\xi_{wind}(t)$ with v^{th} order at time step *t*. The quantile of chance constraints can, therefore, be calculated through (4-18)-(4-20), and applied as the deterministic form in (4-17). The formulation of other chance constraints in (4-16i) can be accordingly transferred to deterministic constraints by the similar expressions shown in (4-18) to (4-20).

4.4.3. Overall Methodology

The methodology developed to solve the chance-constrained energy hub optimization is described by the following steps:

- Step 1. Acquire data: energy hub load, distributions of renewable generations, and system parameters.
- Step 2. Build the optimization problem with the given constraints, and chance constraints formulated in (4-16).
- Step 3. Initialize the control vector *u(t)* within the predefined boundary.
- Step 4. Convert the chance constraints into deterministic constraints through (4-17)-(4-20).
- Step 5. Apply the interior-point method to optimize the energy hub system with deterministic constraints.
- Step 6. Determine whether the solution from step 5 satisfies the stopping criteria, and if not, update the control vector *u(t)* and repeat steps 4 to 5 until the stopping criterion is met.

The optimization follows the general procedures of a heuristic algorithm, which is to update the optimal solution for the problem until the stopping criteria are met. However, as indicated in the previous section, the quantile of chance constraints not only depends on the probability level but also correlates with other control variables. Therefore, in updating the control variables, the chance constraints need to be circularly transferred to deterministic constraints at each iteration. The interior-point approach is then implemented to solve the deterministic problem to find the best solutions.

4.5 EVPI and VSS Model

To evaluate the effect of applying stochastic programming to solve the optimization problem, the results from the CCP are compared with those from the expected value of

perfect information (EVPI) and value of the stochastic solution (VSS), both of which use deterministic programming to solve the optimization. The EVPI calculates the maximum amount a decision maker is willing to pay when uncertain information is perfectly known [31]. By assuming the uncertainty is modelled by various scenarios each with a known probability, the wait-and-see solution (WS) is derived by summing the optimal solution from each scenario multiplied by probability. The EVPI is calculated by (4-21), and SS is the solution from the CCP.

$$EVPI = SS - WS \tag{4-21}$$

The VSS reflects the benefits from explicitly modelling the uncertain distributions. It is mathematically formulated as the difference between the expected value (EV) of the optimal solution where uncertain variables are replaced by their mean values and the stochastic solutions [31].

$$VSS = EV - SS \tag{4-22}$$

4.6 Case Study

The approaches of deriving PDF and CDF curves are illustrated in this section, and the convergence behaviour of the optimization technique is obtained and analysed by implementing the CCP on an example sample. Additionally, two cases are demonstrated and discussed in this section to validate the proposed model. The energy hub system in Fig. 4-2 is applied and the simulated time horizon is set as T=24. The chance constraints on gas and power flows between adjacent hubs are separately applied to the optimization problem in the first and second cases to investigate the impact of different chance constraints on system optimization performance. The system setup and data acquisition are indicated as follows.

4.6.1. Data Setup

The uncertainty in renewable energy generation, including solar energy and wind energy, are modelled in this paper. The CCP is used in this paper because a short period of overloading is tolerable for energy networks between communities, and hence a slight error is permissible.

Literature suggests that the characteristics of solar and wind energy generally follow Beta [30] and Weibull distributions [20]. Thus, the probability density functions of solar and wind energy injection at each time step are derived by fitting the historical data into

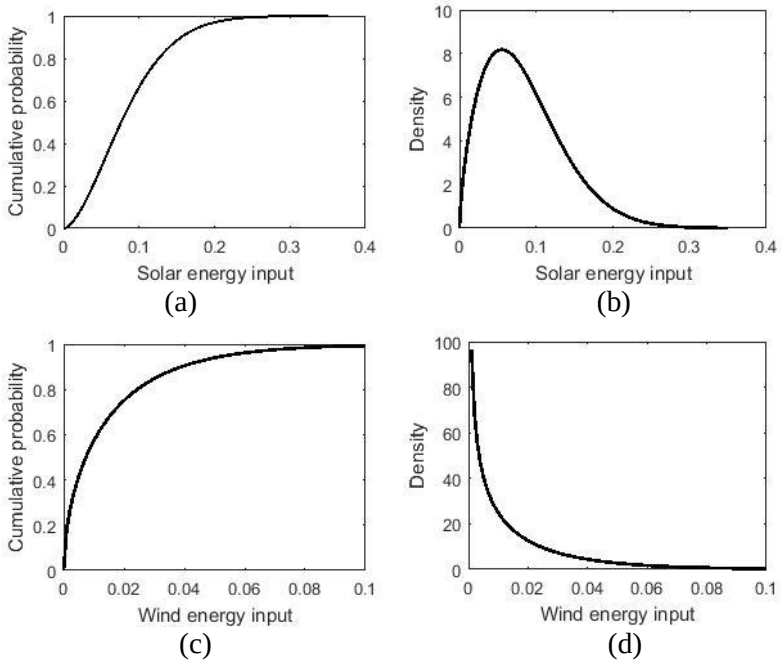

Fig. 4-3. PDF and CDF curves of renewable energies inputs at step 9

Table 4-1.ENERGY HUB SYSTEM PARAMETERS AND CONSTRAINTS

System parameters	
Line 1-2	Z_{12}=0.3+j0.9 p.u., Y_{12}=j1.5·10^{-6} p.u.
Line 1-3	Z_{13}=0.2+j0.6 p.u., Y_{12}=j2.5·10^{-6} p.u.
Line 2-3	Z_{23}=0.1+j0.4 p.u., Y_{12}=j3.5·10^{-6} p.u.
G_1	V_1=1∠0^{o}, a_{G1}=0, b_{G1}=10 £/p.u., c_{G1}=0.001 £/p.u.^{2}
G_2	a_{G2}=0 b_{G2}=12 £/p.u., c_{G2}=0.0012 £/p.u.^{2}
Pipe lines	GHV·k_{12}=4.5 GHV·k_{13}=3.0 GHV·k_{23}=2.0
Compressor	GHV·k_{com}=0.5
N	p_1=1 p.u., a_N=0, b_N=5 £/p.u., c_N=0 £/p.u.^{2}
CHP	η_e=0.33, η_{gh}=0.57
GF	η_F=0.75
Storage	E_h^{stb}=0.5, e_h^+= e_h^-=0.9
Renewables	η_{so}=0.117, v_{ci}=4m/s, v_{co}=25m/s, v_{rs}=16m/s, P_{rated}=0.3p.u.
Constraints	
Nodes	$0.8 \le \lvert V_m \rvert \le 1.2$ p.u.
m=1, 2, 3	$p_m \le 1.2$ p.u.
G_2	$0 \le P_{G2} \le 4$ p.u., $0 \le \lvert Q_{G2} \rvert \le 4$ p.u., $0 \le \lvert P_{G2}+jQ_{G2} \rvert \le 5$ p.u.
Compressor	$1.2 \le p_m / p_k \le 1.8$
Storage	$0 \le E_h \le 6$ p.u. $-3 \le M_h \le 3$ p.u.
CHP input	$0 \le P_{CHP,input} \le 1$ p.u.
GF/GSHP	$0 \le P_{GSHP/GF\_input} \le 1.5$ p.u.

Beta and Weibull distributions respectively, the shape factors of these distributions are then estimated. The cumulants are calculated based on the shape factors. The probability density function (PDF) curves and CDF curves of the solar and wind energy

inputs at time step 9 are shown in Fig. 4-3 as an example. Here, figures (a) and (b) denote the characteristics of solar input, figures (c) and (d) indicate the wind input's PDF and CDF.

In addition to renewable uncertainties, the load profiles for the energy hub system are modelled by the electricity and thermal load profile simulation models [32] and [33]. The parameters and constraints for other elements in the energy hub system are taken from [8, 13, 28], which are described in Table 4-1. The system is considered as in a per unit (p.u.) system and the monetary unit is assumed to be GBP (£).

4.6.2. Derivation of PDF and CDF Curves

The results of CCP on the 3-hub system are analyzed with their PDF and CDF curves. All curves are sufficiently accurate to observe their characteristics when 500 samples are applied. The change to the curves are imperceptible when more samples are implemented, but the computational burden is exponentially heavy. Therefore, 500 samples are analyzed to acquire the PDF and CDFs plots. Generally, the two functions can be obtained by the following key procedures as shown in Fig. 4-4.

- Step 1: Implement the CCP optimization for the 3-hub system in terms of 500 samples, where each sample represents the CCP with different probabilities of

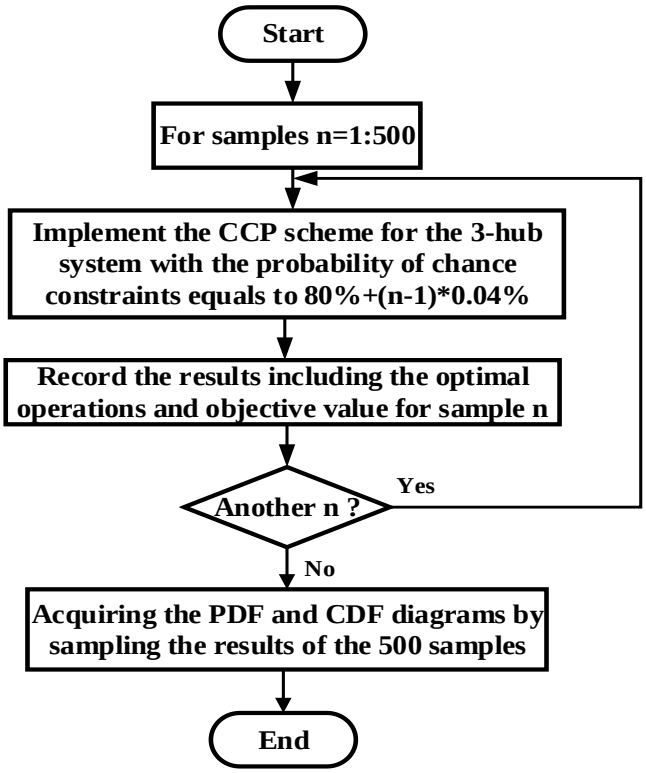

Fig. 4-4.Flowchart of obtaining PDF and CDF curves from CCP

chance constraints. For example, to acquire the PDF and CDF curves with chance constraint probability higher than 80%, the corresponding probability level of chance constraints equals to 80%+(n-1) *0.04% with n growing from 1 to 500.

- Step 2: Record the optimization results, including the optimal operations and objective value of each sample.
- Step 3: Build PDF and CDF curves by running 500 samples.

4.6.3. Case 1-Gas Flows with Chance Constraints

1) Convergence analysis of CCP

The optimization problem (4-16) is formulated as a multi-period problem, which is non-convex. Due to the high complexity of the problem, the global minimum is not guaranteed with the used interior-point method. However, the interior-point method is capable of resolving the non-linear problem compared with the linear programming methods. To demonstrate that the algorithm is capable of achieving a local minimum when applied to CCP, a single run of the 3-hub system is analyzed with the probability level of the chance constraints set as 80%, and the convergence behaviour of the optimization is derived and shown in Fig. 4-5. The algorithm stopping criteria is specified as follows: the maximum iterations are 3000, both the constraints and function tolerances are 10^{-6}, and the maximum function evaluations are 3000000. It can be seen that the value of the objective function dramatically declines from iteration 1 to 5. It then slightly increases until iteration 23, the curve continually drops from iteration 23 to 30, and remains stable thereafter. It demonstrates that the optimization converges around iteration 41 and achieves the minimum value of £522.33. It is, therefore, reasonable to conclude a local minimum has been met. In fact, the optimization converges for each sample after approximately 40 iterations. Additionally, previous

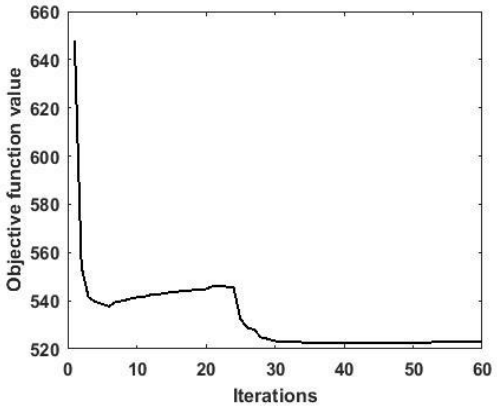

Fig. 4-5.The convergence of CCP implementing on the 3-hub system

literature has proved that the interior-point method applied to CCP is capable of converging to a minimum solution when solving problems with similar complexity [1, 8, 34].

2) Different probability levels of chance constraints

The maximum value of the chance constraint (i.e. the gas flow between adjacent hubs) is set as 0.8 p.u., and different probability levels of 80%, 85%, 90%, and 95% are applied to investigate how chance constraints affect the optimization.

The CDF curves of the optimized total cost are shown in Fig. 4-6, which are derived by optimizing 500 samples for the 3-hub system with the chance constraints level higher than the above probability levels. The optimized total costs of the three-hub system vary from approximately £521.5 to £527 with the cumulative probability changing from 0 to 1. All CDF curves perform similar characteristics with the optimization results derived from different chance constraint probability levels.

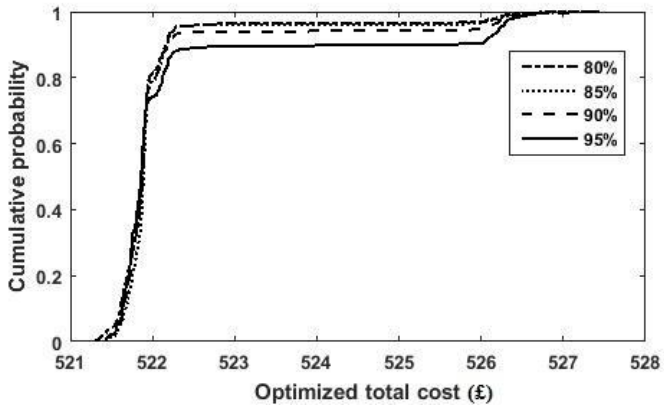

Fig. 4-6.Case 1-CDF curve of the optimized total cost

Since the load is relatively high at time step 9 compared to other time steps, the optimal operation for the energy hub at this time step is of interest for further investigation. The CDF curves of the total gas injection to the network at time step 9 with different chance constraints probability levels are in Fig. 4-7.

Fig. 4-7 indicates that all of the CDF curves gradually rising until the cumulative probability reaches 0.2, and then the curves rapidly increase to the cumulative probability of 1. The CDF curves with different probability levels of chance constraints present similar variation. The CDF curves in Fig. 4-7 present completely different characteristics with the CDF curves in Fig. 4-6. This is mainly due to the non-linearity

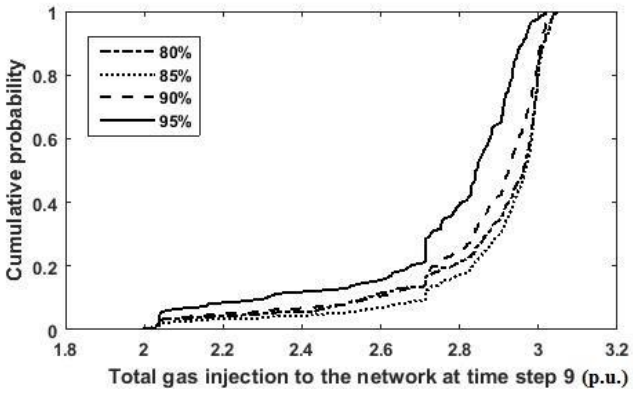

Fig. 4-7.Case 1-CDF curve of the total gas injection at time step 9

between gas flow and the total system cost. Additionally, since the hub system presents high flexibility, the change of gas flows between hubs could lead to an unpredictable impact on the total cost. For example, the constraints on the quantity of gas flows could lead to less gas injection into the energy hub. The demand could be satisfied by accordingly adjusting the operations of other elements within the energy hub system such as discharging the storage or switching on other converters. Since the problem is a multi-period problem with high complexity, the cost of the adjustments is not predictable. Therefore, the CDF curves of the optimized total cost perform differently with the CDF curve of the gas flows between hubs.

4.6.4. Case 2-Power Flows with Chance Constraints

1) Different probability levels of chance constraints

The power flows between adjacent hubs are restricted by the chance constraints for the second case. Considering system safety limits, the maximum power flows between hubs are assumed to be 50% of branch capacity. With the different chance constraints probability levels of 80%, 85%, 90% and 95 %, the CDF curves of the total gas injection

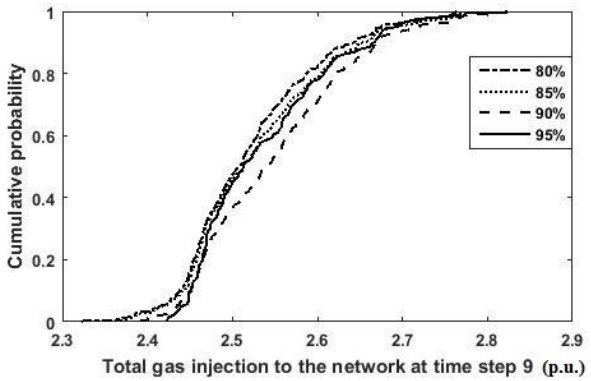

Fig. 4-8.Case 2-CDF curve of the total gas injection at time step 9

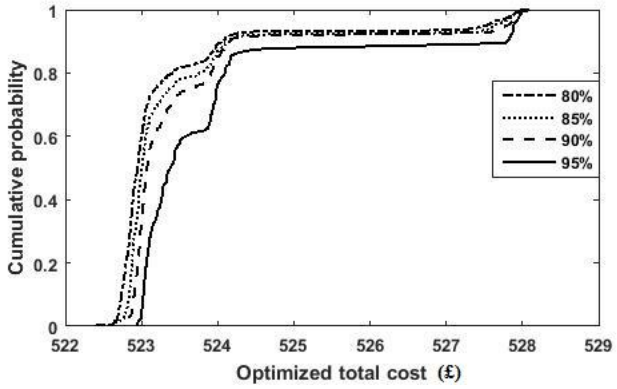

Fig. 4-9.Case 2-CDF curve of the optimized total cost

to the network at time step 9 are shown in Fig. 4-8, and the CDF curves of the optimized total cost are depicted in Fig. 4-9. 500 optimization results are sampled to derive the curves.

As seen from Fig. 4-8, the total gas injection at time step 9 varies from approximately 2.32 p.u. to 2.82 p.u.. The CDF curve generally spans wider when the chance constraints probability level is lower, and the optimal operations tend to be more stable with fewer variations when the probability level of chance constraints is higher.

The characteristics of the CDF curves in Fig. 4-8 are different from the CDF curves in Fig. 4-7 in terms of shape and gradient. Additionally, the abscissa of the CDF curves in Fig. 4-7 spans from approximately 2 to 3, spanning greater distance compared with the CDF curves in Fig. 4-8. Hence the total gas injection to the network is more affected when the gas flows between hubs are restricted by the chance constraints.

Conversely, the CDF curves of the optimized total cost in Fig. 4-9 present similar characteristics with the curves in Fig. 4-6. However, the abscissa of the CDF curves in Fig. 4-9 spans wider than the curves in Fig. 4-6, which means that the optimized total cost is more sensitive when the power flows between hubs are constrained by chance constraints. Therefore, when the restriction of chance constraints on gas flows change to power flows, the impacts to the optimal operations of every element within the energy hub system are completely different.

2) The optimal strategy for energy hub system

The optimal operation of hub 1 in terms of electrical load over 24 hours is shown in Fig. 4-10, where the probability levels of chance constraints are set higher than 80%. As seen, the total electrical load represented by the histogram and power injection to GSHP

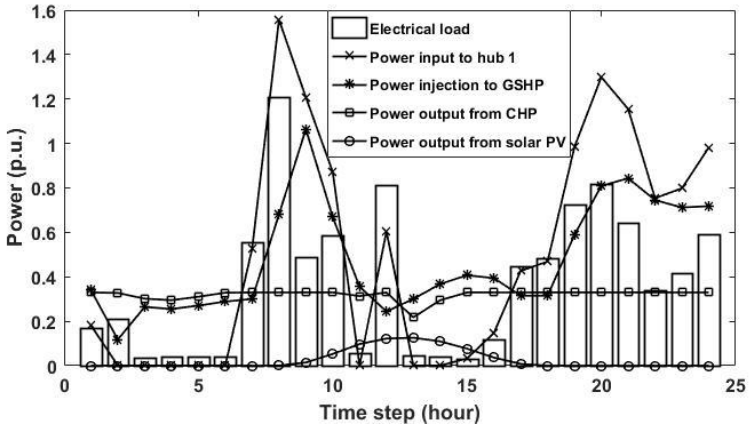

Fig. 4-10.Optimal operations of hub 1 over 24 hours

(denoted by stars) are met by the grid power (denoted by crosses), CHP output (denoted by squares), and solar PV output (denoted by circles). The peak loads are 1.21 p.u. and 0.92 p.u., which appear at time steps of 8 and 20; the power injections to the hub over 24 hours approximately follow the same variations as the load, and the maximum power injections are at time steps of 8 and 20 with the values of 1.55 p.u. and 1.30 p.u. respectively. The electric output from CHP generally remains at 0.33 p.u. over 24 hours, which is close to the maximum CHP power output. Since the energy efficiency of the CHP is higher than those of other converters and the CHP is thus more profitable, it is operated at the maximum power over the whole time horizon.

3) Sensitivity analysis

By assuming that the power flows between hubs are restricted by chance constraints, the probability levels of chance constraints are set to be 80%, 82%… to 99.9%. The optimal dispatch factors of the three hubs at time step 9 under these probability levels are shown in Fig. 4-11. Figures (a) and (b) indicate the variations of v_e and v_g under different chance constraint probabilities, with the horizontal and vertical axis

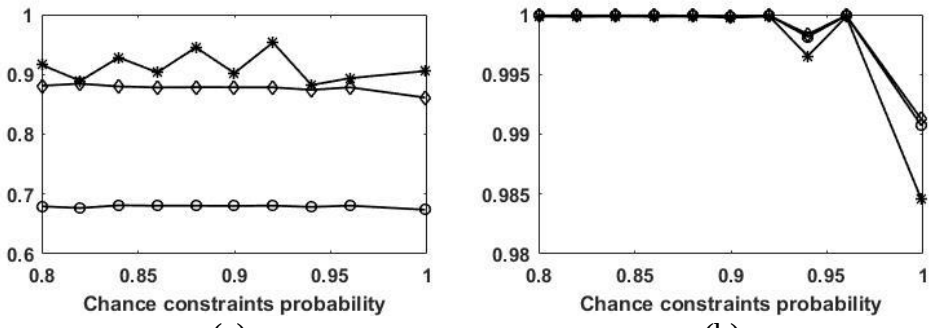

(a) (b)

Fig. 4-11.Dispatch factors under different chance constraints probability

representing the chance constraint probability and the value of dispatch factors. The diamonds, stars, and circles represent the dispatch factors of hubs 1, 2, and 3 respectively. As seen, the dispatch factors v_e of hubs 1 and 3 remain flat when the probability changes and the dispatch factor of hub 2 shows irregular variations. Moreover, the changing probability levels hardly affect the dispatch factors vg of the three hubs because the profits from the CHP are higher than those of the GF.

4) Importance of CCP

To highlight the importance of CCP and compare its results with those from deterministic approaches, EVPI and VSS are calculated by solving the same 3-hub system optimization with deterministic constraints. In other words, the maximum power flows between hubs are restricted to be lower than 50% of the capacity with 100% certainty. The value of WS is calculated by using scenario methods, where the probability of each scenario is assumed to be perfectly known. Scenario-generating methods are used in [5, 15-21], and hence the EVPI can be used to measure the impact between using CCP and scenario methods to solve an energy hub optimization problem with uncertainties.

In this paper, WS is derived by applying the 2PEM in [19, 20] to solve the energy hub optimization with uncertainties. In terms of system total cost, WS and EV are calculated as £524.02 and £522.92 respectively. The solution of CCP (SS) is £527.96 when the probability level of chance constraints is set at 99.99% (100% is not possible because the quantile derived through Cornish-Fisher Expansion will be infinite). The EVPI and VSS are £3.94 and £5.04 by using (4-21) and (4-22). The EVPI indicates that the difference between optimized system costs from CCP and 2PEM is £3.94, and the VSS suggests that there is an extra cost of £5.04 due to uncertainties.

4.6.5. Comparison between the Two Cases

The PDF diagrams of the optimized objective derived from the two cases are shown in Fig. 4-12, where both the probability levels of chance constraints are set as 80%. The upper and lower diagrams represent the distributions of probability densities for case 1 and 2 respectively. The possible optimized total cost varies from £521.31 to £527.45 in case 1, and £522.39 to £528.10 in case 2. The span of the possible optimization results in case 1 is wider compared with the results derived from case 2. Additionally, the expense derived from case 2 is holistically higher than the expense in case 1.

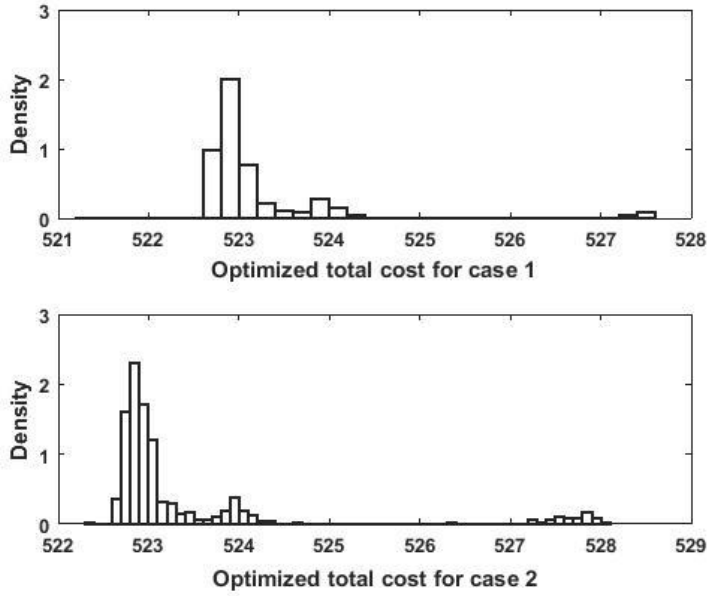

Fig. 4-12.PDF diagrams of the optimized total cost with the probability of chance constraints higher than 80% derived from the two cases

It is observed from the lower diagram in Fig. 4-12 that, the PDF curve derived from case 2 presents relatively high fluctuations around £524 and £528 in addition to the high probability density around the total cost of £523. On the other hand, the probability density for the upper PDF curve is generally centralized around the total cost of £523, which shows stabilized characteristics. Therefore, by comparing the total costs of the two cases, it suggests that the energy hub system tends to be more unstable and system cost is comparatively high when the power flows between hubs are restricted by chance constraints. Thus, the system should be carefully operated with the electricity power flows limited by chance constraints.

Since the heat storage is equipped within the energy hub system and optimized by CCP, the impacts of chance constraints to the operations of heat storages are investigated. The optimal operation of the heat storage in hub 1 is studied as an example. The energy level of heat storage quantifies the percentage of energy stored in it divided by its capacity, and the CDF curves of the maximum energy level of heat storage in hub 1 with different chance constraints probability levels are shown in Fig. 4-13. The upper and lower CDF curves are derived from case 1 and 2 respectively. As seen in Fig. 4-13, the CDF curves perform similar variation tendency for each individual case. However, the differences between the CDF curves in case 2 are more distinct compared to case 1, and the CDF curves have a broader span in case 2. It could be seen that the energy hub

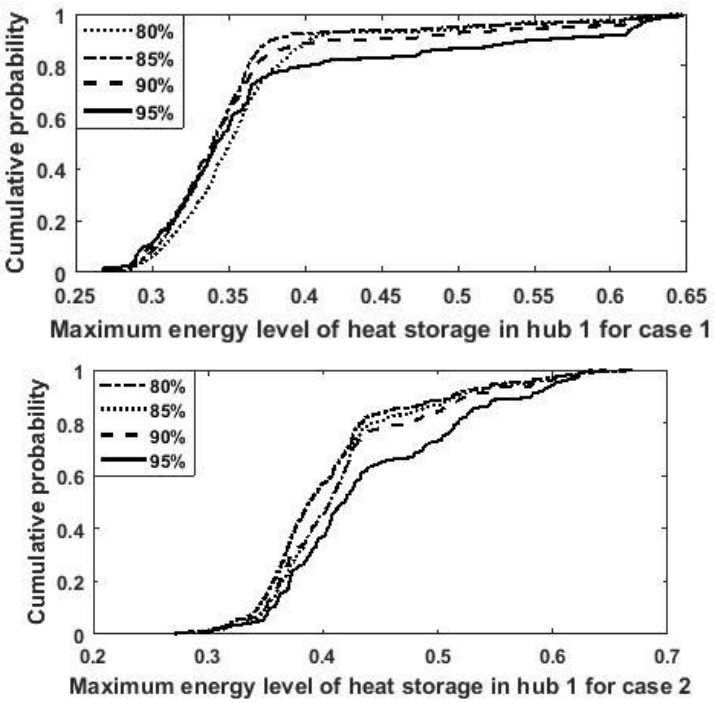

Fig. 4-13.CDF curves of Maximum energy level for two cases

system tends to be more unstable when the chance constraints limit the power flows between hubs.

The results also suggest that the capacity of heat storage should be accordingly extended when the power flows between hubs are restricted by chance constraints since the maximum energy level in case 2 is higher than case 1.

4.7 Conclusion

To model the intelligent operations of smart energy city with uncertainties, this paper applies the energy hub concept to optimize community renewable energy resources with uncertainty parameters. Chance-constrained programming is applied in this paper to solve the optimal energy flow problem for the energy hub system. The main findings are as follows:

- The uncertain elements of the energy hub system should be appropriately modelled since the stochastic nature can significantly affect energy hub system operations and costs.
- Chance-constrained programming is effective in optimizing energy hubs with uncertain factors, enabling the realistic operation of the energy hub system with minimum costs.

- Results demonstrate that chance constraints on power flows have a relatively high impact on energy hub system optimization. The results could be more unstable compared with the case of modelling gas flows with chance constraints.

Future work will incorporate other optimization schemes existing in smart energy cities, such as demand response and unit commitment by chance-constrained programming into the energy hub optimization. Additionally, the correlations of input random variables, such as wind outputs, will be considered as well by joint distributions in energy hub optimization.

4.8 Chapter Summary

Based on the work of chapter 3, where the interconnected energy hubs are optimised under steady state, this chapter extends the work by considering the access of uncertain renewable generations to the energy hub system. The wind farm and solar panel are considered to be equipped within the system, and their stochastic characteristics and probability density function curves are obtained by fitting historic data. The effect of uncertainty on the interconnected energy hub system is analysed through the chance constraint, which restricts the normal constraint by a pre-defined probability. Compared with scenario-based methods, which have been widely applied in previous literature, the chance-constrained programming mitigates the computational burden in contrast to Monte Carlo Simulation, and better captures the stochastic nature of uncertain variables compared with scenario-reduction methods.

To model the uncertainty more accurately, the correlations between uncertain renewable generations are of interest to investigate, and the related effects on energy hub system should be studied. The chance-constrained programming on energy hub system is improved by considering the renewable generations' correlations, which is illustrated in next chapter.

Chapter 5

Chance-Constrained Multi Energy System Optimisation with Correlated Wind Generation

This chapter proposes to apply chance-constrained programming to analyse and resolve the integrated energy hub optimisation with demand response, the correlated wind power generations is also modelled and investigated within the optimisation scheme.

Chapter Overview

Chapter 4 proposes to employ chance-constrained programming to optimise the probabilistic energy hub problem by restricting the energy flows between hubs with chance constraints. To enrich the research of stochastic energy hub optimisation and model the uncertainty more accurately, the correlations between renewable power generations are explicitly considered in this chapter. In fact, the renewable power generations are very likely to depend on each other, especially for interconnected energy hubs which are locally distributed, the dependent uncertain variables can be formulated by joint distributions. However, the correlations have not been investigated within the energy hub system, and hence the effects of uncertainty on energy hub operations analysed from previous literature may be inaccurate. Some expansion methods can be applied to estimate the probability density function of the joint distribution, however requires prohibitively high computational efforts when the joint distribution is formulated for multiple uncertain variables, thus not suitable for multi-hub optimisation.

In order to address this issue, this chapter proposes to model the relation between geographically close wind farms' power generations by fitting historical data, and models the correlations with Pearson correlation. Strong linear relationship between the wind farm outputs could be observed, thus this chapter proposes to approximate the relation between wind farm outputs with linear formulation, hence the distribution of one farm output can be derived by other farm's power generation and their correlation.

Additionally, this chapter considers the customers' response to probabilistic energy hub optimisation and varying energy prices, it is implemented by integrating the demand response scheme into the energy hub optimisation with the objective of reducing total energy costs. This research thus benefits both the system operators and customers by advising them with optimal operations under uncertain renewable generations. Conclusively, the contributions of this chapter can be summarised as follows:

i) Chance-constrained programming is implemented for the interconnected energy hub optimisation by considering both the customer demand response and correlated wind farms' generations.
ii) The correlated wind farm outputs indicates strong dependency from historical data, and are thus modelled by Pearson correlation.

iii) The chance constraints are applied to restrict the energy flows between energy hubs, which are solved by Cornish-Fisher Expansion.

Statement of Authorship

This declaration concerns the article entitled:			
Chance-Constrained Multi Energy System Optimisation with Correlated Wind Generation			
Publication status: Submitted			
Publication details (reference)	None.		
Candidate's contribution to the paper	The candidate and the second author jointly proposed the idea of the paper, and they designed the methodology. The candidate executed all the coding to derive the experimental results. Other authors helped the candidate with the design of case studies, format of the paper, and improvement of academic writing. The percentage of the candidate did compared with the whole work is indicated as follows: Formulation of ideas: 70% Design of methodology: 80% Simulation work: 90% Presentation of data in journal format: 80%		
Statement from candidate	This paper reports on original research I conducted during the period of my Higher Degree by Research candidature.		
Signed	Da Huo	Date	01/09/2018

5.1 Abstract

Energy hubs can exploit the value of multi energy carriers by coupling them to benefit both system operators and customers with increased flexibility and reduced energy costs, but uncertain renewable generation and customer interaction with the carriers complicate the modelling and operation.

This paper develops chance-constrained optimisation for energy hub systems by restricting energy flows between hubs with relaxing overloading constraints. The correlations between geographically close wind farms in energy hubs are considered by establishing their relations using historical data. In addition, demand response is incorporated to further increase the flexibility of energy hub systems and customers' benefits. The model optimally schedules demand and the energy hub system over a whole time horizon to achieve the minimum energy cost. Cornish-Fisher Expansion is employed to translate chance constraints into deterministic constraints to formulate a multi-period problem. The proposed chance-constrained optimisation model is demonstrated on an interconnected 2-hub system where each hub is assumed to equip with a wind farm. Results illustrate that it can maximally exploit the capability of the interconnected hubs to increase the energy supply flexibility, incorporate customer interaction, and capture wind power correlation. The method can thus benefit the hub system operators and customers with reduced energy infrastructure investment costs and energy bills.

5.2 Introduction

The energy hub can coordinate various energy vectors and infrastructure to satisfy demand, hence significantly improves the efficiency [1, 2]. Communities such as universities or hospitals can be modelled as energy hubs, where the benefits of both the system operators and customers can be maximised by optimally scheduling the energy flows between them [1, 3].

On the other hand, demand response (DR) scheme has been employed to encourage customers to re-allocate energy usage in response to variant energy carrier prices [4-6]. From the perspective of operating energy hub systems, energy demand could be satisfied by consuming cheaper energy to reduce costs. For example, instead of using relatively expensive electricity from the grid to meet the energy hub electricity demand, the Combined Heat and Power (CHP) can be switched on to consume gas to produce

electricity and heat. Therefore, combining DR with energy hub can bring further profits by responding to energy prices. Instead of solely altering the load pattern, the integrated DR with energy hub can also vary energy conversion patterns between energy vectors [7, 8]. In [4], the electric and thermal loads of an energy hub are assumed to be responsive to the day-ahead market to minimise the energy cost. [5] proposes to implement the integrated DR to benefit both customers and utility companies in real-time pricing scheme.

However, the DR program and energy hub operations are highly affected by uncertainties, such as the renewable generation. Inappropriate modelling approaches may cause damage to system components or exorbitantly high costs [9]. Additionally, renewable generation of each hub such as wind turbines may have correlations when they are geographically close [10]. This characteristic challenges the multi-carrier system operations when the wind power generation is rich. Therefore, the modelling of correlated uncertainties is essential for energy hubs. The dependent uncertain variables can be formulated by joint distributions, but they could complicate the optimisation. Some expansion methods introduced in [11] can estimate the probability density function of the joint distributions with joint moments and cumulants. However, the calculation of joint cumulants is complex when uncertain variables number increases, hence the expansion methods are improper to solve the optimisation problem with multiple correlated uncertain variables. In [10, 12], the Cholesky decomposition is adopted to convert the correlated variables to uncorrelated variables to simplify the computation.

In solving the energy hub optimisation problem with uncertainty, Monte Carlo simulation has been applied in [13, 14] to model the uncertain inputs to energy hubs but heavy computational burden is required due to a large number of scenarios. The scenario-reduction methods are also applied in [4, 7, 8, 15, 16], but the reduced scenarios may fail to completely reflect the randomness of uncertainties. Furthermore, the correlated uncertain variables are not considered in the work reported in the above literature. The chance-constrained programming (CCP) is more flexible for optimising energy hub systems with uncertainties compared to scenario-generation methods. CCP is a promising approach for system optimisation since temporary overloading is tolerable on some transmission networks, such as electricity and natural gas. Given the distributions of uncertain variables, chance constraints are restricted by the boundaries

of acceptable probability levels and the CCP is then implemented by satisfying both the deterministic and chance constraints [17, 18].

In this paper, a CCP for multi-energy hub optimisation is proposed, considering customer interaction with the multi-carrier system and the correlation of renewable energy at different hubs. The CCP is implemented to reduce the energy costs by optimally determining the energy hub operations with regard to the correlated wind farms' generations. It restricts the energy flows between hubs by chance constraints because temporary power system overloading is allowable. The correlation of outputs of multi-wind generation is also considered, approximated by the linear Pearson Correlation. Additionally, customer demand response responding to various energy carriers and hub operation conditions is considered via demand elasticity. The Cornish-Fisher Expansion (CF) is applied to convert the chance constraints into deterministic constraints with given uncertainty distributions and confidence levels. The problem is therefore formulated as a multi-period non-linear deterministic problem, solved by the interior-point method in this paper. The CCP is demonstrated on an interconnected 2-hub system, where two adjacent wind farms located in the 2 hubs are included. Optimisation results are modelled by its cumulative distribution function (CDF) curves derived from different chance constraints probability levels.

The main contributions of the paper are: i) it develops the energy hub system optimisation considering customer DR and the output correlation of wind farms; ii) it models the correlations between uncertain wind farm output across various hubs that are geographically close with Pearson Correlation; iii) it uses chance constraints to restrict energy flows between hubs in the optimisation, solved by Cornish-Fisher Expansion.

The rest of the paper is organised as follows: the energy hub system with the power and gas networks are mathematically illustrated in section II. The demand response with price elasticity and renewable correlation are presented in section III, The optimisation problem is formulated in section IV, and the methodology is introduced. Case studies are presented and discussed in section V. Section VI concludes the paper.

5.3 Energy Hub System Modelling

5.3.1. Energy Hub

The energy hub system investigated in this paper utilises electricity, gas, and wind

energy to meet electrical and thermal load with energy converters, including the Gas Furnace (GF), Combined Heat and Power (CHP), Ground Source Heat Pump (GSHP), and Wind Turbine (WT). GF is a widely-used converter to generate heat by combusting natural gas; CHP simultaneously generates electricity and heat by consuming natural gas, which has a higher overall efficiency compared to GF [19]; GSHP consumes electricity to produce heat by extracting heat from the ground, which has been extensively applied in Europe and America; WT converts kinetic wind energy into electricity power.

The outputs of GSHP (P_{HP_out}) and GF (P_{GF_out}) at time step t are in (5-1) and (5-2)

$$P_{HP\_out}(t) = COP \cdot P_{HP}(t) \tag{5-1}$$

$$P_{GF\_out}(t) = \eta_F \cdot P_{GF}(t) \tag{5-2}$$

where, η_{GF} is the GF efficiency, and COP denotes the Coefficient of Performance of the GSHP. P_{HP} and P_{GF} respectively are the power and gas inputs to GSHP and GF.

The electrical output ($P_{CHP,E}$) and heat output ($P_{CHP,H}$) of the CHP at time step t are formulated by the natural gas injection (P_{CHP}) in (5-3)

$$P_{CHP,E}(t) = \eta_e \cdot P_{CHP}(t) \tag{5-3a}$$

$$P_{CHP,H}(t) = \eta_{th} \cdot P_{CHP}(t) \tag{5-3b}$$

Where, η_e and η_{th} are the electric efficiency and thermal efficiency.

All converters need to be safely operated by limiting their outputs within rated capacity. Additionally, the output of the CHP is also constrained by its ramp rate e_{ramp}:

$$-e_{ramp} \leq P_{CHP,E}(t) - P_{CHP,E}(t-1) \leq e_{ramp} \tag{5-4}$$

The wind generation is expressed in terms of the wind speed v_w by piecewise function in (5-5) [20, 21], where P_{rated} is the wind turbine rated power. v_{ci}, v_{rd}, v_{ct} respectively represent the cut-in, rated, and cut-out wind speeds.

$$P_w = \begin{cases} 0, & (v_w < v_{ci}, v_w > v_{ct}) \\ P_{rated} \cdot \left(\frac{v_w - v_{ci}}{v_{rd} - v_{ci}}\right), & (v_{ci} \le v_w \le v_{rd}) \\ P_{rated}, & (v_{rd} < v_w < v_{ct}) \end{cases} \quad (5\text{-}5)$$

An example of a single energy hub is depicted in Fig. 5-1 with the above converters equipped. The energy transformation through the energy hub system at time step *t* can be expressed in (5-6), where the output matrix (*L*) is equal to the converter coupling matrix (*C*) multiplied by the input matrix (*P*).

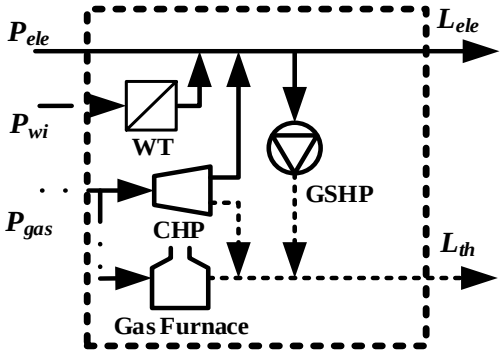

Fig. 5-1.A single energy hub

$$\begin{bmatrix} L_{ele}(t) \\ L_{th}(t) \end{bmatrix} = \begin{bmatrix} 1 - v_e(t) & \eta_{WT}(1 - v_e(t)) & v_g(t)\eta_e(1 - v_e(t)) \\ v_e(t)COP & v_e(t)\eta_{WT}COP & v_g(t)\left(\eta_{gh} + \eta_e v_e(t)COP\right) + (1 - v_g(t))\eta_F \end{bmatrix} \times \begin{bmatrix} P_{ele}(t) \\ P_{wi}(t) \\ P_{gas}(t) \end{bmatrix} \quad (5\text{-}6)$$

Equation (5-6) shows that the electrical demand (L_{ele}) and thermal demand (L_{th}) at time step *t* are satisfied by utilising electricity (P_{ele}), natural gas (P_{gas}), and wind energy (P_{wi}) with the converters. v_e and v_g are dispatch factors. v_e is the percent of electricity input into the GSHP over the total electricity consumption, and v_g is the proportion of gas injected to the CHP relative to the total gas input.

5.3.2. Electricity Network Modelling

The electricity network connects energy hubs for power transmission. The equilibrium of complex power at bus *m* is in (5-7) [1, 2], where S_{mn} represents the complex power between buses *m* and *n*, S_m is the total complex power injected at bus *m*, and *N* denotes the total number of buses in the system.

$$S_m = \sum_{n=1}^{N} S_{mn} \tag{5-7}$$

The complex power flow S_{mn} is formulated in (5-8) in terms of bus voltages V_m and V_n, and line parameters.

$$S_{mn} = \frac{|V_m|^2}{\tilde{Z}_{mn}^*} - \frac{V_m V_n^*}{Z_{mn}^*} \tag{5-8}$$

The line between buses are assumed to follow the π equivalent circuit, and hence $\tilde{Z}_{mn}$ is formulated in (5-9)

$$\tilde{Z}_{mn} = \left(\frac{1}{Z_{mn}} + \frac{Y_{mn}}{2}\right)^{-1} \tag{5-9}$$

where Z_{mn} and Y_{mn} respectively represent the series impedance and shunt admittance.

5.3.3. Gas Network Modelling

Gas networks also connect energy hubs to transmit gas with compressors to regulate pressures. Similar to electricity networks, the gas flow balance at node *m* is in (5-10) [1, 2],

$$Q_m = \sum_{n=1}^{N} Q_{mn} \tag{5-10}$$

where Q_m is the total gas injection to node *m*, and Q_{mn} represents the gas flow between nodes *m* and *n*.

Specifically, Q_{mn} is expressed in terms of the upstream pressure p_m and downstream pressure p_n:

$$Q_{mn} = k_{mn} sn_{mn} \sqrt{sn_{mn}(p_m^2 - p_n^2)} \tag{5-11a}$$

$$sn_{mn} = \begin{cases} +1, & \text{if } p_m \geq p_n \\ -1, & \text{else} \end{cases} \tag{5-11b}$$

Where k_{mn} is the coefficient to reflect pipeline's physical properties.

The energy consumed by the compressor is

$$Q_{com} = k_{com} Q_{mn} (p_m - p_k) \tag{5-12}$$

where p_m and p_k are the suction and discharge pressures at the two sides of the compressor. k_{com} is the coefficient measuring its characteristics.

Additionally, Q_{mn} can be utilised to express the gas power flow P_{mn} by multiplying the gross heating value of gas (GHV):

$$P_{mn} = GHV \cdot Q_{mn} \tag{5-13}$$

5.4 Demand Response and Renewable Correlation

5.4.1. Demand Response with Price Elasticity

Customers can change demand in response to the variation of energy carrier prices, defined as demand elasticity [22], so as to save costs. The elastic demand is considered in energy hub optimisation to increase system flexibility. The sensitivity of demand in relation to the changing of energy price is quantified by price elasticity [23, 24]:

$$L = a \cdot P^{\varepsilon} \tag{5-14}$$

Where L is load, P is energy price, and ε represents the price elasticity. a is a coefficient, formulated by a given reference load L_{ref} and price P_{ref} as shown in (5-15).

$$a = \frac{L_{ref}}{P_{ref}^{\varepsilon}} \tag{5-15}$$

Specifically, the reference price P_{ref} is input by customers, and P represents the real time energy price for DR. L_{ref} is customers' load before implementing the DR scheme, and L is the new load after response. The price elasticity over the entire simulation time horizon is assumed to be constant.

For the energy hubs, the demand of one energy carrier can be satisfied from other energy carriers with energy converters. For example, CHP can be switched on to meet the electricity load to avoid importing expensive electricity from the grid during high-tariff periods. Therefore, the DR should be operated in response to energy prices, while considering energy hub operation conditions to achieve the minimum energy cost. The problem is therefore defined as optimally scheduling the load by considering both the variations of energy prices and energy hub operations to achieve the minimum cost.

5.4.2. Correlated Wind Generation

Energy hubs are normally geographically close, as they mainly model adjacent buildings, communities, etc. Hence, a wind farm located in each hub is close to the other in another hub, which yields strong correlations between their power outputs. To observe the output correlation between graphically closed wind farms, historical data of hourly wind speed over a year is derived from two close observation stations in Cardiff [25]. Assuming there are two wind farms separately located at the two observation points with same parameters including rated power, cut-in, cut-out, and rated wind speed, the hourly power outputs are accordingly derived by (5-5). The hourly wind farm outputs from 00:00 to 04:00 over one year are plotted in Fig. 5-2. The x-axis represents the power generation at wind farm 1, and the y-axis is the power generation at wind farm 2.

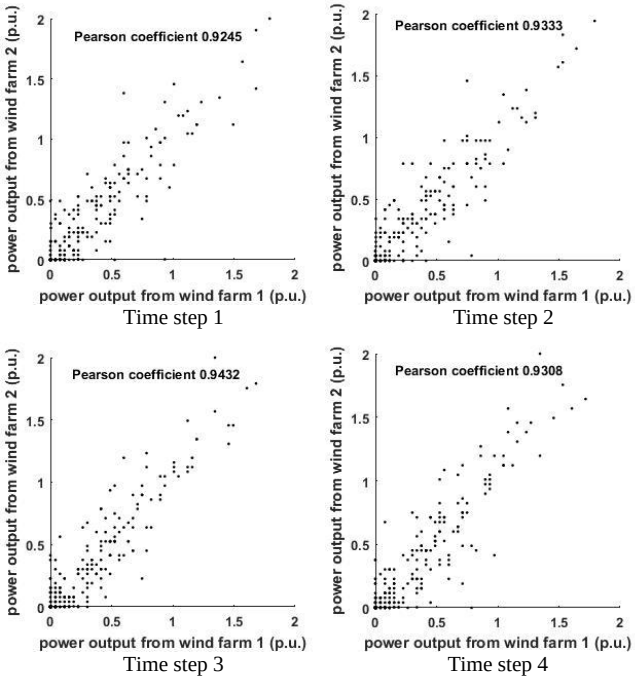

Fig. 5-2.Power outputs from wind turbines at farm 1 and 2

As seen, the power outputs of farms 1 and 2 show approximately linearly, which can be expressed by correlation to indicate the intensity and orientation of the relationship. The correlation is modelled through the Pearson correlation coefficient because it measures the linearity of two random variables, and a value nearer to 1 indicates a stronger linear relation. The coefficient ρ between two random variables α and β is

$$\rho(\alpha,\beta) = \frac{\mathrm{cov}(\alpha,\beta)}{\sigma(\alpha)\sigma(\beta)} \tag{5-16}$$

Where cov(α,β) is the covariance matrix between α and β, and σ is the standard deviation.

It is observed from Fig. 5-2 that Pearson correlation over all time steps is higher than 0.9. Hence this paper proposes to approximate the relation between wind generations at each time step *t* by the linear formulation shown in (5-17).

$$\xi_2(t) = f_1(t) \cdot \xi_1(t) + f_2(t) \tag{5-17}$$

Where ξ_1 and ξ_2 are the power outputs of farm 1 and 2, f_1 and f_2 are factors expressing the linear relations.

The values of f_1 and f_2 at all time steps can be derived by accordingly fitting the historical data. Therefore, the power distribution of one farm can be derived by modelling the other farm's power generation and correlation, by using (5-17).

5.5 Problem Formulation and Methodology

By modelling the energy flows between hubs with chance constraints due to uncertain renewable generation, the proposed DR scheme is formulated through the chance-constrained programming. The optimisation problem is mathematically presented in this section, together with the method of converting chance constraints into deterministic constraints. The overall flowchart of the method is also presented.

5.5.1. CCP Optimisation Formulation

An interconnected 2-hub system in Fig. 5-3 is used to illustrate the concept. Each hub represents a community-level building. The power injection and gas injection to the

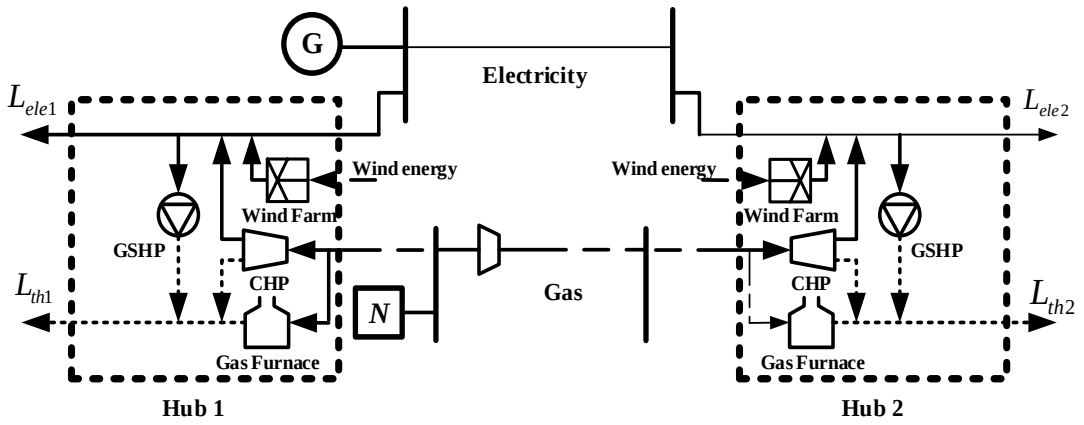

Fig. 5-3.The two-hub interconnected system.

system are at the bus/node near hub 1, where hubs 1 and 2 are connected by the electricity and gas networks. Each hub contains a wind farm, and heating converters, including CHP, GF, and GSHP. The electrical and thermal demand of each hub is satisfied by the cooperation of all converters by consuming electricity and gas.

The objective is to minimise the energy hub system total cost over the whole time horizon. The control variables include: the real-time electricity price, scheduled electricity load, power and gas input to each hub, power and gas flows between hubs, voltage at each bus, gas pressure at each node, compressor pressure, and the dispatch factors of each hub. The above variables are included in the control vector *u(t)*

$$u(t) = [P_{ele,i}(t), P_{gas,i}(t), V_i(t), P_G(t), P_N(t), S_{i,j}(t), p_i(t),$$

$$Q_{i,j}(t), p_{com,i}(t), v_{e,i}(t), v_{g,i}(t), \Pi_{ele}(t), L_{ele,i}(t)] \quad \forall i, \forall t \tag{5-18}$$

In (5-18), the subscript *i* and *j* denote the indexes of energy hubs and *t* is the time step. $P_G(t)$ and $P_N(t)$ are the complex power and gas injections at time step *t*. $\Pi_{ele}(t)$ is the real-time electricity price at time step *t*. The definitions of other variables are in previous section.

The optimisation objective is to minimise the total system cost (*TC*), quantified by adding electricity and gas costs together over the whole time horizon. The variant tariffs are applied to the electricity demand, and a constant price rate is assumed for gas. The CCP objective problem is

Objective:

$$\text{Min } TC = \sum_{t=1}^{T}(P_G(t) \cdot \Pi_{ele}(t) + P_N(t) \cdot \Pi_{gas}(t) \tag{5-19a}$$

Subject to:

$$\begin{cases} \text{Equality constraints: } (5-1)-(5-3), (5-5)-(5-15) \\ \text{Inequality constraints: } (5-4), \\ 0 \le v_{e,i}(t) \le 1 \quad 0 \le v_{g,i}(t) \le 1 & (5-19\text{b}) \\ 0 \le P_G(t) \le P_{G,max}(t) \quad 0 \le P_N(t) \le P_{N,max}(t) & (5-19\text{c}) \\ 0 \le P_{ele,i}(t) \le P_{ele,i,max}(t) \quad 0 \le P_{gas,i}(t) \le P_{gas,i,max}(t) & (5-19\text{d}) \\ 0 \le p_i(t) \le p_{i,max}(t) \quad 0 \le V_i(t) \le V_{i,max}(t) & (5-19\text{e}) \\ p_{com,i,min}(t) \le p_{com,i}(t) \le p_{com,i,max}(t) & (5-19\text{f}) \\ 0 \le P_{CHP,i}(t) \le P_{CHP,i,max}(t) \quad 0 \le P_{GF,i}(t) \le P_{GF,i,max}(t) & (5-19g) \\ 0 \le P_{GSHP,i}(t) \le P_{GSHP,i,max}(t) & (5-19h) \\ \text{Chance constraints:} \\ \Pr\{Q_{i,j}(t) \le Q_{i,j}^{max}\} \ge \alpha \quad \Pr\{S_{i,j}(t) \le S_{i,j}^{max}\} \ge \alpha & (5-19\text{i}) \end{cases}$$

Equation (5-19a) indicates that the total cost is the objective to be minimised, where $\Pi_{ele}(t)$ and $\Pi_{gas}(t)$ represent the electricity and gas prices at time step *t* with the units of m.u. (monetary units)/p.u. (power units). *T* is the number of total time steps. The inequality constraints are to consider the safety of operating the energy hub system. (5-19b) indicates that the value of dispatch factors should be within the boundary of 0 and 1. (5-19c) specifies the minimum and maximum power and gas input to the energy hub system. (5-19d) is the limitations of the energy inputs to each hub. (5-19e) reflects the voltage and pressure constraints at each bus and node. (5-19f) is the constraint on gas pressures. (5-19g) and (5-19h) are the minimum and maximum power outputs for converters.

Because temporary overloading along branches is tolerable, the chance constraints are applied to restrict the power and gas flows between hubs in (5-19i). *Pr* is the probability of the chance constraint, where a probability level α is established to restrict the deterministic constraints. Equation (5-19i) means that the probability of energy flows less than the maximum allowable energy flows should be higher than α. Therefore, solving problem (5-19) is to optimise the energy hub systems while considering the safety and chance constraints, with renewable energy randomly generated according to the distributions.

5.5.2. Cornish-Fisher Expansion

The problem (5-19) is a stochastic problem with chance constraints. To properly solve it, this paper proposes to apply the Cornish-Fisher Expansion (CF) method to convert the chance constraints into deterministic constraints so that deterministic optimisation approaches can be applied.

Equation (5-19i) could be converted into (5-20) because the quantile presents monotone relation with its inverse CDF [26].

$$q_{Q_{i,j}}(\alpha) \leq Q_{i,j,max} \qquad q_{S_{i,j}}(\alpha) \leq S_{i,j,max} \tag{5-20}$$

In (5-20), q is defined as the quantile, which quantifies the inverse function of the random variable's Cumulative Distribution Function (CDF) with the given probability level α. The CF is expressed as a function to calculate the quantile of a random variable in terms of its cumulants, and it is formulated in (5-21) in terms of α with five orders of

cumulants [11].

$$q(\alpha) = A(\alpha) + \frac{A^2(\alpha)-1}{6}\kappa_3 + \frac{A^3(\alpha)-3A(\alpha)}{24}\kappa_4 - \frac{A^3(\alpha)-5A(\alpha)}{36}\kappa_3^2 + \frac{A^4(\alpha)-6A^2(\alpha)+3}{120}\kappa_5 - \frac{A^4(\alpha)-5A^2(\alpha)+2}{24}\kappa_3\kappa_4 + \frac{12A^4(\alpha)-53A^2(\alpha)+17}{324}\kappa_3^2 \quad (5\text{-}21)$$

Where A is the quantile of the standard normal distribution when the probability is α, and κ_v is the cumulants with order v.

To calculate the quantiles of chance constraints by CF, they need to be firstly converted into the formulation in terms of the uncertain variables and other control variables. The polynomials containing uncertain variables can then be expressed with the CF to derive the quantile. The process of deriving the quantiles of chance constraints Q_{12} is illustrated as an example through (5-22) and (5-23). By combining all constraints in (5-1)-(5-14), Q_{12} at each time step t can be expressed by the outputs of two wind farms ξ_1 and ξ_2 and other control variables x in (5-22).

$$Q_{1,2}(t) = a_1\xi_1(t) + a_2\xi_2(t) + Co(t) \quad (5\text{-}22)$$

In (5-22), *Co(t)* represents the function comprising the polynomials of control variables. a_1 and a_2 are the coefficients related to the two uncertain variables. With the linear relation between the outputs of two wind farms as illustrated in (5-17), (5-22) could be converted into:

$$Q_{1,2}(t) = (a_1 + a_2 \cdot f_1(t))\xi_1(t) + f_2(t) + Co(t) \quad (5\text{-}23)$$

With CF, the uncertain variable $\xi_1(t)$ can be expanded by (5-21) when the probability level is α. The quantile of Q_{12} can be calculated via (5-21)-(5-23), modelled as a deterministic value in (5-20). When the same method is applied to other chance constraints, the stochastic problem of CCP can be converted into a deterministic problem.

5.5.3. Overall Flowchart of the Methodology

The flowchart of implementing the CCP on energy hub system optimisation is shown in Fig. 5-4. Firstly, data including energy hub load, distributions of renewable generations, and system parameters are acquired, and the optimisation problem is built.

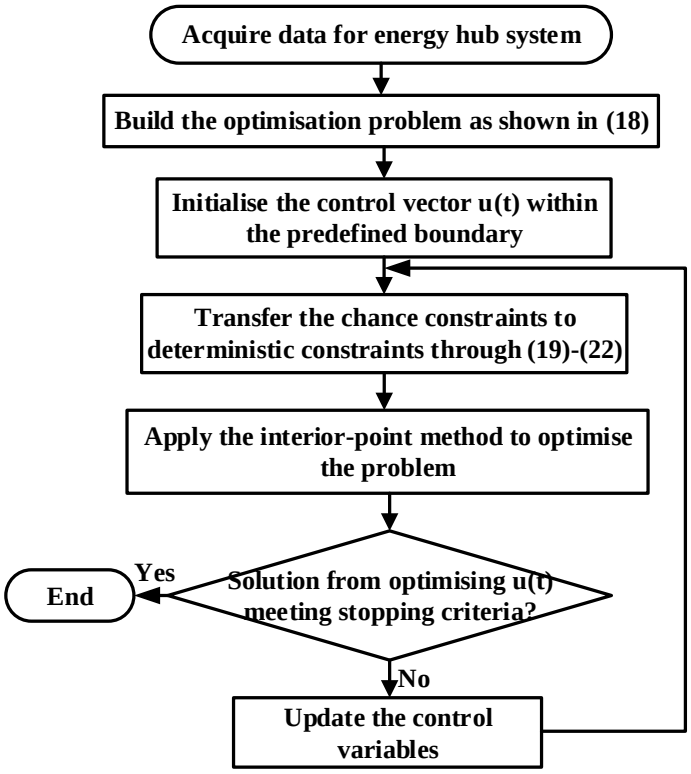

Fig. 5-4.Flowchart of CCP-based energy hub optimisation

Then, the control vector *u(t)* is initialised based on the lower and upper boundaries. The chance constraints are then transformed into deterministic constraints by using CF. The interior-point method is heuristically applied to solve the model.

It should be noted that the quantiles of chance constraints depend on both the control variables and uncertain variables with given probability levels. Hence the chance constraints need to be iteratively translated into deterministic constraints when the control variables are updated at each iteration.

5.6 Case Study

Two cases studies are presented in this section for demonstration, where chance constraints are separately applied to restrict the power flow and gas flow between hubs. The CCP is applied to investigate the effects of uncertainties on integrated DR with energy hub optimisation.

5.6.1. Data Setup

According to [15, 27], the wind speed generally follows the Weibull distribution. Therefore, the historic data of wind speed at each time step is fitted through the Weibull distribution to derive the probability density function (PDF) at each time step. By using

the random numbers generated from the distributions of wind speeds, Monte Carlo method is applied to evaluate the distributions of wind farms in the 2-hub interconnected system, shown in Fig. 5-3. As an example, Fig. 5-5 (a) shows wind speed distribution observed at wind farm 1 at time step 9, Fig. 5-5 (b) presents the related distribution of power output from wind farm 1. The cumulants with different orders could then be calculated by the samples of wind farm generations. As the correlation between the two wind farms' outputs is established, the distribution of power output from wind farm 2 at each time step and related cumulants can be accordingly derived by (5-17).

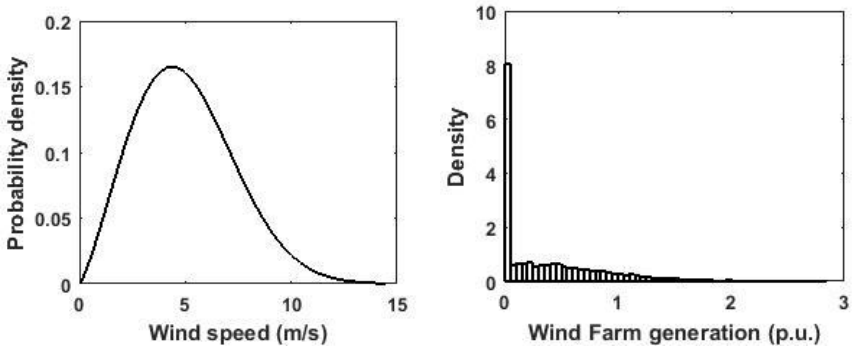

Fig. 5-5.PDF of wind speed and power generation derived at wind farm 1 at time step 9

The reference electricity price P_{ref} input by customers over 24 hours is adopted from [28], shown in Fig. 5-6. The electricity load of hubs 1 and 2 are assumed to be price elastic, the price elasticities of hub 1 and 2 are adopted from [24] as -0.8 and -1.4. The gas price is assumed to be constant with 0.04 m.u./p.u. over the whole time period. The electrical load and thermal load of the energy hub system over 24 hours are modelled according to [29] and [30] respectively. The constraints and system parameters required for the optimisation are given in Table 5-1, which are derived from [1, 3, 13, 21, 31].

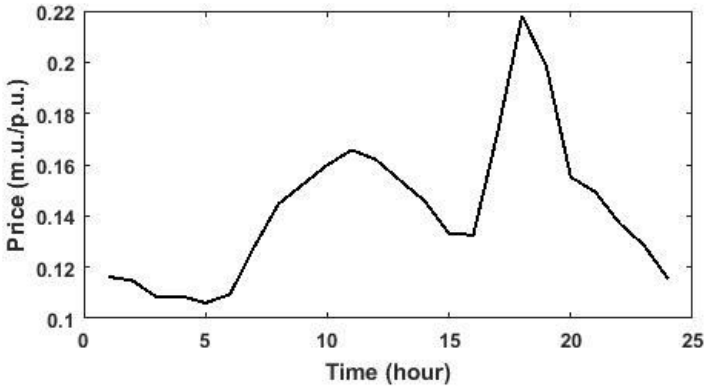

Fig. 5-6.Electricity price over 24 hours.

Table 5-1.ENERGY HUB SYSTEM PARAMETERS AND CONSTRAINTS

System parameters	
Line 1-2	Z_{12}=0.3+j0.9 p.u., Y_{12}=j1.5·10^{-6} p.u.
Line 1-3	Z_{13}=0.2+j0.6 p.u., Y_{12}=j2.5·10^{-6} p.u.
Pipe lines	GHV·k_{12}=4.5 GHV·k_{13}=3.0
Compressor	GHV·k_{com}=0.5
CHP	η_e=0.33, η_{gh}=0.57
GF	η_F=0.75
Storage	E_h^{stb}=0.5, e_h^+= e_h^-=0.9
WT	v_{ci}=4m/s, v_{co}=25m/s, v_{rs}=16m/s, P_{rated}=3p.u.
Constraints	
Nodes	$0.8 \leq \lvert V_m \rvert \leq 1.2$ p.u.
m=1, 2, 3	$p_m \leq 1.2$ p.u.
Compressor	$1.2 \leq p_m / p_k \leq 1.8$
CHP input	$0 \leq P_{CHP,input} \leq 1$ p.u.
GF/GSHP	$0 \leq P_{GSHP/GF\_input} \leq 1.5$ p.u.

5.6.2. Case 1-Power Flow Restricted by Chance Constraints

1) Optimisation under Different Probability Levels of Chance Constraints

The optimisation is carried out with different probability levels of chance constraints to investigate how the CCP influences the DR scheme and energy hub system operations. The maximum power flow between hubs are assumed to be 1.6 p.u. and restricted by chance constraints for case 1. Four probability levels 80%, 85%, 90%, 95% are separately applied to limit the chance constraints.

All results are analysed through their cumulative distribution function (CDF) curves, obtained by sampling the optimisation results of 200 different samples. Between the probability of 80% and 99.99%, 200 probability levels are uniformly adopted and applied to each sample to restrict the chance constraints.

The CDF curves of the optimisation results in terms of system total costs are shown in Fig. 5-7, where the chance constraints' probability levels are higher than 80%, 85%, 90%, and 95% respectively. As seen, the optimised total costs vary between 5.47 m.u. and 6.26 m.u for all probability levels, and the CDF curves vary with similar gradients.

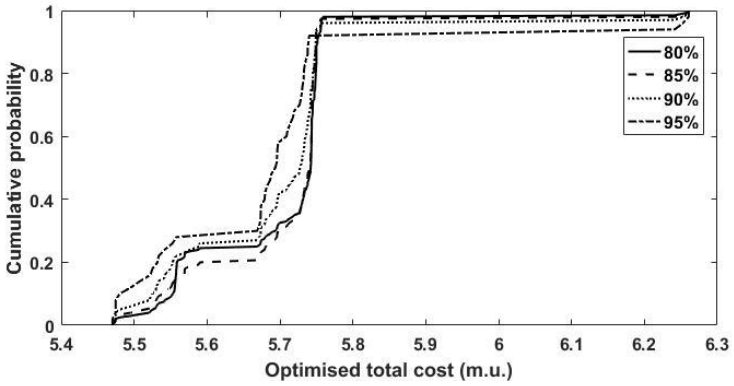

Fig. 5-7.CDF curves of optimised total cost.

It can be observed that all CDF curves have two major increases when the possible optimised total costs vary from 5.47 m.u. to 5.56 m.u., and 5.68 m.u. to 5.74 m.u.. It indicates high probability density and the possible optimised costs are centralised in these intervals.

The electrical and thermal loads are relatively high at time step 9, hence the optimal operations at this time step are of interest to investigate. The CDF curves of the active power injection to hub 2 at time step 9 are shown in Fig. 5-8. With the chance constraints restricted by different probability levels, the CDF curves of total active power injection present similar characteristics. All CDF curves dramatically increase from 0.02 p.u. to approximately 0.21 p.u. with the cumulative probability increase to the boundary between 80% and 95%, and gradually increase from 0.21 p.u. to 1.89 p.u. with the cumulative probability reaches 100%. Since the power flow between hubs is restricted by chance constraint, and the CHP can be switched on to supply the electricity load, the magnitudes of active power input to hub 2 are therefore less, which concentrate on the interval between 0.02 p.u. and 0.21 p.u..

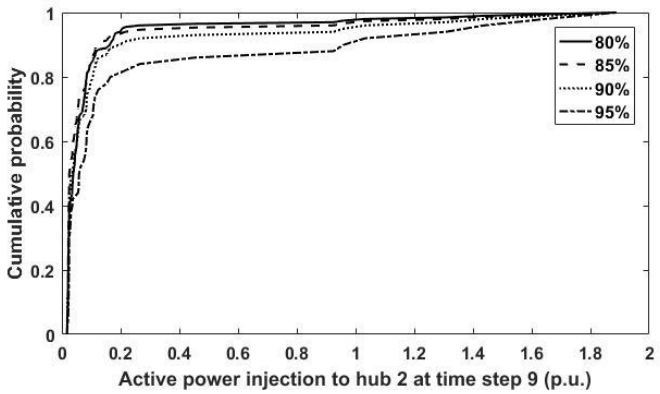

Fig. 5-8.CDF curves of the active power input to hub 2 at time step 9.

Because the relationship between the energy hub active power injection and total cost is non-linear, the CDF curves in Fig. 5-8 show completely different characteristics with the CDF curves in Fig. 5-7 in terms of shape and gradient. The value of active power injection could be non-linearly affected by the gas injection, re-scheduled load, and possible wind power, leading to an unpredictable variation in system total cost. Additionally, the optimisation problem is formulated as a complicated multi-period problem, the operations at current time step could non-linearly affect the operations of following steps. Hence, the high flexibility could result in a random change in system total cost when the total active power input changes.

2) Variation of Load Pattern

After implementing the optimisation with the chance constraints restricted by 80%, most of the optimal electricity prices during high tariff period from 17 to 24 are increased compared with the reference prices, the majority of prices at other time steps are decreased. The comparison between the optimised electricity loads (dotted line) of hub 1 and 2 with their original loads (solid line) are depicted in Fig. 5-9 and 5-10.

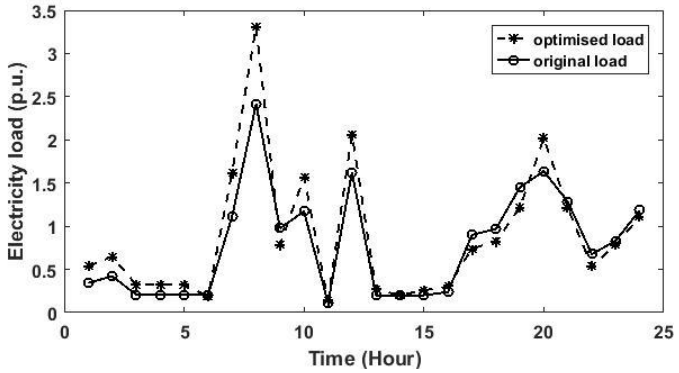

Fig. 5-9.Electricity demand of hub 1 over 24 hours

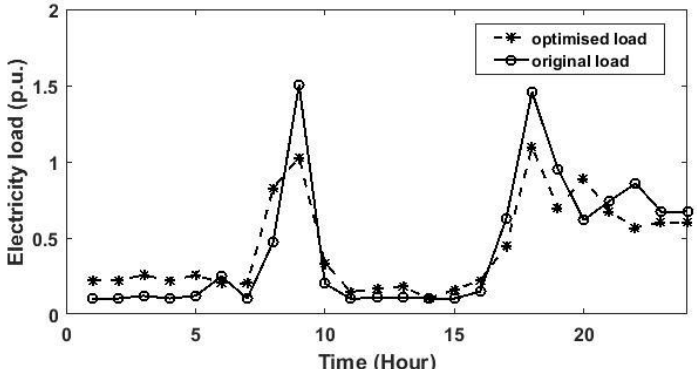

Fig. 5-10.Electrical demand of hub 2 over 24 hours.

Regarding to the same amount of change of electricity price, the loads in hub 2 vary

more broadly compared with hub 1 due to different price elasticities considered in each hub.

If the effect of energy hub is excluded, it can be derived from (5-14) and (5-15) that the electricity consumption cost is monotonically decreasing with electrical load if the elasticity is greater than -1, and monotonically increasing with load if the elasticity is less than -1. The price elasticities of hub 1 and 2 are -0.8 and -1.4 respectively, and the holistic load of hub 1 is higher than hub 2, hence reducing electricity price and enhancing load would be relatively cheaper.

When the effect of energy hub is considered, it can be observed from Fig. 5-9 and 5-10 that the majority of re-scheduled loads are increased compared with the reference load, and the loads over high-tariff period are slightly decreased. It is because that the energy cost can thus be reduced by increasing the electricity load as aforementioned. Additionally, the electricity load can also be satisfied by consuming relatively cheaper natural gas with CHP or importing the free wind power generation, which further decreases the energy cost.

The optimal operations of converters in hub 2 to satisfy the electrical demands are shown in Fig. 5-11. The power injection to hub 2 (denoted by crosses), the power output from CHP (denoted by diamonds), and the average power output from WT (denoted by circles) are co-ordinately operated to meet the electrical load (denoted by histograms) and the power input to GSHP (denoted by stars).

It could be observed from Fig. 5-11 that the power inputs to hub 2 are zero at most time steps. It is because the WT and CHP are substantially generating power, since the cost of consuming gas to generate power is relatively low, and the wind energy is free.

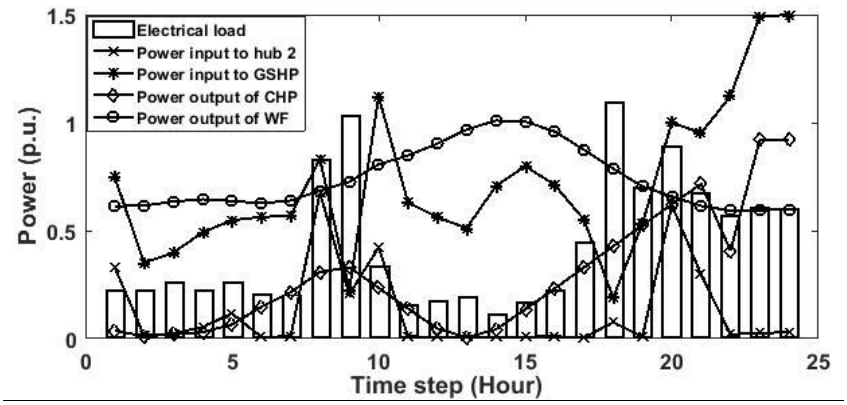

Fig. 5-11.Optimal operations of hub 2 over 24 hours

Therefore, not only responding to the varying electricity price, the demand also varies according to the operations of renewable generators and other converters.

5.6.3. Case 2-Gas Flow Restricted by Chance Constraints

The gas flow between energy hubs is restricted by chance constraints in this case. By setting the maximum gas flow between hubs as 1.8 p.u., the probability levels of 80%, 85%, 90%, 95% are separately applied to restrict the chance constraints of maximum gas flow. Similar to case 1, 200 samples are optimised to acquire the CDF curves to examine the effects of CCP. The CDF curves of the optimisation results in terms of the system total cost are shown in Fig. 5-12.

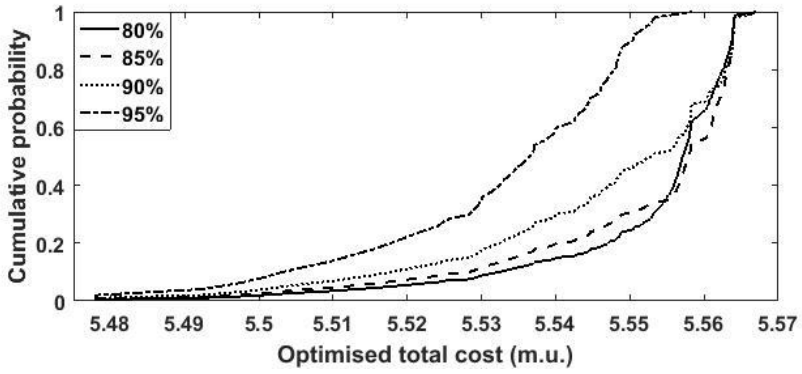

Fig. 5-12.CDF curves of optimised total cost.

As seen, for the probability levels of chance constraints higher than 80%, 85%, and 90%, the CDF curves of optimised total costs vary between 5.48 p.u. and 5.57 p.u. with the cumulative probability increase from 0 to 1. When the probability of chance constraint is higher than 95%, the possible total costs change from 5.48 p.u. to 5.55 p.u..

Compared with the CDF curves in Fig. 5-7, the CDF curves are more similar to each other in Fig. 5-12 when different probability levels are applied to restrict chance constraints. Moreover, the possible optimised total cost of all CDF curves in Fig. 5-12 span narrower than the curves in Fig. 5-7. The above phenomena suggest that the optimisation for carrying out DR scheme on energy hub system may be more affected when the power flow between hubs are restricted by chance constraints.

The CDF curves of the active power injection to hub 2 at time step 9 with different chance constraints probabilities are presented in Fig. 5-13. The possible values of the active power injection change from 3.39 p.u. to 3.41 p.u. with the cumulative

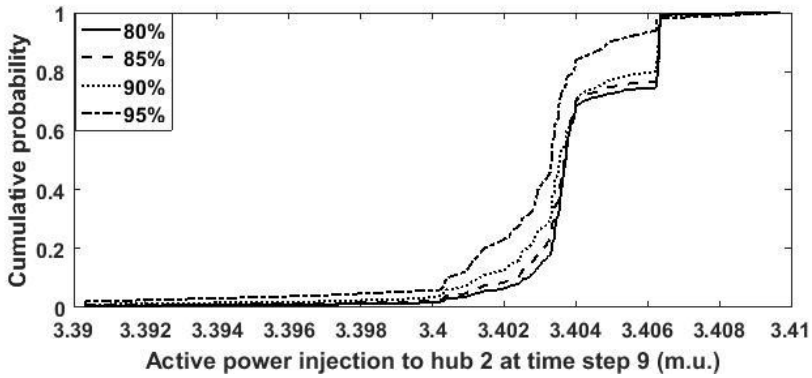

Fig. 5-13.CDF curves of the active power input to hub 2 at time step 9.

probability increase from 0 to 1. Most of the values of active power input concentrate on the interval between 3.40 p.u. and 3.406 p.u., which are significantly improved compared with Fig. 5-8. It is because the gas flow between hubs is restricted by chance constraints, and the power generation from CHP is limited, hence more power should be imported from the grid.

The values of total active power input are changing within the boundary of 0.019 p.u., which is much less than the value changed on the abscissa in Fig. 5-8. It also demonstrates that the optimisation is less influenced when the gas flow between hubs is restricted by chance constraints.

5.7 Conclusion

The chance-constrained programming is proposed in this paper to solve the energy hub optimisation considering both demand response and the correlation between the outputs of different wind power through extensive demonstrations, the main findings are as follows:

- Chance-constrained programming is capable to solve energy hub optimisation with DR and correlation of wind power, considering temporary overloading is permitted.
- Customer load pattern is significantly affected in response to the variations of energy prices and energy hub operations. The holistic loads are increased, and the loads over high-tariff periods are slightly decreased.
- The effects of chance-constrained programming on energy hub optimisation are relatively high when the chance constraints are restricting power flow between hubs.

The optimal operation is more stable when gas flow between hubs is restricted by chance constraints.

The proposed chance-constrained programming is useful for hub operators to efficiently operate the hubs and make the best of system capacity for benefiting themselves and customers with reduced investment and bill costs. The model is easy to expand to energy hub systems with more smart appliances, such as storage and solar power.

5.8 Chapter Summary

By explicitly modelling the correlations between geographically close wind farms with Pearson correlation, this chapter improves the chance-constrained programming for interconnected energy hubs optimisation developed in chapter 4. Additionally, the customers' reaction to smart scheduling is also reflected by considering elastic demand, and incorporating demand response into energy hub optimisation. The optimisation scheme benefits both the operators and end customers with reduced investments and energy costs by maximally utilise the flexibility of energy hub system.

Chapter 6

Optimisation for Interconnected Energy Hub System with Combined Ground Source Heat Pump and Borehole Thermal Storage

This chapter investigates the optimal operations of borehole thermal storage within the interconnected energy hubs, by respectively adopting the Finite Element and transfer function to model the performance of borehole thermal storage.

Chapter Overview

Previous chapters investigate the optimisation for interconnected energy hub system under steady state or considering uncertainty. From the prospect of operating future smart grids, the energy hub system is foreseen to be cooperative with other system operating or smart technologies to increase power system flexibility or achieve some optimisation objectives. Therefore, the optimisation of energy hub system with other technologies are of interest to research.

As indicated in section 2.2.5, the combined ground source heat pump and borehole thermal storage raised researchers' attention in recent years due to their high efficiency and stable performance. The energy hub system can benefit from the combined system to efficiently satisfy the thermal load, the mixture of power and thermal of the system can also well fit into the energy hub modelling. Therefore, the optimal operations of combined ground source heat pump and borehole thermal storage are investigated within the interconnected energy hubs in this chapter. The main contributions of this chapter is summarised as follows:

i) The borehole thermal storage is assumed to be equipped to support a residential community, which is modelled by an interconnected energy hub system. The optimisation for the community is investigated.

ii) The Finite Element model is employed to model the performance of the borehole thermal storage in response to the varying input boundary conditions. An equivalent transfer function model is proposed to model the borehole storage in order to reduce the computational time.

iii) The optimisation problem is formulated as a multi-period, non-convex problem, which is resolved by applying the decomposed Particle Swarm Optimisation approach proposed in chapter 3.

Statement of Authorship

This declaration concerns the article entitled:			
Optimisation for Interconnected Energy Hub System With Combined Ground Source Heat Pump and Borehole Thermal Storage			
Publication status: Published			
Publication details (reference)	Da HUO, Wei WEI, Simon Le BLOND. Optimisation for interconnected energy hub system with combined ground source heat pump and borehole thermal storage[J]. Front. Energy,, (): 0-.		
Candidate's contribution to the paper	The candidate and the second author jointly proposed the idea of the paper, and they designed the methodology. The candidate designed the case studies, and executed most of the coding to derive the experimental results. The third author helped the candidate with the format of the paper, and improvement of academic writing. The percentage of the candidate did compared with the whole work is indicated as follows: Formulation of ideas: 70% Design of methodology: 80% Simulation work: 90% Presentation of data in journal format: 70%		
Statement from candidate	This paper reports on original research I conducted during the period of my Higher Degree by Research candidature.		
Signed	Da Huo	Date	31/08/2018

6.1 Abstract

Ground source heat pumps (GSHP) give zero-carbon emission heating at a residential level. However, as the heat is discharged, the temperature of the ground drops, leading to a poorer efficiency. Borehole inter-seasonal thermal storage coupled with GSHP maintains the efficiency at a high level. To adequately utilize the high performance of combined GSHP and the borehole system to further increase system efficiency and reduce cost, such a combined heating system is incorporated into the interconnected multi-carrier system to support the heat load of a community. The borehole finite element (FE) model and an equivalent borehole transfer function are proposed and respectively applied to the optimisation to analyze the variation of GSHP performance over the entire optimisation time horizon of 24 h. The results validate the borehole transfer function, and the optimisation computation time is reduced by 17 times compared with the optimisation using the FE model.

6.2 Introduction

In order to reduce the pollution caused by utilizing fossil fuels and adopt a sustainable economy, the UK government aims to reduce carbon emissions by 80% before 2050 compared with the 1990 baseline [1]. Domestic buildings consume 40% of the total energy of the society [2], which implies that there is a great potential for saving energy and increasing energy efficiency at domestic level. The energy hub modelling approach could, therefore, be employed to adequately exploit renewable energy, increasing energy efficiency and sustainability without compromising on energy security. The energy hub modelling framework provides an effective way to holistically harness different energy infrastructures by considering them as an integrated system. The corresponding co-generation or tri-generation technology enables flexible energy management among all available energy carriers [3].

A typical energy hub provides the functions of importing, exporting, converting, and storing energy. Conventional converters such as gas furnace and micro-turbine have been analysed within the energy hub system [4, 5]. Recently, research efforts have been made to address the application of low-carbon and high efficiency converters in energy hub systems, such as combined heat and power plant (CHP) [6, 7] and heat pumps [8]. The efficiency of the heat pump is dependent on the heat source temperature and indoor temperature. The application of the borehole storage can significantly increase the

GSHP performance since the thermal storage provides a high temperature source, raising the coefficient of performance (CoP) of ground source heat pumps (GSHP). Therefore, the combination of GSHP and borehole thermal storage is studied in this paper.

Energy storage system is a viable solution for the multi-carrier system to stabilise and balance system equilibrium [9, 10]. Borehole thermal storage uses the ground as a heat source and storage medium. High temperature fluid flows through the borehole pipes and stores the heat energy into the surrounding ground and this process is done by heat transfer [11]. After the fluid dumps the heat into the borehole, the temperature settles down in the borehole wall area and when the heat is needed from the borehole, the fluid extracts the heat from borehole wall and provides high temperature source. The relationship between borehole wall temperature and charging/discharging energy is analysed by applying the finite element method which is used to synthesise an equivalent borehole wall temperature transfer function. In the FE model, the mesh number is enormous, which wastes more time. As a result, it is significant to simplify the borehole model. Borehole transfer function model uses the borehole wall temperature response to the input heat flux to create a simplified borehole model.

To sufficiently utilize the high performance of combined GSHP and borehole system to further decrease the overall system cost, the combined GSHP and borehole system operations are optimised within the context of the energy hub in this paper.

In addition to the traditional optimisation of the single energy hub, the interconnecting heterogeneous energy infrastructure at a local level can best leverage renewable generation and pooled storage without suffering from large distance transmission losses and enable self-sufficient energy communities. Additionally, the energy management between buildings enables adequate utilization of energy redundancy in each building, which comprehensively achieves the system optimisation. Hence the interconnected energy hub approach at the residential level has a huge potential for reducing the energy costs and increasing the energy efficiency. The optimisation considering both the power flow and energy hub operations within the interconnected energy hub system has been implemented in Refs. [4, 7, 12–14]. However, when the mathematical model of heat storage such as borehole is explicitly considered, the coordination of GSHP and heat storage within the context of energy hub optimisation has not been studied. This paper investigates the optimisation of an interconnected energy hub system with different

heating converters equipped within each hubs. Such a heating network considers the effective cooperation between the conventional gas heating, CHP and a combined GSHP and borehole storage system.

To effectively reduce the cost of the energy hub system, an optimal policy needs to be determined against the time-varying energy tariffs, converter efficiency etc. The performance of GSHP at each time step is related to the wall temperature of the borehole, which is derived by analysing the heat flux input/output from the borehole over the whole time horizon. Besides, due to the ramp rate restriction for CHP, the operations of a CHP between each time step are interdependent. Therefore, the optimisation of the interconnected energy hub system is formulated as a non-convex multi-period optimisation problem. Different approaches have been implemented to solve energy hub optimisation problems with similar complexity. In Refs. [12, 15], the model predictive control scheme is applied to optimally control the operations of three interconnected energy hub systems. The multi-agent genetic algorithm is utilized to optimise the power and gas flows between energy hubs in Refs. [4, 16]. The multiagent-based consensus algorithm and the event-triggered control scheme are respectively applied in Refs. [17, 18] to optimise the multi-carrier system within the context of energy internet. The existence of Nash equilibrium is researched for the optimisation of multiple energy hub systems in Refs. [19–22]. A modified version of the teaching-learning-based optimisation is proposed and carried out in [5] for the energy hub system where the converters present a non-constant efficiency. Among the above optimisation techniques, the global minimum cannot be guaranteed when solving the highly-complex problem, and the mathematical problem is relatively easy when the global minimum could be found. A decomposed approach for implementing particle swarm optimisation (PSO) [23] is proposed in [14], which presents a high performance with a fast converging speed when solving the highly-constrained interconnected energy hub problem. The decomposed technique is, therefore, utilized in this paper to optimise the operations of the energy hub system together with the borehole system.

To sum up, in this paper, the optimal operations of combined GSHP and borehole system is investigated within the optimisation scheme of energy hub, an equivalent transfer function of the borehole model is presented, and the decomposed technique of applying PSO is incorporated to the interconnected energy hub optimisation.

6.3 Modelling

Since domestic buildings consume approximately 40% of the total energy, in which the electricity consumption accounts for around 68% [2], the power system can significantly benefit from optimally dispatching the application of various energy carriers among residential houses. As any scale of energy systems can be modelled by energy hub [24], and different energy infrastructures such as electricity, gas, and heat are generally equipped within domestic houses, the energy hub is, therefore, applied to model the residential house. In this paper, the optimal operations of multiple residential houses with borehole system are investigated.

The configuration of *K* number of interconnected energy hubs is shown in Fig. 6-1. The system represents a community including *K* residential houses where electricity and heat could be co-ordinated between each other. The power adjustment between hubs could be achieved through the electrical connection indicated in Fig. 6-1. For example, the electricity transfer from hub *K*–1 to hub *K* is achieved by injecting electricity to the grid from hub *K*–1, and extracting the same amount of electricity from the grid to hub *K*. The heat sharing is assumed to be available between adjacent hubs. The borehole storage is set up within the community, which supplies the GSHP equipped within each house. The heating converter including micro-combined heat and power systems (micro-CHP) and gas furnace are also included. Each house is modelled as an energy hub.

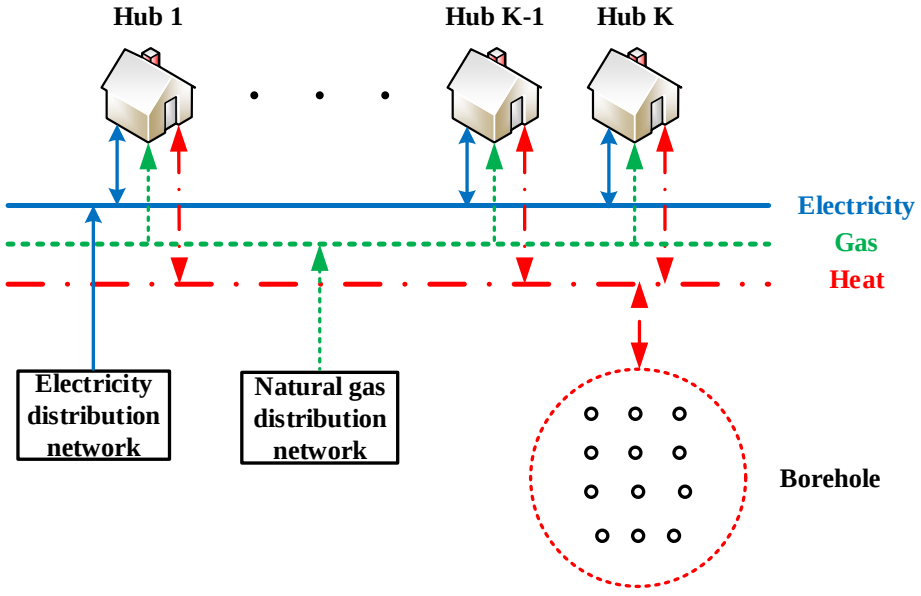

Fig. 6-1.Eleven interconnected energy hubs system

The optimisation for the interconnected energy hub systems is implemented by determining the operations of each hub over the whole time horizon to reach a minimum system cost, with the knowledge of the prices of energy carriers, load profile, system parameters, etc. To mathematically model the optimisation problem, detailed mathematical models of converters, borehole, and energy hub are illustrated in the following sub-sections.

6.3.1. Micro-CHP

The micro-CHP simultaneously generate power and heat by using gas. Compared with conventional heating converters, such as a gas furnace, micro-CHP produces a higher overall efficiency and a lower carbon emission [25]. The micro-CHP employed in the energy hub model is assumed to be steady-state with a constant electric efficiency and thermal efficiency. In addition to the constraint of maximum CHP output, the ramp rate of CHP is considered in this research and given by

$$e_{\mathrm{p}}(t-1) - e_{\mathrm{ramp}} \leq e_{\mathrm{p}}(t), \tag{6-1}$$

$$e_{\mathrm{p}}(t-1) + e_{\mathrm{ramp}} \geq e_{\mathrm{p}}(t), \tag{6-2}$$

where e_{p} is the power output of the micro-CHP, the variable t corresponds to the time step number in discrete time, so that any variable that is a function of time is fixed during time step t, and e_{ramp} is the micro-CHP maximum ramp rate.

6.3.2. Ground Source Heat Pump

In 2014, the Renewable Heat Incentive (RHI) was launched in the UK to increase the installation of low carbon technologies [26]. Heat pumps have lower carbon emissions than the conventional heating methods such as a boiler. Ground source heat pumps (GSHP) are widely used since they have a higher and more stable CoP over other heat pump types, due to the fact that ground temperatures remain constant throughout the whole year. The definition of CoP is

$$H = \mathrm{CoP} \cdot P_{\mathrm{e}}, \tag{6-3}$$

where H is the heat energy output and P_{e} is the electricity required by the heat pump.

The CoP equations for this paper is obtained from the real world project, CHOICES [27]. The CoP value depends on the condenser water outlet temperature, the evaporator inlet temperature, and the GSHP installation capacity which is the maximum heat

energy that GSHP can generate. GSHP is connected to the borehole storage which will provide a higher evaporator inlet temperature. GSHP consumes electricity and generates heat energy to meet the heat demand. Within each condenser temperature category and capacity limit, the CoP value can be seen as a linear function between the GSHP cut-off temperatures.

$$\mathrm{CoP}_{\mathrm{new}} = a \cdot T + b, \tag{6-4}$$

where T (°C) is the borehole wall temperature , a and b are constants. The calculation of CoP values with response to different heat pump evaporator inlet temperatures (borehole wall temperature T) at each condenser outlet temperature category is demonstrated in Table 6-1.

In this system, the GSHP is used for space heating, so that the condenser water outlet temperature is set to 55°C which is the water temperature running in the radiator in houses.

Table 6-1.GSHP COP CALCULATION

Condenser water outlet temperature /°C	CoP (T represents the evaporator inlet (borehole) temperature)
30	$0.1362 \times T + 4.8002$
35	$0.1265 \times T + 4.2335$
40	$0.1135 \times T + 3.7365$
45	$0.1002 \times T + 3.2873$
50	$0.0918 \times T + 2.8072$
55	$0.0850 \times T + 2.3483$

6.3.3. Borehole

Borehole thermal storage comprises of an array of vertical holes drilled under the ground. The depth of each borehole could be up to one hundred and fifty meters into the bedrock. The temperature of the soil remains steady throughout the whole year. In winter, the temperature of the soil is generally higher than the ambient air temperature which helps to create a high and stable GSHP output [28]. There are three mediums in the borehole system, antifreeze agent water, grout (backfill material), and the surrounding soil. The borehole system can be built up in the FE model and there are different input boundary conditions such as temperature, density, heat capacity, the coefficient of heat conduction, heat source (heat flux), etc. With the input information,

each medium is subdivided into a massive number of meshes and the value of each mesh node is solved by the partial differential equation toolbox in the MATLAB technical computing environment.

This paper uses the borehole system from the CHOICES project with 12 boreholes to supply the community modelled by the energy hub system. The CHOICES borehole FE model generates thousands of temperature points at each time step. Table 6-2 lists the borehole parameters used in the FE model. In the FE model, with heat flux injection/extraction, heat transfer happens between boundaries, and the temperature of the whole area is represented by each node as is depicted in Fig. 6-2. The temperature rises as it gets closer to the borehole centre. However, the temperatures needed in the system are the borehole wall temperatures. In the FE model, the temperature distribution across the borehole storage is represented by millions of nodes, and as a result, the borehole wall temperature is obtained by calculating the mean value of the

Table 6-2. BOREHOLE PARAMETERS

Parameter	Ground	Grout	Fluid
Density/(kg·m^{-3})	2770	1550	1052
Heat capacity/(j·(kg·K)$^{-1}$)	826	1000	3795
Thermal conductivity/(W·(m·K)$^{-1}$)	2.61	2.1	0.5
Diameter/m	---	0.15	0.07

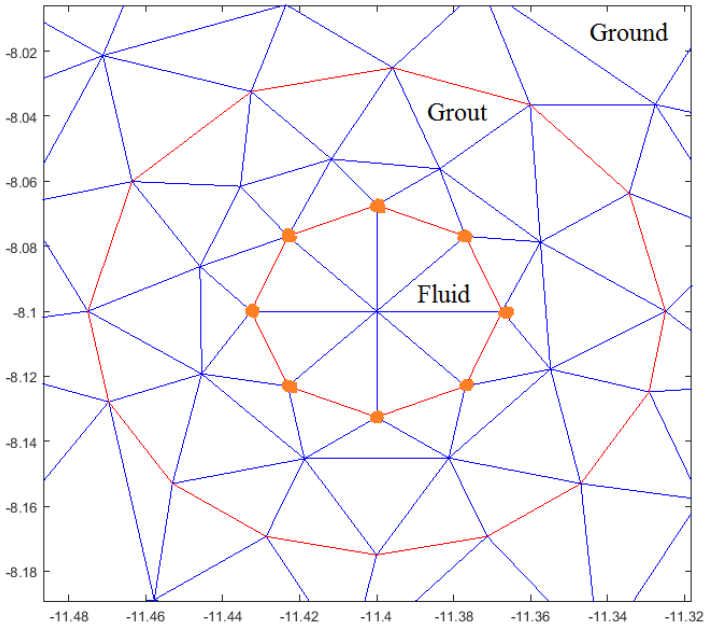

Fig. 6-2.Single FE borehole model cross section view

borehole wall area nodes as the orange nodes shown in Fig. 6-2. After the charging period, the temperature settles in the borehole wall area, and during the heating season, the borehole wall temperature is treated as the GSHP inlet temperature. As a result, the borehole wall temperature is the key aspect of this system which is affected by the heat flux extraction during the heating season.

With the borehole wall defined, Fig. 6-3 gives an example of temperature response to the heat flux output. With constant heat flux (example, 1000 W/m^3) in each time step for 30 hours, the borehole wall temperature decreases (as shown in Fig. 6-3).

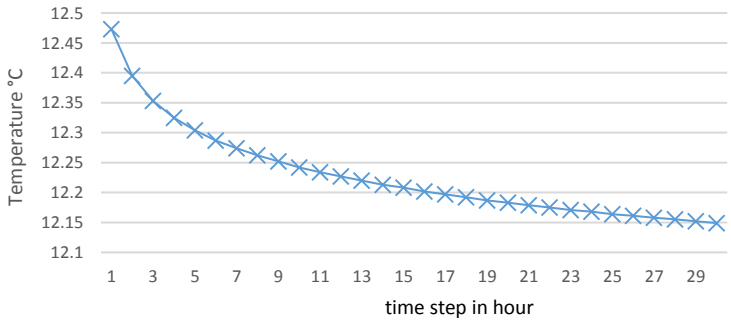

Fig. 6-3.Variation of borehole wall temperature with constant heat flux output

This paper focuses on the heating season so that the starting borehole wall temperature is set to an initial temperature. The borehole system is considered to be an isolated system such that the temperature exchange between the borehole unit and the far surrounding soil can be ignored due to the short simulation time. It is assumed that the borehole wall starting temperature is 20°C after the charging period which is not considered in this simulation. However, it is worth noting that in practice, the borehole wall temperature could be charged to a higher level to obtain higher CoP values over the heating season.

To accelerate optimisation, instead of using the complex borehole FE model, an equivalent borehole wall temperature transfer function is used. By using the borehole wall temperature response to the different heat flux input information from the FE model, a transfer function model is generated. It takes much less computation time for the transfer function to solve the relationship between the input heat flux and the borehole wall temperature. The transfer system is obtained by the system identification toolbox in the MATLAB using the temperature and heat flux relationship over the time.

$$H = \frac{T}{\mathrm{hf}} = \frac{8.693\times10^{-8}\, s+3.625\times10^{-13}}{s^2+0.0001488s+1.079\times10^{-10}}, \tag{6-5}$$

where T (°C) is the borehole wall temperature, hf (W/m^3) represents the heat flux, s refers to the s domain complex frequency parameter used in the transfer function.

By expressing the transfer function in the time domain, Eq. (6-5) can be used to model how the heat input in a previous time step leads to the temperature change in the current time step. Fig. 6-4 exhibits the difference of borehole wall temperature change between the FE model and the transfer function with the same heat flux output over 30 hours. The average temperature difference is 0.07 °C as shown in the figure.

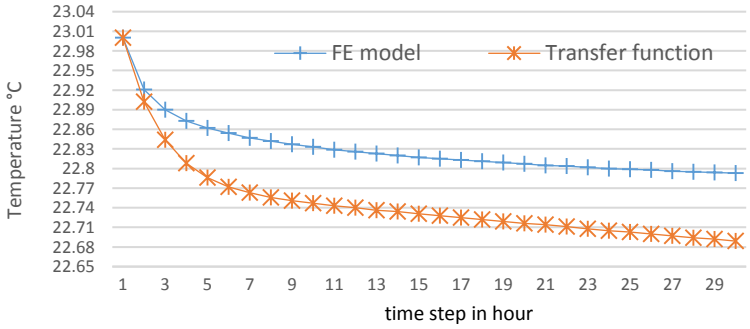

Fig. 6-4.Comparison of FE model and transfer function

6.3.4. Energy Hub Model

Different heating converters are equipped within the energy hub system. In order to efficiently analyse the system, a general formulation of energy hub model including a micro-CHP, a gas furnace, and a GSHP is proposed, as displayed in Fig. 6-5. The transformation between the individual hub output and input is expressed in Eq. (6-6).

$$\begin{bmatrix} L_{\mathrm{ele},i}(t) + E_{ij}(t) \\ L_{\mathrm{th},i}(t) + H_{ij}(t) \end{bmatrix} = \begin{bmatrix} 1 - \nu_{1,i}(t) & 1 - \nu_{1,i}(t) \times \nu_{2,i}(t) \times \eta_e \\ \nu_{1,i}(t) \times \mathrm{CoP}(t) & \nu_{1,i}(t) \times \nu_{2,i}(t) \times \eta_e \times \mathrm{CoP}(t) + \nu_{2,i}(t) \times \eta_{\mathrm{th}} + (1 - \nu_{2,i}(t)) \times \eta_{\mathrm{gf}} \end{bmatrix} \times \begin{bmatrix} P_{\mathrm{ele},i}(t) \\ P_{\mathrm{gas},i}(t) \end{bmatrix} \quad (6\text{-}6)$$

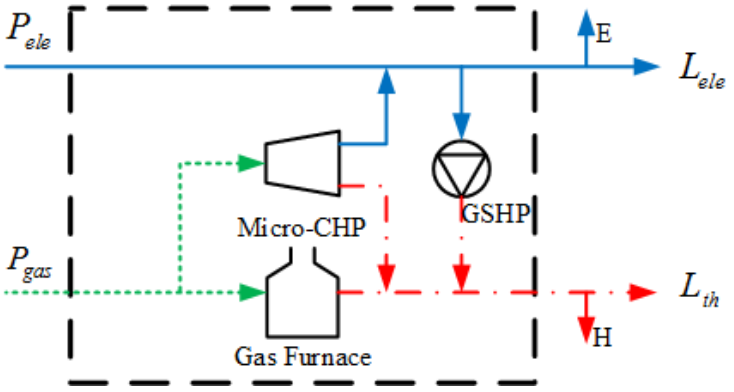

Fig. 6-5.Example of single energy hub

where *i* and *j* denote the hub number; L_{ele} and L_{th} represent the electricity and heat load, respectively; P_{ele} and P_{gas} represent the power input and the gas input; η_{e} and η_{th} are the micro-CHP electric efficiency and thermal efficiency; η_{gf} is the gas furnace efficiency; ν_1 is the dispatch factor, which, in this context, means the ratio of electricity injected to the heat pump divided by the total electricity input to the energy hub; ν_2 denotes the ratio of gas injection to the micro-CHP compared with the total gas injection; and E_{ij} and H_{ij} indicate the power and heat import and export between hub *i* and other hubs.

6.4 Problem formulation and methodology

As illustrated in Section 6.3, the CoP of GSHP is related to the borehole temperature, which is non-linearly affected by the heat flux output at each time step. Additionally, the variations of borehole wall temperature over the whole optimisation time horizon are derived based on the heat flux output at every time step by using the FE model or the transfer function. Therefore, the optimisation for the system needs to be conducted by considering the operations over the whole time period, which generates a multi-period, non-convex problem. With the knowledge of load profile of the hubs, system parameters, prices of energy carriers, and system safety constraints, the optimisation is implemented for the energy hub system to minimise the energy costs over the whole time horizon. The variables to be optimised include the input of the energy carriers, the energy adjustments between hubs, the dispatch factors, and the variations of the CoPs of GSHP over the whole time horizon.

The decomposed approach of applying PSO to the complicated non-convex problem has been demonstrated to be capable of reaching a global minimum comparing with conventional algorithms with better performance [14], and hence it is applied in this paper. The problem formulation and the decomposed approach of applying PSO are illustrated in following sub-sections.

6.4.1. Optimisation problem formulation

The decomposed approach of utilizing PSO is applied to the interconnected energy hub system to perform an optimisation over 24 hours on a typical winter day. Each hour represents one time step. The electricity load, heat load, energy price, the efficiency of each converter and the initial temperature of the borehole field at the first time step are

assumed to be known. The optimisation is then implemented to determine the operation of every hub at each time to give minimum overall system costs.

However, traditional algorithms such as linear programming or other numerical methods are not capable of solving this problem. The electricity price varies between each time step. In addition, along with the variation of borehole wall temperature, the CoP of GSHP is also time dependent. Therefore, the energy hub operations at the current time step may affect the operations at other time steps. Hence, the optimisation is formulated as a multi-period problem. The efficiency of the GSHP changes at each time step, hence the problem is a non-convex optimisation problem [7]. The decomposed approach of using PSO is capable of searching the entire feasible region to find the global minimum. The optimisation is conducted in the MATLAB environment based on the ETH Zurich open source PSO code [29]. The optimisation problem is formulated as follows:

Minimize

$$\sum_{t=1}^{N}\sum_{i=1}^{K}[P_{\mathrm{ele},i}(t)\times\Pi_{\mathrm{ele}}(t)+P_{\mathrm{gas},i}(t)\times\Pi_{\mathrm{gas}}(t)]. \tag{6-7}$$

Subject to (6-1)–(6-6)

$$L_i(t)=C_i(t)\times P_i(t),\forall i,\forall t, \tag{6-8}$$

$$0\le v_i(t)\le 1\ \forall i,\forall t. \tag{6-9}$$

Electricity

$$P_{\mathrm{ele},i,\min}(t)\le P_{\mathrm{ele},i}(t)\le P_{\mathrm{ele},i,\max}(t),\forall i,\forall t, \tag{6-10}$$

$$E_{ij,\min}(t)\le E_{i,j}(t)\le E_{ij,\max}(t),\forall i,\forall t. \tag{6-11}$$

Heat

$$H_{ij,\min}(t)\le H_{ij}(t)\le H_{ij,\max}(t),\forall i,\forall t. \tag{6-12}$$

Gas

$$P_{\mathrm{gas},\min}(t)\le P_{\mathrm{gas},i}(t)\le P_{\mathrm{gas},\max}(t),\forall t. \tag{6-13}$$

Heat pump

$$P_{\mathrm{HP},i,\min}(t)\le \mathrm{CoP}_i(t)\times P_{\mathrm{ele},i}(t)\times v_i(t)\le P_{\mathrm{HP},i,\max}(t),\forall i,\forall t. \tag{6-14}$$

Gas furnace

$$P_{\mathrm{GF,min}}(t) \leq P_{\mathrm{gas}}(t) \times \eta_{\mathrm{gf}} \leq P_{\mathrm{GF,max}}(t), \forall t. \tag{6-15}$$

Micro-CHP

$$e_{\mathrm{p}}(t-1) - e_{\mathrm{ramp}} \leq e_{\mathrm{p}}(t) \leq e_{\mathrm{p}}(t+1) + e_{\mathrm{ramp}}, \forall t \tag{6-16}$$

$$e_{\mathrm{p,min}} \leq e_{\mathrm{p}}(t) \leq e_{\mathrm{p,max}}, \forall t. \tag{6-17}$$

The control vector $u(t)$ is illustrated in Eq. (6-18)

$$u(t) = \left[P_{\mathrm{ele},i}(t), P_{\mathrm{gas},i}(t), E_{ij}(t), H_{ij}(t), v_i(t), \mathrm{CoP}(t)\right], \forall i, \forall t. \tag{6-18}$$

where Π(t) denotes the energy price. Eq. (6-8) is the energy hub transformation function corresponding to Eq. (6-6). *N* is the number of total time steps, and in this research the time step size is one hour, thus *N* is equal to 24. *K* represents the number of energy hubs modelled in the community. Eq. (6-9) indicates the limitation for dispatch factors, and Eqs. (6-10) and (6-13) denote the minimum and maximum energy input to each hub. Eqs. (6-11) and (6-12) illustrate the adjustment of energy transmission limitation between hubs. Eqs. (6-14), (6-15), and (6-17) indicate the minimum and maximum power output of each converter. Eq. (6-16) specifies the ramp rate for micro-CHP. The optimisation is carried out by determining the control vector shown in Eq. (6-18), which contains the power and gas inputs, the energy adjustments between hubs, the dispatch factors within all hubs, and the CoP of GSHP at all time steps.

6.4.2. Decomposed PSO

The concept of PSO is proposed based on the behaviour of flocking birds or fish schools. Each particle represents a solution to the problem, and the fitness score of the particle denotes the performance of the particle. The group of particles updates at each iteration towards the global minimum based on the two factors of best particle ever achieved P_i^g and the best position of particle i P_i^k. The updating of all particles follows the mechanism as follows.

For particle *i* at iteration *k+1*, the position *X* is indicated as shown in Eq. (6-19).

$$X_i^{k+1} = X_i^k + V_i^{k+1}, \tag{6-19}$$

where V_i^{k+1} means the velocity of particle *i* at iteration *k+1*, which is derived in Eq. (6-20).

$$V_i^{k+1} = \omega V_i^k + c_1 r_1 \left(P_i^k - X_i^k\right) + c_2 r_2 \left(P_i^g - X_i^k\right), \tag{6-20}$$

where ω, c_1, and c_2 are coefficients, r_1 and r_2 indicate two random numbers between 0 and 1. The decomposed approach of utilizing PSO to solve Eqs. (6-7) – (6-18) is illustrated in Fig. 6-6 based on the equations above.

Eq. (6-7) represents a highly-constrained non-convex optimisation problem. The decomposed PSO decouples the complicated problem into sub-problems, namely the scheduling of heat fluxes between GSHPs and borehole, and other elements of the interconnected energy hub system. As shown in Fig. 6-6, the information of heat fluxes over the whole time horizon is initialised and contained in each particle, and all particles are forced into the feasible region. The numerical method of the 'interior-point' method is then applied to optimise other hub elements over the whole time horizon based on

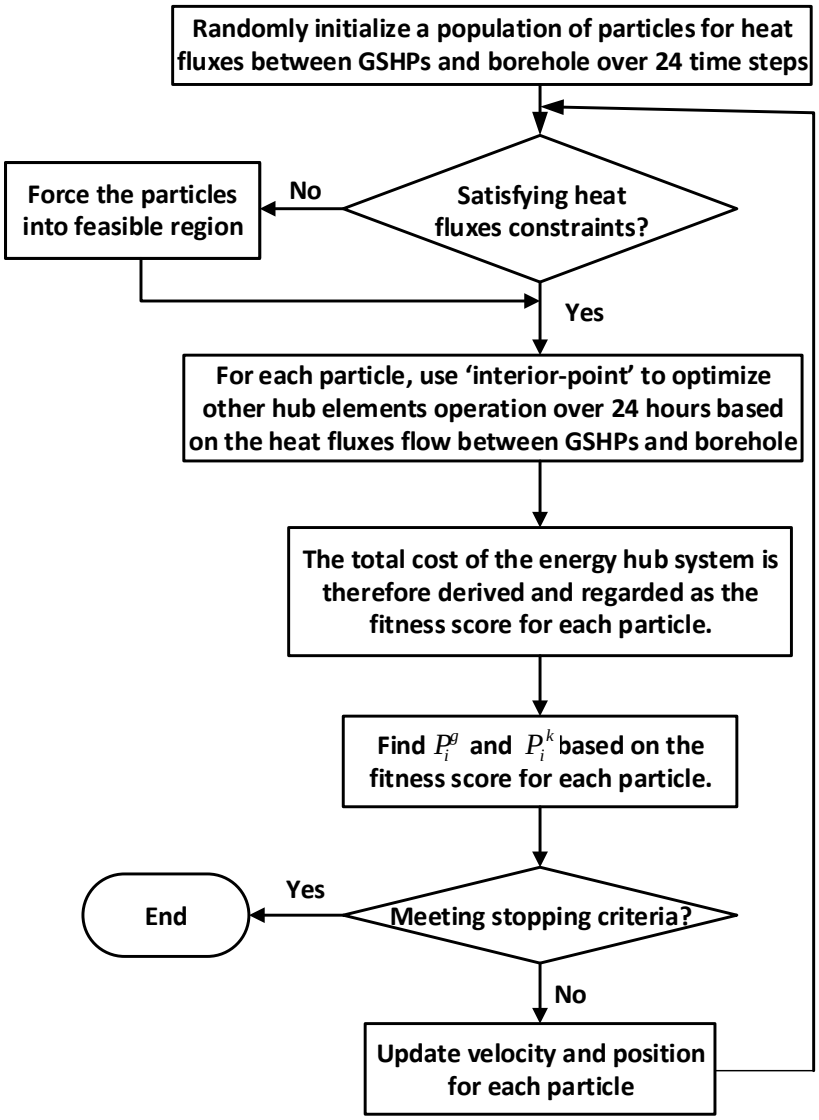

Fig. 6-6.Working flow of the decomposed technique of applying PSO

heat fluxes information, and the total cost of the system can be derived and regarded as the fitness score for each particle. All particles update according to Eqs. (6-19) and (6-20) until the stopping criteria are met.

6.5 Case studies and results

6.5.1. System setup

Case studies are conducted for a community including 11 houses. The borehole storage is set up within the community, which supplies the GSHP equipped within houses 1, 3, 4, 6, 8, 10, and 11. The micro-CHP and gas furnace are included in houses 2 and 5, and 7 and 9 respectively. The electricity load and heat load for the 11 hubs over 24 hours are generated based on [30, 31], and it is assumed that the customer behaviours of the 11 houses are different, and hence the energy load profiles are various. The specific energy consumptions over the whole time horizon of hub 1 are shown in Fig. 6-7 as an example, in which the electricity peak loads appear at around 17:00, and the heat peak loads are at approximately 9:00 and 20:00. The efficiencies of hub devices are derived

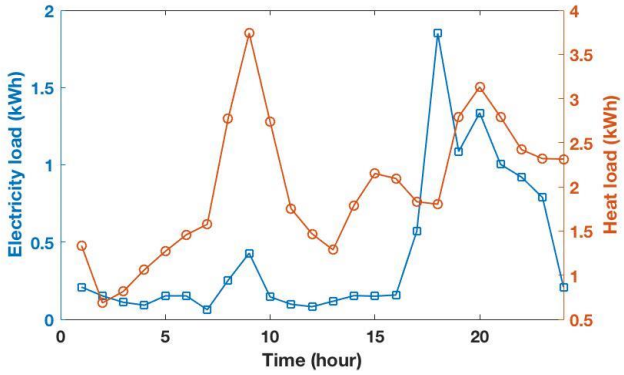

Fig. 6-7. Energy consumptions of hub 1 over 24 hours

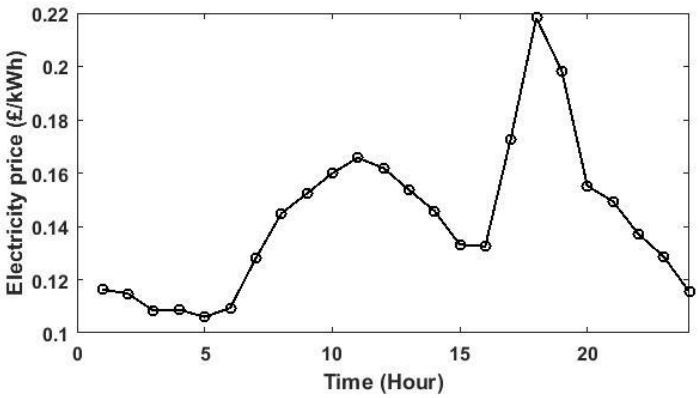

Fig. 6-8.Variant electricity prices against time

from Refs. [5, 6, 25]. The varying electricity price over the 24 hours is obtained from Ref. [32] and shown in Fig. 6-8. Other parameters simulated in this paper are given in Table 6-3.

Table 6-3. PARAMETERS FOR ELEVEN HUBS

Parameter	Value
$e_{ramp}/(kW \cdot min^{-1})$	0.15
e_p/kW	0–0.3
η_{gf}	0.75
η_e	0.3
$\Pi_{gas}/£$	0.04
H_{th}	0.57
P_{HP}/kW	0–8.3

Four cases are presented and optimised in this paper. It is assumed that both the four cases are carried out to optimise the 11-hub system. The electricity and heat loads, system constraints, system parameters including converters efficiencies, borehole model, and the prices of the energy carriers of the four cases are the same. Comparing with using the FE model to calculate the borehole wall temperature, a transfer function model is proposed in this paper. The FE model is applied in Cases 1 and 3, and the transfer function model is applied in Cases 2 and 4 respectively. The related results are discussed to investigate the accuracy of applying the transfer function model in energy hub optimisation. In order to examine the benefits from interconnecting energy hubs, it is assumed that there is no power or heat connection between hubs for Cases 1 and 2, all hubs are directly connected with the grid, and the heat load in each hub is satisfied by applying its own heating converter. The energy sharing is available as indicated in Fig. 6-1 for Cases 3 and 4.

6.5.2. Convergence analysis

To demonstrate that the decomposed PSO is capable of converging to a near-global point, an optimisation is performed for the 11-hub community where the FE model for calculating the borehole wall temperature is utilized. Under the conservative stall generations (30) and stall tolerance settings (£0.0001), a population of 40 particles is utilized to implement the optimisation. The value of the objective function at each iteration is indicated in Fig. 6-9. It could be derived that the best particle achieves the value of £42.12 when all particles are initially generated. The optimisation result rapidly drops from iteration 1 to 44, and trends to be flat after iteration 45. The optimisation

eventually converges to £37.17 after 132 iterations, which demonstrates that the application of the decomposed PSO enables a near-global minimum when solving the optimisation problem proposed in this paper.

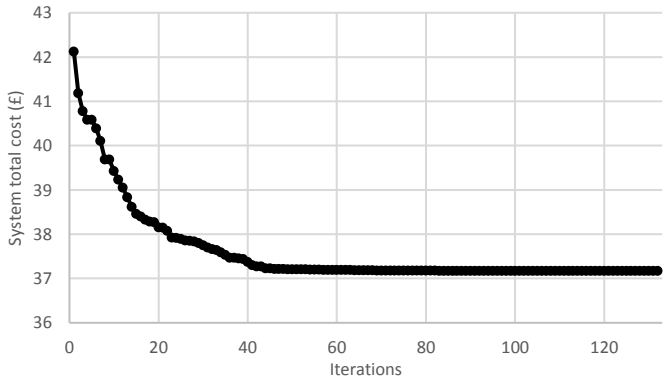

Fig. 6-9.Convergence behavior for the decomposed PSO applying to Case 3

6.5.3. Results and analysis

The total energy cost over the 24 hours for each case is shown in Table 6-4.

Table 6-4. ENERGY COST FOR EACH CASE

Case number	Energy cost/£	Computation time/s
1	39.32	N/A
2	39.36	N/A
3	37.16	5998
4	37.30	248

As shown in Table 6-4, when the energy sharing is available between hubs, the eleven-hub energy cost can be reduced by £2.16 and £2.06 respectively for the FE model and the transfer function model being employed during the optimisation. It can also be concluded that although the FE model is more accurate to estimate the borehole wall temperature, the transfer function model can achieve the results within an acceptable error (0.38%), and the computation time can be reduced by a factor of 17.

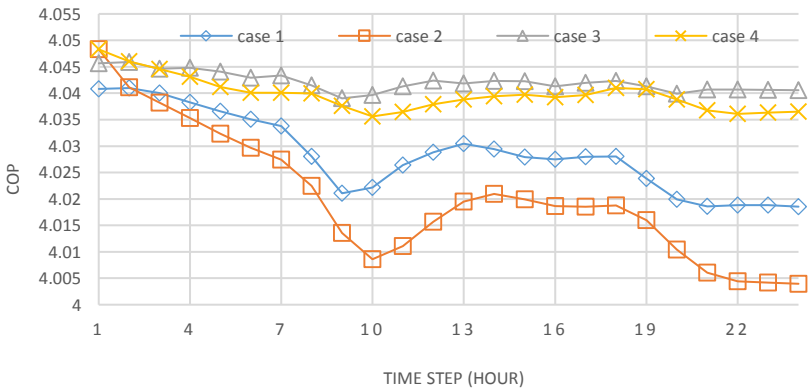

Fig. 6-10.CoP for GSHP over 24 hours for each case

The CoP of GSHP located at each individual residential house at each time step in terms of the four cases is shown in Fig. 6-10. Since the CoP of GSHP is linearly correlated with the borehole wall temperature as indicated in Eq. (6-4), and both the FE model and transfer function model are applied to derive the borehole wall temperature, hence the differences of CoPs between Cases 3 and 4 reflect the accuracy of applying the two models. As seen from Fig. 6-10, the CoPs over the 24 hours differ in Cases 3 and 4, but have similar variations where the CoPs difference at each time step is less than 0.01. This demonstrates that the transfer function model is capable of deriving the borehole wall temperature for energy hub optimisation over the 24 hours with error less than 0.2%.

Compared with the cases that there are energy sharing between hubs, the CoP of GSHPs over the 24 hours obtained from Cases 1 and 2 has a greater variation. Especially the CoP varies between the boundary of 4 and 4.05 for Case 2. Conversely, when the energy hubs are interconnected, the CoP derived from Cases 3 and 4 has a similar variation. This demonstrates that the operations of combined GSHP and borehole system tends to be more stable when the energy sharing between hubs is available.

Since the electricity price reaches the peak value around the time steps of 17 and 18, it can be seen from Fig. 6-10 that for optimisation Cases 3 and 4, the CoP does not drop around the high-electricity price period, which means the utilization of GSHP is accordingly reduced. Alternatively, other heating devices are activated to support the heat load.

It can also be derived from Fig. 6-10 that, according to the second law of thermal dynamics, when the heat is extracted from the borehole, the borehole wall temperature decreases, which generates a high temperature gradient between the wall and the surrounding storage volume. As a result, the heat replenishment from the surrounding volume to the wall occurs. When this is greater than the heat extraction from the GSHP, it will lead to a rise in temperature of the borehole wall, which explains the slight increase in the CoP value seen in Fig. 6-10 in the time steps of 10–14.

The total electricity injection to the eleven-hub system over the 24 hours is depicted in Fig. 6-11. Compared with Cases 1 and 2 where no energy sharing or optimisation is carried out, the electricity consumption in Cases 3 and 4 are reduced at every time step, especially during the peak price period. The reason for this is that the micro-CHP is

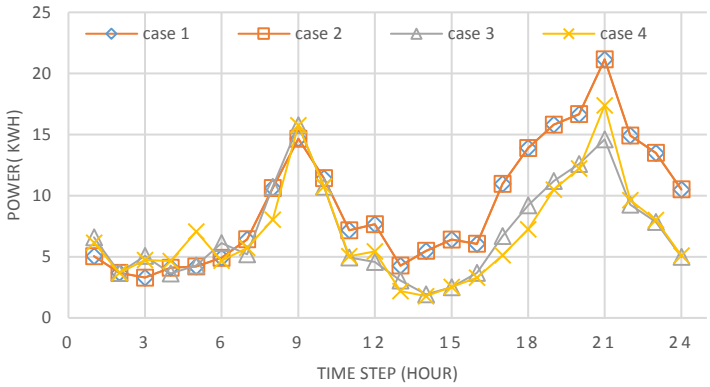

Fig. 6-11.Total electricity injection to 11-hub system over 24 hours for each case

operated during this period, and thus the generated power and heat could be exported to other hubs, avoiding the need for grid import. Meanwhile, the gas furnace is switched on to supply most of the heating instead of electricity driven GSHP in this period.

6.6 Conclusions and future work

This paper presents the optimisation of an interconnected energy hub system including a combined GSHP and a borehole heating system, a micro-CHP, and a gas furnace. The borehole FE model and transfer function model are respectively applied to the optimisation to simulate the borehole wall temperature based on the given discharging heat flux at each time step. The main findings are concluded as follows:

- When the borehole transfer function model is employed the optimisation produces approximately the same results compared with the optimisation where the FE model is applied.
- The computation time is significantly reduced by applying the borehole transfer function model.
- The combined GSHP and borehole system tends to be more stable when the energy hubs are interconnected.
- The total energy cost of the community can be significantly reduced by applying the energy hub optimisation scheme.

Future work will be centred on investigating the optimal control policy for combined GSHP and boreholes within energy hub communities on seasonal time scales.

6.7 Chapter Summary

This chapter contributes to the optimisation for energy hub system incorporated with other smart grid technologies. It innovatively integrates the ground source heat pump and borehole thermal storage to supply a community of residential houses, which are modelled by interconnected energy hubs. The decomposed technique of applying Particle Swarm Optimisation developed in chapter 3 is employed to optimally scheduling the operations of energy hub system together with the borehole storage.

The extra heat can be stored in the borehole thermal storage in summer and discharge during heating seasons, hence the borehole system performs efficiently for inter-seasonal operations. Future work will be carried out to operate the energy hub system with borehole on seasonal time scales.

Chapter 7

Conclusion

This chapter summarises the thesis by outlining the major contributions and findings from the research.

The energy hub presents a powerful concept to advise system operators of how to dispatch, convert, and store various energy infrastructures in order to achieve an optimal condition. Due to the challenges introduced by the increasing utilisation of uncertain renewable generations, distributed generation, distributed multi-energy generation, and the advance of smart grid optimisation schemes, the energy hub concept is therefore proposed to incorporate them to function in the smart city.

The interconnected energy hub system increases system flexibility and profits by maximally exploiting the value of available energy carriers, energy converters, and storages in each hub. Thus, this thesis intensively investigates the optimisation of the interconnected energy hub system to benefit the community and residential users, meanwhile address the challenges to the modern power system. Previous researches may fail to propose robust technique to solve non-convex multi-period energy hub problem, the uncertainty has not been well modelled, and the integration between energy hub and other smart grid technologies might be ignored. This thesis investigates the interconnected energy hub optimisation problem in terms of the aforementioned aspects. From the perspective of operating power system, this thesis benefits both the system operator and customers with improved optimisation performance, less energy infrastucture cost, reduced carbon emission, increased system flexibility and network security. The conclusions and main findings are drawn as follows.

Optimising Energy Hub with Decomposed PSO Approach

The optimisation for interconnected energy hub system is generally formulated as a complicated multi-period, non-convex problem considering the inclusion of complex energy transmission networks and energy storages. The optimisation algorithms applied in previous researches fail to prove their capability of achieving a global minimum in solving the energy hub problem with a massive number of constraints and variables. In order to address it, a comprehensive interconnected energy hub system is firstly modelled by considering converters with non-constant efficiency converters and battery storage system, the battery lifetime cost is considered to better utilise the battery without unnecessary degradation. A novel decomposed approach of applying PSO hybridised with interior-point method is proposed to solve the optimisation problem. The main findings are indicated as follows:

- The performance of the proposed approach of utilising combined PSO with interior-point is validated by a simple 2-hub system, where the theoretical minimum can be analytically derived.
- The optimisation is carried out for a 3 residential energy hub system over 24 hours. By considering the battery lifetime cost within the objective function, it is observed that the utilisation of battery varies between 60% and 90% to avoid unnecessary degradation of the battery lifetime, while achieving the minimum cost. Comparatively, the state of charge of the battery varies from 50% to 100% if the battery lifetime cost is not considered. It demonstrates that the battery lifetime consumes faster when it is operated during a lower state of charges.
- Compared with the conventional PSO, the decomposed approach of utilising PSO hybridised with interior-point method achieves a 58% greater energy saving for the 3-hub optimisation with 98% saving of computation time. The optimisation demonstrably reaches very near to the global minimum. This method can be applied in a receding time horizon approach for solving a practical system of size around 10 hubs, always leveraging the most up to date load prediction.

Chance-Constrained Programming for Energy Hub

In order to better model the uncertain renewable generations compared with the traditional methods such as Monte Carlo simulation and scenario-generation methods, the chance-constrained programming is proposed to solve the energy hub optimisation with uncertainty. The chance constraints innovatively restrict the power and gas flows between adjacent hubs, due to the fact that the temporary overloading is tolerable in the power system. This research contributes to maximally penetrate the renewable generations into the energy hub system at the lowest cost in a smart city, and the impact of chance constraints on energy hub optimisation is extensively explored. The main findings are illustrated as follows:

- By applying Cornish-Fisher Expansion to translate chance constraints into deterministic constraints, the stochastic chance-constrained programming problem is mathematically transferred to a deterministic problem, the interior-point method is applied to optimise the problem. It is demonstrated that the algorithm is capable of achieving a minimum in solving the proposed 3-hub problem.

- The optimisation results for the 3-hub problem derived from chance-constrained programming are compared with the results from 2 point estimate method through the Expected Value of Perfect Information and Value of the Stochastic Solution models. The comparison suggests that the optimised system cost from CCP is £3.94 higher compared with 2PEM, and the system needs to spend extra £5.04 to deal with the uncertain renewable generations.
- The energy hub operations could be more unstable if the power flows between hubs are restricted by chance constraints. It shows stable characteristics when the chance constraints restrict gas flows. However, the total gas injection into the network is more affected when the gas flows are restricted by the chance constraints.

Chance-Constrained Programming for Integrated Demand Respond with Energy Hub Considering Correlated Wind Generations

In order to further improve the simulation for uncertain renewable generations to acquire more accurate results for energy hub optimisation with uncertainty, the correlation between geographically closed wind generations is considered and quantified by Pearson correlation coefficient. Additionally, the integrated demand response with energy hub optimisation is considered to reflect customers' reaction to varying energy prices and energy hub operations. This work benefits both the system operators and customers with reduced energy infrastructure investment costs and energy bills. The main contributions and findings are indicated as follows:

- Chance-constrained programming is capable of solving energy hub optimisation with demand response while considering the correlations between wind power generations. The historical data of wind speeds observed at two geographically closed stations display strong linear relationship for each hour, hence the Pearson correlation is utilised to quantify the linearity and applied in the expressions of chance constraints.
- The results demonstrate that the effects of chance-constrained programming on energy hub optimisation are more obvious when the power flow between hubs is restricted by chance constraints, compared with the case that gas flow is restricted by chance constraints.

- After implementing the integrated demand response with energy hub optimisation, the loads over the high-tariff period are slightly decreased, and the loads at other time steps are increased compared with the reference load. It demonstrates that the energy hub optimal operations respond to both the varying energy prices and the elements within the energy hub system.

Energy Hub Optimisation with Combined GSHP and Borehole Thermal Storage

The combined GSHP with borehole thermal storage effectively reduces the carbon emission at the residential level and improves the energy utilisation efficiency since the borehole storage is regarded as a stable heat source with high temperature, which results in high efficiency of GSHP. In order to accommodate the utilisation of the combined system for domestic users, it is investigated within the interconnected energy hub system to support the thermal load of a community of residential houses. The borehole finite element (FE) model and an equivalent borehole transfer function are proposed and respectively applied to the optimisation to analyse the variation of GSHP performance over the entire optimisation time horizon of 24 h. The main contributions and findings are illustrated as follows:

- The decomposed approach of applying the hybrid PSO and interior-point method proposed in this thesis is employed in this work to resolve the energy hub optimisation problem. It is demonstrated that the approach is capable to achieve a near global minimum.
- The optimisation results validate the equivalent transfer function model, which produces approximately the same results compared with the case that the FE model is applied. Additionally, the computational time is reduced by a factor of 17 times by using the equivalent transfer function model.
- Compared with the case that the electricity and heat connection between hubs are unavailable, the combined GSHP and borehole system tends to be more stable when the energy hubs are interconnected, the coefficient of performance of GSHP slightly varies in supporting the interconnected energy hub system over the whole optimisation time horizon.

Chapter 8

Future Work

This chapter presents the potential future work to enrich the optimisation methodologies for multi-carrier energy system, as well as the interaction with other smart grid technologies or frameworks.

In the future, the following work is important because the specific trading scheme between energy hubs should be built to consider the market participants' willingness to exchange energies; the operating constraints of the distributed generation need to be included in the energy hub optimisation for more accurate simulation; the uncertain variables may not comply with the empiric distributions, and hence the risk management can be employed to optimise the energy hub system with low risk; the control method should be implemented for energy hub operations to maintain the system stability. Detailed future work is illustrated as follows.

Considering Peer to Peer Trading between Energy Hubs

The interconnected energy hub system is optimised in order to achieve the minimum energy cost for the holistic system, the energies including renewable energies, electricity, gas, and heat are assumed to be flexibly shared among all hubs. From the prospective of reducing energy cost, the more robust energy converters, free renewable generations, and energy storage systems are more likely to be utilised by all hub participants through the energy transmission networks. However, the willingness of the customers to share their energies or robust technologies with others is ignored, the metering and trading scheme between different hub users have not been investigated in previous researches.

In recent years, with the increasing utilisation of DERs and DGs among residential, commercial, and industrial users, the traditional consumers are transferred to prosumers as they both consume and generate energy. The prosumers may wish to sell the extra energy from their DERs or DGs to other consumers to make profits, and the trading paradigm is defined as the Peer to Peer (P2P) trading. Within the context of P2P, each energy hub participant can be regarded as a single entity to trade in the market. The conventional P2P paradigm generally considers the trading of electricity and renewable energies, however, the P2P established between multi-carrier energy systems can include the trading of other energy infrastructures such as gas and heat, while considering the optimal operations of energy hub system. Therefore, considering the P2P trading between energy hubs proposes a more explicit trading scheme, which could bring further energy saving and better meet customers' multiple demands. Additionally, it practically models the application of interconnected energy hub system with energy

markets. The work benefits the system coordinator with enhanced transparency of the trading between all hub participants.

Unit Commitment with Energy Hub Optimisation

Presently, the interconnected energy hub system is considered to be equipped with various energy storages, renewable generators, CHP, heat pumps, and other efficient energy converters to collectively meet customers' demands. Most of the studies simulate the energy converters and storages with constant efficiency, some researches models the efficiency with quadratic function in terms of the energy input. However, some constraints such as start-up/shut-down costs are excluded, where the related optimal operations can be inaccurate.

The unit commitment problem is defined as optimising the production of a series of electricity generators in order to meet the energy demands with minimum cost or carbon emissions. The unit commitment considers more explicitly for the generators with the operational constraints such as ramp up/down rate, minimum up/down time constraints. Unit commitment has not been investigated within energy hub system. Therefore, based on the work presented in this thesis, unit commitment can be applied to interconnected energy hubs with uncertainty to contribute more practical optimisation for the operations of the energy converters and storage.

Risk Management in Energy Hub Optimisation

Uncertain variables such as the renewable generations and customer loads of the energy hub system are generally modelled by their distributions, which are derived empirically by fitting historical data. The optimisation for energy hub is therefore implemented based on the distributions. However, the uncertainty existed in the energy hub system is mostly time-varying and stochastic, which may significantly depend on the factors such as customers' behaviour and weather condition. The uncertain variables may not comply with the empiric distributions, hence the optimal operations are inaccurate and the energy hub system is in risks.

To address this issue and operate the energy hub system with acceptable risks, the risk management model can be employed into the optimisation problem to search for the trade-off between energy saving and risks. Risk management was initially proposed to deal with natural disasters and constitute financial policies. The risk is quantitatively

measured within the management scheme and has been applied to some power system planning and pricing problems. However, it has never been applied to energy hub problem. Within the context of the multi-carrier energy system, future work can incorporate risk management scheme to determine the optimal policy with acceptable risk, and investigates the effect of risks on the dependency between various energies.

Energy Hub System Stability Analysis

The energy hub optimisation in most researches is assumed to be carried out under steady-state, where the loads, energy prices, and system parameters are assumed to be constant. Uncertainty can be considered in the system optimisation, however, they are typically simulated through deterministic approaches to analyse the effects of uncertainty on system operations. In fact, some dynamic phenomenon exists in the power system such as the variations in voltage and frequency, which could generate small transients or larger disturbance in the system. Stability can be applied to quantify the capability of the system that recovers to an equilibrium after undergoes a physical disturbance. Conclusively, the system stability influences whether the system operations can be continually implemented without majorly affecting any customers after an incentive. The energy hub system theoretically improves the system stability because the system demands depend on various energy carriers, the energy storage system can also provide reserves to hedge the risks from uncertainty. However, the stability of the energy hub system has not been analysed in the previous literature.

Future work can be carried out to optimally plan the energy hub system while maintains the system stability. Novel control approaches such as stochastic distribution control theory can be applied to optimise the energy hub problem. The system reliability and network investment security can thus be improved.

Publications

Huo, D, Gu, C, Ma, K, Wei, W, Xiang, Y & Le Blond, S 2018, 'Chance-Constrained Optimization for Multi Energy Hub Systems in a Smart City' IEEE Transactions on Industrial Electronics.

Huo, D, Le Blond, S, Gu, C, Wei, W & Yu, D 2018, 'Optimal operation of interconnected energy hubs by using decomposed hybrid particle swarm and interior-point approach' International Journal of Electrical Power and Energy Systems, vol. 95, pp. 36-46. DOI: 10.1016/j.ijepes.2017.08.004

Huo, D, Wei, W & Le Blond, S 2018, 'Optimisation for interconnected energy hub system with combined ground source heat pump and borehole thermal storage' Frontiers in Energy. DOI: 10.1007/s11708-018-0580-0

Huo, D, Gu, C, Wang Z, 'Chance-Constrained Multi Energy System Optimisation with Correlated Wind Generation', IEEE Transactions on Power System. (under review)

Huo, D, Gu, C, Yang, G & Le Blond, S 2017, 'Combined domestic demand response and energy hub optimisation with renewable generation uncertainty' Energy Procedia, vol. 142, pp. 1985-1990. DOI: 10.1016/j.egypro.2017.12.399

Huo, D, Liu, Y, Gu, C & Le Blond, S 2015, Optimal flow of energy-hub including heat pumps at residential level. 50th International Universities Power Engineering Conference, UPEC 2015. DOI: 10.1109/UPEC.2015.7339899

Wei, W, C. Gu, Huo. D, S. Le Blond, and X. Yan, "Optimization of Borehole Energy Storage Charging Strategy within a Low Carbon Space Heating System," IEEE Access (under review)

Wei, W, Huo. D and Le Blond, S, "Comparison between FE Model and Transfer Function for Short-term Borehole Charging Optimization," in 2017 IEEE Power and Energy Society General Meeting (PESGM), 2017, pp. 1-5.

Wei, W, Huo, D & Le Blond, S 2016, 'Borehole active recharge benefit quantification on a community level low carbon heating system'. Power and Energy Society General Meeting, PESGM 2016. DOI: 10.1109/PESGM.2016.7741352

Yu, D, Zhang, H, Huo, D & Le Blond, S 2017, CHP sizing and domestic building energy cost optimization. 51st International Universities Power Engineering Conference, UPEC 2016. DOI: 10.1109/UPEC.2016.8113990

Reference

Chapter 1

[1] C. Buccella, C. Cecati, and H. Abu-Rub, "An Overview on Distributed Generation and Smart Grid Concepts and Technologies," *Power Electronics for Renewable Energy Systems, Transportation, and Industrial Applications*, pp. 50-68, 2014.

[2] F. Urban and J. Nordensvärd, "Low carbon development : key issues," 2013.

[3] K. Richardson, W. Steffen, H. Schellnhuber, J. Alcamo, T. Barker, D. Kammen, *et al.*, *Climate Change: global risks challenges and decisions*, 2009.

[4] OECD, *Transition to a Low-Carbon Economy*, 2010.

[5] S. Paudyal, C. A. Canizares, and K. Bhattacharya, "Optimal Operation of Industrial Energy Hubs in Smart Grids," *Ieee Transactions on Smart Grid*, vol. 6, pp. 684-694, Mar 2015.

[6] "Exploring how the UK can meet the 2050 emission reduction target using the web-based 2050 Calculator [Online] Available https://www.gov.uk/2050-pathways-analysis."

[7] "The UK low carbon transition plan: national strategy for climate and energy, available at https://www.gov.uk/government/publications/the-uk-low-carbon-transition-plan-national-strategy-for-climate-and-energy," 2009.

[8] "Siemens UK, "Clarity on the future UK electricity mix", available at http://www.siemens.co.uk/en/insights/government-policy-on-future-uk-electricity-mix.htm."

[9] B. Zhao, X. S. Zhang, J. Chen, C. S. Wang, and L. Guo, "Operation Optimization of Standalone Microgrids Considering Lifetime Characteristics of Battery Energy Storage System," *Ieee Transactions on Sustainable Energy*, vol. 4, pp. 934-943, Oct 2013.

[10] J. Villar, R. Bessa, and M. Matos, "Flexibility products and markets: Literature review," *Electric Power Systems Research*, vol. 154, pp. 329-340, Jan 2018.

[11] M. T. Digambar, "Distributed Generation (DG) and Distributed Resources (DR)," in *Electricity Power Generation:The Changing Dimensions*, ed: Wiley-IEEE Press, 2011, p. 352.

[12] "DTI, Department of Trade and Industry. Review of distributed generation. A joint Government/Ofgem report; 2007b."

[13] G. Allan, I. Eromenko, M. Gilmartin, I. Kockar, and P. McGregor, "The economics of distributed energy generation: A literature review," *Renewable & Sustainable Energy Reviews*, vol. 42, pp. 543-556, Feb 2015.

[14] E. A. M. Cesena, T. Capuder, and P. Mancarella, "Flexible Distributed Multienergy Generation System Expansion Planning Under Uncertainty," *Ieee Transactions on Smart Grid*, vol. 7, pp. 348-357, Jan 2016.

[15] G. Chicco and P. Mancarefla, "Distributed multi-generation: A comprehensive view," *Renewable & Sustainable Energy Reviews*, vol. 13, pp. 535-551, Apr 2009.

[16] M. Geidl, "Integrated Modeling and Optimization of Multi-Carrier Energy Systems," *PhD dissertation, Power Systems Laboratory, ETH Zurich,* 2007.

[17] M. Geidl, G. Koeppel, P. Favre-Perrod, B. Klockl, G. Andersson, and K. Frohlich, "Energy hubs for the future," *Ieee Power & Energy Magazine,* vol. 5, pp. 24-30, Jan-Feb 2007.

[18] P. Favre-Perrod, M. Geidl, B. Klock, and G. Koeppel, "A vision of future energy networks," *IEEE Power Engineering Society Inaugural 2005 Conference and Exposition in Africa,* pp. 13-17, 2005.

[19] F. Kienzle, P. Favre-Perrod, M. Arnold, and G. Andersson, "Multi-energy delivery infrastructures for the future," in *Infrastructure Systems and Services: Building Networks for a Brighter Future (INFRA), 2008 First International Conference on*, 2008, pp. 1-5.

[20] M. Houwing, R. R. Negenborn, and B. De Schutter, "Demand Response With Micro-CHP Systems," *Proceedings of the Ieee,* vol. 99, pp. 200-213, Jan 2011.

[21] M. Mohammadi, Y. Noorollahi, B. Mohammadi-ivatloo, M. Hosseinzadeh, H. Yousefi, and S. T. Khorasani, "Optimal management of energy hubs and smart energy hubs - A review," *Renewable & Sustainable Energy Reviews,* vol. 89, pp. 33-50, Jun 2018.

[22] M. C. Bozchalui, S. AhsanHashmi, H. Hassen, C. A. Canizares, and K. Bhattacharya, "Optimal Operation of Residential Energy Hubs in Smart Grids," *Ieee Transactions on Smart Grid,* vol. 3, pp. 1755-1766, Dec 2012.

[23] D. Huo, S. Le Blond, C. Gu, W. Wei, and D. Yu, "Optimal operation of interconnected energy hubs by using decomposed hybrid particle swarm and interior-point approach," *International Journal of Electrical Power & Energy Systems,* vol. 95, pp. 36-46, 2018/02/01/ 2018.

[24] M. Almassalkhi and I. Hiskens, "Impact of Energy Storage on Cascade Mitigation in Multi-energy Systems," *2012 Ieee Power and Energy Society General Meeting,* 2012.

[25] X. H. Guan, Z. B. Xu, and Q. S. Jia, "Energy-Efficient Buildings Facilitated by Microgrid," *Ieee Transactions on Smart Grid,* vol. 1, pp. 243-252, Dec 2010.

[26] F. Adamek, M. Arnold, and G. Andersson, "On Decisive Storage Parameters for Minimizing Energy Supply Costs in Multicarrier Energy Systems," *Sustainable Energy, IEEE Transactions on,* vol. 5, pp. 102-109, 2014.

[27] A. Shabanpour-Haghighi and A. R. Seifi, "Energy Flow Optimization in Multicarrier Systems," *Ieee Transactions on Industrial Informatics,* vol. 11, pp. 1067-1077, Oct 2015.

[28] S. Bahrami and A. Sheikhi, "From Demand Response in Smart Grid Toward Integrated Demand Response in Smart Energy Hub," *Ieee Transactions on Smart Grid,* vol. 7, pp. 650-658, Mar 2016.

[29] M. Moeini-Aghtaie, A. Abbaspour, M. Fotuhi-Firuzabad, and E. Hajipour, "A Decomposed Solution to Multiple-Energy Carriers Optimal Power Flow," *Ieee Transactions on Power Systems,* vol. 29, pp. 707-716, Mar 2014.

[30] H. Yu, C. Y. Chung, K. P. Wong, and J. H. Zhang, "A Chance Constrained Transmission Network Expansion Planning Method With Consideration of Load

and Wind Farm Uncertainties," *Ieee Transactions on Power Systems,* vol. 24, pp. 1568-1576, Aug 2009.

[31] F. Kienzle, P. Ahcin, and G. Andersson, "Valuing Investments in Multi-Energy Conversion, Storage, and Demand-Side Management Systems Under Uncertainty," *Ieee Transactions on Sustainable Energy,* vol. 2, pp. 194-202, Apr 2011.

[32] M. C. Bozchalui, C. A. Canizares, and K. Bhattacharya, "Optimal Energy Management of Greenhouses in Smart Grids," *Ieee Transactions on Smart Grid,* vol. 6, pp. 827-835, Mar 2015.

[33] S. Chen, Z. N. Wei, G. Q. Sun, K. W. Cheung, and Y. H. Sun, "Multi-Linear Probabilistic Energy Flow Analysis of Integrated Electrical and Natural-Gas Systems," *Ieee Transactions on Power Systems,* vol. 32, pp. 1970-1979, May 2017.

[34] B. M.-i. A. Dolatabadi, M. Abapour and S. Tohidi, "Optimal Stochastic Design of Wind Integrated Energy Hub," *IEEE Transactions on Industrial Informatics,* vol. 13, pp. 2379-2388, 2017.

[35] N. Neyestani, M. Yazdani-Damavandi, M. Shafie-Khah, G. Chicco, and J. P. S. Catalao, "Stochastic Modeling of Multienergy Carriers Dependencies in Smart Local Networks With Distributed Energy Resources," *Ieee Transactions on Smart Grid,* vol. 6, pp. 1748-1762, Jul 2015.

[36] M. Rastegar, M. Fotuhi-Firuzabad, H. Zareipour, and M. Moeini-Aghtaie, "A Probabilistic Energy Management Scheme for Renewable-Based Residential Energy Hubs," *IEEE Transactions on Smart Grid,* vol. PP, pp. 1-11, 2016.

[37] M. Moeini-Aghtaie, P. Dehghanian, M. Fotuhi-Firuzabad, and A. Abbaspour, "Multiagent Genetic Algorithm: An Online Probabilistic View on Economic Dispatch of Energy Hubs Constrained by Wind Availability," *Ieee Transactions on Sustainable Energy,* vol. 5, pp. 699-708, Apr 2014.

[38] M. Alipour, K. Zare, and M. Abapour, "MINLP Probabilistic Scheduling Model for Demand Response Programs Integrated Energy Hubs," *Ieee Transactions on Industrial Informatics,* vol. 14, pp. 79-88, Jan 2018.

Chapter 2

[1] M. Geidl and G. Andersson, "A modeling and optimization approach for multiple energy carrier power flow," in *Power Tech, 2005 IEEE Russia*, 2005, pp. 1-7.

[2] M. Geidl and G. Andersson, "Optimal Power Flow of Multiple Energy Carriers," *Power Systems, IEEE Transactions on,* vol. 22, pp. 145-155, 2007.

[3] M. Geidl, "Integrated Modeling and Optimization of Multi-Carrier Energy Systems," *PhD dissertation, Power Systems Laboratory, ETH Zurich*, 2007.

[4] M. R. Almassalkhi and A. Towle, "Enabling City-scale Multi-energy Optimal Dispatch with Energy Hubs," *2016 Power Systems Computation Conference (Pscc)*, 2016.

[5] J. X. Wang, H. W. Zhong, Z. M. Ma, Q. Xia, and C. Q. Kang, "Review and prospect of integrated demand response in the multi-energy system," *Applied Energy,* vol. 202, pp. 772-782, Sep 15 2017.

[6] M. Qadrdan, M. Chaudry, J. Z. Wu, N. Jenkins, and J. Ekanayake, "Impact of a large penetration of wind generation on the GB gas network," *Energy Policy*, vol. 38, pp. 5684-5695, Oct 2010.

[7] A. Q. Huang, M. L. Crow, G. T. Heydt, J. P. Zheng, and S. J. Dale, "The Future Renewable Electric Energy Delivery and Management (FREEDM) System: The Energy Internet," *Proceedings of the Ieee*, vol. 99, pp. 133-148, Jan 2011.

[8] Y. Maniyali, A. Almansoori, M. Fowler, and A. Elkamel, "Energy Hub Based on Nuclear Energy and Hydrogen Energy Storage," *Industrial & Engineering Chemistry Research*, vol. 52, pp. 7470-7481, Jun 5 2013.

[9] M. Mohammadi, Y. Noorollahi, B. Mohammadi-Ivatloo, and H. Yousefi, "Energy hub: From a model to a concept - A review," *Renewable & Sustainable Energy Reviews*, vol. 80, pp. 1512-1527, Dec 2017.

[10] "U.S. DOE combined heat and power installation database; 2016. Available at: https://doe.icfwebservices.com/chpdb/."

[11] S. Martinez, G. Michaux, P. Salagnac, and J. L. Bouvier, "Micro-combined heat and power systems (micro-CHP) based on renewable energy sources," *Energy Conversion and Management*, vol. 154, pp. 262-285, Dec 15 2017.

[12] "Department for Business, Energy & Industrial Strategy, "Combined heat and power", available at https://www.gov.uk/guidance/combined-heat-and-power."

[13] M. Houwing, R. R. Negenborn, and B. De Schutter, "Demand Response With Micro-CHP Systems," *Proceedings of the Ieee*, vol. 99, pp. 200-213, Jan 2011.

[14] M. Abbaspour, M. Satkin, B. Mohammadi-Ivatloo, F. H. Lotfi, and Y. Noorollahi, "Optimal operation scheduling of wind power integrated with compressed air energy storage (CAES)," *Renewable Energy*, vol. 51, pp. 53-59, Mar 2013.

[15] A. Lucas and S. Chondrogiannis, "Smart grid energy storage controller for frequency regulation and peak shaving, using a vanadium redox flow battery," *International Journal of Electrical Power & Energy Systems*, vol. 80, pp. 26-36, Sep 2016.

[16] P. C. Del Granado, Z. Pang, and S. W. Wallace, "Synergy of smart grids and hybrid distributed generation on the value of energy storage," *Applied Energy*, vol. 170, pp. 476-488, May 15 2016.

[17] M. Arnold, R. R. Negenborn, G. Andersson, and B. De Schutter, "Model-Based Predictive Control Applied to Multi-Carrier Energy Systems," *2009 Ieee Power & Energy Society General Meeting, Vols 1-8*, pp. 4592-4599, 2009.

[18] M. Moeini-Aghtaie, A. Abbaspour, M. Fotuhi-Firuzabad, and E. Hajipour, "A Decomposed Solution to Multiple-Energy Carriers Optimal Power Flow," *Ieee Transactions on Power Systems*, vol. 29, pp. 707-716, Mar 2014.

[19] H. Yu, C. Y. Chung, K. P. Wong, and J. H. Zhang, "A Chance Constrained Transmission Network Expansion Planning Method With Consideration of Load and Wind Farm Uncertainties," *Ieee Transactions on Power Systems*, vol. 24, pp. 1568-1576, Aug 2009.

[20] M. C. Bozchalui, C. A. Canizares, and K. Bhattacharya, "Optimal Energy Management of Greenhouses in Smart Grids," *Ieee Transactions on Smart Grid*, vol. 6, pp. 827-835, Mar 2015.

[21] M. Alipour, K. Zare, and M. Abapour, "MINLP Probabilistic Scheduling Model for Demand Response Programs Integrated Energy Hubs," *Ieee Transactions on Industrial Informatics,* vol. 14, pp. 79-88, Jan 2018.

[22] S. Paudyal, C. A. Canizares, and K. Bhattacharya, "Optimal Operation of Industrial Energy Hubs in Smart Grids," *Ieee Transactions on Smart Grid,* vol. 6, pp. 684-694, Mar 2015.

[23] M. C. Bozchalui, S. AhsanHashmi, H. Hassen, C. A. Canizares, and K. Bhattacharya, "Optimal Operation of Residential Energy Hubs in Smart Grids," *Ieee Transactions on Smart Grid,* vol. 3, pp. 1755-1766, Dec 2012.

[24] N. Neyestani, M. Yazdani-Damavandi, M. Shafie-Khah, G. Chicco, and J. P. S. Catalao, "Stochastic Modeling of Multienergy Carriers Dependencies in Smart Local Networks With Distributed Energy Resources," *Ieee Transactions on Smart Grid,* vol. 6, pp. 1748-1762, Jul 2015.

[25] J. Peschon, D. W. Bree, and L. P. Hajdu, "Optimal Power-Flow Solutions for Power-System Planning," *Proceedings of the Institute of Electrical and Electronics Engineers,* vol. 60, pp. 64-&, 1972.

[26] C. C. Shao, X. F. Wang, M. Shahidehpour, X. L. Wang, and B. Y. Wang, "An MILP-Based Optimal Power Flow in Multicarrier Energy Systems," *Ieee Transactions on Sustainable Energy,* vol. 8, pp. 239-248, Jan 2017.

[27] F. Adamek, M. Arnold, and G. Andersson, "On Decisive Storage Parameters for Minimizing Energy Supply Costs in Multicarrier Energy Systems," *Sustainable Energy, IEEE Transactions on,* vol. 5, pp. 102-109, 2014.

[28] A. Sheikhi, M. Rayati, S. Bahrami, and A. M. Ranjbar, "Demand Side Management in a group of Smart Energy Hubs as price anticipators; the game theoretical approach," *2015 IEEE Power & Energy Society Innovative Smart Grid Technologies Conference (ISGT),* 2015.

[29] A. Sheikhi, M. Rayati, S. Bahrami, and A. M. Ranjbar, "Integrated Demand Side Management Game in Smart Energy Hubs," *Ieee Transactions on Smart Grid,* vol. 6, pp. 675-683, Mar 2015.

[30] A. Sheikhi, M. Rayati, S. Bahrami, A. M. Ranjbar, and S. Sattari, "A cloud computing framework on demand side management game in smart energy hubs," *International Journal of Electrical Power & Energy Systems,* vol. 64, pp. 1007-1016, Jan 2015.

[31] F. Kamyab and S. Bahrami, "Efficient operation of energy hubs in time-of-use and dynamic pricing electricity markets," *Energy,* vol. 106, pp. 343-355, Jul 1 2016.

[32] A. Shabanpour-Haghighi and A. R. Seifi, "Energy Flow Optimization in Multicarrier Systems," *Ieee Transactions on Industrial Informatics,* vol. 11, pp. 1067-1077, Oct 2015.

[33] S. Bahrami and A. Sheikhi, "From Demand Response in Smart Grid Toward Integrated Demand Response in Smart Energy Hub," *Ieee Transactions on Smart Grid,* vol. 7, pp. 650-658, Mar 2016.

[34] S. Althaher, P. Mancarella, and J. Mutale, "Automated Demand Response From Home Energy Management System Under Dynamic Pricing and Power and

Comfort Constraints," *Ieee Transactions on Smart Grid*, vol. 6, pp. 1874-1883, Jul 2015.

[35] A. G. Hossam, "Perspectives of Demand‐Side Management Under Smart Grid Concept," in *Energy Conservation in Residential, Commercial, and Industrial Facilities*, ed: Wiley-IEEE Press, 2018, p. 352.

[36] A. Sheikhi, S. Bahrami, and A. M. Ranjbar, "An autonomous demand response program for electricity and natural gas networks in smart energy hubs," *Energy*, vol. 89, pp. 490-499, Sep 2015.

[37] C. L. Su and D. Kirschen, "Quantifying the Effect of Demand Response on Electricity Markets," *Ieee Transactions on Power Systems*, vol. 24, pp. 1199-1207, Aug 2009.

[38] C. Y. Zhao, J. H. Wang, J. P. Watson, and Y. P. Guan, "Multi-Stage Robust Unit Commitment Considering Wind and Demand Response Uncertainties," *Ieee Transactions on Power Systems*, vol. 28, pp. 2708-2717, Aug 2013.

[39] P. R. Thimmapuram, J. Kim, A. Botterud, and Y. Nam, "Modeling and Simulation of Price Elasticity of Demand Using an Agent-Based Model," *2010 Innovative Smart Grid Technologies Conference (Isgt)*, 2010.

[40] "About the Domestic Renewable Heat Incentive (RHI), available at https://www.ofgem.gov.uk/environmental-programmes/domestic-rhi/about-domestic-rhi."

[41] C. F. Song and Q. Tian, "Research on the Utilization of Ground Heat Resource and the Numerical Simulation of the Heat Exchange of Underground U-tube," *Iceet: 2009 International Conference on Energy and Environment Technology, Vol 1, Proceedings*, pp. 804-809, 2009.

[42] B. Sanner, C. Karytsas, D. Mendrinos, and L. Rybach, "Current status of ground source heat pumps and underground thermal energy storage in Europe," *Geothermics*, vol. 32, pp. 579-588, Aug-Dec 2003.

[43] Z. Jizhong, "Uncertainty Analysis in Power Systems," in *Optimization of Power System Operation*, ed: Wiley-IEEE Press, 2015, p. 664.

[44] "National Centers for Environmental Information, Available at https://www.ncei.noaa.gov/."

[45] M. Aien, A. Hajebrahimi, and M. Fotuhi-Firuzabad, "A comprehensive review on uncertainty modeling techniques in power system studies," *Renewable & Sustainable Energy Reviews*, vol. 57, pp. 1077-1089, May 2016.

[46] F. Kienzle, P. Ahcin, and G. Andersson, "Valuing Investments in Multi-Energy Conversion, Storage, and Demand-Side Management Systems Under Uncertainty," *Ieee Transactions on Sustainable Energy*, vol. 2, pp. 194-202, Apr 2011.

[47] B. M.-i. A. Dolatabadi, M. Abapour and S. Tohidi, "Optimal Stochastic Design of Wind Integrated Energy Hub," *IEEE Transactions on Industrial Informatics*, vol. 13, pp. 2379-2388, 2017.

[48] M. Moeini-Aghtaie, P. Dehghanian, M. Fotuhi-Firuzabad, and A. Abbaspour, "Multiagent Genetic Algorithm: An Online Probabilistic View on Economic Dispatch of Energy Hubs Constrained by Wind Availability," *Ieee Transactions on Sustainable Energy*, vol. 5, pp. 699-708, Apr 2014.

[49] M. Rastegar, M. Fotuhi-Firuzabad, H. Zareipour, and M. Moeini-Aghtaie, "A Probabilistic Energy Management Scheme for Renewable-Based Residential Energy Hubs," *IEEE Transactions on Smart Grid,* vol. PP, pp. 1-11, 2016.

[50] M. Wendt, P. Li, and G. Wozny, "Nonlinear chance-constrained process optimization under uncertainty," *Industrial & Engineering Chemistry Research,* vol. 41, pp. 3621-3629, Jul 24 2002.

[51] G. Dorini, P. Pinson, and H. Madsen, "Chance-Constrained Optimization of Demand Response to Price Signals," *Ieee Transactions on Smart Grid,* vol. 4, pp. 2072-2080, Dec 2013.

[52] H. Zhang and P. Li, "Chance Constrained Programming for Optimal Power Flow Under Uncertainty," *Ieee Transactions on Power Systems,* vol. 26, pp. 2417-2424, Nov 2011.

[53] Z. Wu, P. L. Zeng, X. P. Zhang, and Q. Y. Zhou, "A Solution to the Chance-Constrained Two-Stage Stochastic Program for Unit Commitment With Wind Energy Integration," *Ieee Transactions on Power Systems,* vol. 31, pp. 4185-4196, Nov 2016.

[54] J. Z. Liu, H. Chen, W. Zhang, B. Yurkovich, and G. Rizzoni, "Energy Management Problems Under Uncertainties for Grid-Connected Microgrids: A Chance Constrained Programming Approach," *Ieee Transactions on Smart Grid,* vol. 8, pp. 2585-2596, Nov 2017.

[55] Q. F. Wang, Y. P. Guan, and J. H. Wang, "A Chance-Constrained Two-Stage Stochastic Program for Unit Commitment With Uncertain Wind Power Output," *Ieee Transactions on Power Systems,* vol. 27, pp. 206-215, Feb 2012.

Chapter 3

[1] S. Pazouki and M. R. Haghifam, "Optimal planning and scheduling of energy hub in presence of wind, storage and demand response under uncertainty," *International Journal of Electrical Power & Energy Systems,* vol. 80, pp. 219-239, Sep 2016.

[2] M. Geidl and G. Andersson, "Optimal Power Flow of Multiple Energy Carriers," *Power Systems, IEEE Transactions on,* vol. 22, pp. 145-155, 2007.

[3] M. Geidl, G. Koeppel, P. Favre-Perrod, B. Klockl, G. Andersson, and K. Frohlich, "Energy hubs for the future," *Ieee Power & Energy Magazine,* vol. 5, pp. 24-30, Jan-Feb 2007.

[4] F. Kienzle, P. Favre-Perrod, M. Arnold, and G. Andersson, "Multi-energy delivery infrastructures for the future," in *Infrastructure Systems and Services: Building Networks for a Brighter Future (INFRA), 2008 First International Conference on,* 2008, pp. 1-5.

[5] X. H. Guan, Z. B. Xu, and Q. S. Jia, "Energy-Efficient Buildings Facilitated by Microgrid," *Ieee Transactions on Smart Grid,* vol. 1, pp. 243-252, Dec 2010.

[6] M. Moeini-Aghtaie, A. Abbaspour, M. Fotuhi-Firuzabad, and E. Hajipour, "A Decomposed Solution to Multiple-Energy Carriers Optimal Power Flow," *Ieee Transactions on Power Systems,* vol. 29, pp. 707-716, Mar 2014.

[7] F. Adamek, M. Arnold, and G. Andersson, "On Decisive Storage Parameters for Minimizing Energy Supply Costs in Multicarrier Energy Systems," *Sustainable Energy, IEEE Transactions on,* vol. 5, pp. 102-109, 2014.

[8] M. Arnold, R. R. Negenborn, G. Andersson, and B. De Schutter, "Model-Based Predictive Control Applied to Multi-Carrier Energy Systems," *2009 Ieee Power & Energy Society General Meeting, Vols 1-8,* pp. 4592-4599, 2009.

[9] A. Sheikhi, M. Rayati, S. Bahrami, and A. M. Ranjbar, "Integrated Demand Side Management Game in Smart Energy Hubs," *Ieee Transactions on Smart Grid,* vol. 6, pp. 675-683, Mar 2015.

[10] A. Sheikhi, M. Rayati, S. Bahrami, A. M. Ranjbar, and S. Sattari, "A cloud computing framework on demand side management game in smart energy hubs," *International Journal of Electrical Power & Energy Systems,* vol. 64, pp. 1007-1016, Jan 2015.

[11] S. Bahrami and A. Sheikhi, "From Demand Response in Smart Grid Toward Integrated Demand Response in Smart Energy Hub," *Ieee Transactions on Smart Grid,* vol. 7, pp. 650-658, Mar 2016.

[12] A. Sheikhi, S. Bahrami, and A. M. Ranjbar, "An autonomous demand response program for electricity and natural gas networks in smart energy hubs," *Energy,* vol. 89, pp. 490-499, Sep 2015.

[13] F. Kamyab and S. Bahrami, "Efficient operation of energy hubs in time-of-use and dynamic pricing electricity markets," *Energy,* vol. 106, pp. 343-355, Jul 1 2016.

[14] A. Sheikhi, M. Rayati, S. Bahrami, and A. M. Ranjbar, "Demand Side Management in a group of Smart Energy Hubs as price anticipators; the game theoretical approach," *2015 IEEE Power & Energy Society Innovative Smart Grid Technologies Conference (ISGT),* 2015.

[15] M. Schulze and P. C. Del Granado, "Optimization Modeling in Energy Storage Applied to a Multi-Carrier System," *Ieee Power and Energy Society General Meeting 2010,* 2010.

[16] M. C. Bozchalui, S. AhsanHashmi, H. Hassen, C. A. Canizares, and K. Bhattacharya, "Optimal Operation of Residential Energy Hubs in Smart Grids," *Ieee Transactions on Smart Grid,* vol. 3, pp. 1755-1766, Dec 2012.

[17] B. Zhao, X. S. Zhang, J. Chen, C. S. Wang, and L. Guo, "Operation Optimization of Standalone Microgrids Considering Lifetime Characteristics of Battery Energy Storage System," *Ieee Transactions on Sustainable Energy,* vol. 4, pp. 934-943, Oct 2013.

[18] W. Ongsakul and D. N. Vo, "Artificial Intelligence in Power System Optimization PREFACE," *Artificial Intelligence in Power System Optimization,* pp. V-V, 2013.

[19] T. Y. Lee, "Operating schedule of battery energy storage system in a time-of-use rate industrial user with wind turbine generators: A multipass iteration particle swarm optimization approach," *Ieee Transactions on Energy Conversion,* vol. 22, pp. 774-782, Sep 2007.

[20] M. A. A. Pedrasa, T. D. Spooner, and I. F. MacGill, "Coordinated Scheduling of Residential Distributed Energy Resources to Optimize Smart Home Energy Services," *Ieee Transactions on Smart Grid,* vol. 1, pp. 134-143, Sep 2010.

[21] F. Zhao, J. J. Si, and J. J. Wang, "Research on optimal schedule strategy for active distribution network using particle swarm optimization combined with bacterial foraging algorithm," *International Journal of Electrical Power & Energy Systems*, vol. 78, pp. 637-646, Jun 2016.

[22] C. P. a. S. T. Liu, "“Performance of a commercial hot water boiler,” U.S. Dept. Commerce Technol. Admin., Nat. Inst. Standards Technol., Gaithersburg, MD, USA, Tech. Rep. NISTIR 6226," 1998.

[23] M. E. Baster, "Modelling the performance of Air Source Heat Pump Systems," *Thesis, University of Strathclyde*, 2011.

[24] M. Houwing, R. R. Negenborn, and B. De Schutter, "Demand Response With Micro-CHP Systems," *Proceedings of the Ieee*, vol. 99, pp. 200-213, Jan 2011.

[25] D. P. Jenkins, J. Fletcher, and D. Kane, "Lifetime prediction and sizing of lead-acid batteries for microgeneration storage applications," *Iet Renewable Power Generation*, vol. 2, pp. 191-200, Sep 2008.

[26] J. Kennedy and R. Eberhart, "Particle swarm optimization," in *Neural Networks, 1995. Proceedings., IEEE International Conference on*, 1995, pp. 1942-1948 vol.4.

[27] R. E. Perez and K. Behdinan, "Particle swarm approach for structural design optimization," *Computers & Structures*, vol. 85, pp. 1579-1588, Oct 2007.

[28] S. Ebbesen, P. Kiwitz, and L. Guzzella, "A Generic Particle Swarm Optimization Matlab Function," *2012 American Control Conference (Acc)*, pp. 1519-1524, 2012.

[29] I. Richardson, M. Thomson, D. Infield, and C. Clifford, "Domestic electricity use: A high-resolution energy demand model," *Energy and Buildings*, vol. 42, pp. 1878-1887, Oct 2010.

[30] R. M. Yao and K. Steemers, "A method of formulating energy load profile for domestic buildings in the UK," *Energy and Buildings*, vol. 37, pp. 663-671, Jun 2005.

[31] R. Li, Z. M. Wang, S. Le Blond, and F. R. Li, "Development of Time-of-Use Price by Clustering Techniques," *2014 Ieee Pes General Meeting - Conference & Exposition*, 2014.

[32] F. Kienzle, P. Ahcin, and G. Andersson, "Valuing Investments in Multi-Energy Conversion, Storage, and Demand-Side Management Systems Under Uncertainty," *Ieee Transactions on Sustainable Energy*, vol. 2, pp. 194-202, Apr 2011.

[33] "Photovoltaic Geographical Information System - Interactive Maps, [Online] Available: http://re.jrc.ec.europa.eu/pvgis/apps4/pvest.php#."

[34] T. P. Zhou and W. Sun, "Optimization of Battery-Supercapacitor Hybrid Energy Storage Station in Wind/Solar Generation System," *Ieee Transactions on Sustainable Energy*, vol. 5, pp. 408-415, Apr 2014.

Chapter 4

[1] M. Geidl, "Integrated Modeling and Optimization of Multi-Carrier Energy Systems," *PhD dissertation, Power Systems Laboratory, ETH Zurich*, 2007.

[2] A. Sheikhi, M. Rayati, S. Bahrami, and A. M. Ranjbar, "Integrated Demand Side Management Game in Smart Energy Hubs," *IEEE Transactions on Smart Grid,* vol. 6, no. 2, pp. 675-683, Mar 2015.

[3] A. Sheikhi, S. Bahrami, and A. M. Ranjbar, "An autonomous demand response program for electricity and natural gas networks in smart energy hubs," *Energy,* vol. 89, pp. 490-499, Sep 2015.

[4] M. Geidl, G. Koeppel, P. Favre-Perrod, B. Klockl, G. Andersson, and K. Frohlich, "Energy hubs for the future," *IEEE Power & Energy Magazine,* vol. 5, no. 1, pp. 24-30, Jan-Feb 2007.

[5] F. Kienzle, P. Ahcin, and G. Andersson, "Valuing Investments in Multi-Energy Conversion, Storage, and Demand-Side Management Systems Under Uncertainty," *IEEE Transactions on Sustainable Energy,* vol. 2, no. 2, pp. 194-202, Apr 2011.

[6] S. Bahrami and A. Sheikhi, "From Demand Response in Smart Grid Toward Integrated Demand Response in Smart Energy Hub," *IEEE Transactions on Smart Grid,* vol. 7, no. 2, pp. 650-658, Mar 2016.

[7] M. C. Bozchalui, S. AhsanHashmi, H. Hassen, C. A. Canizares, and K. Bhattacharya, "Optimal Operation of Residential Energy Hubs in Smart Grids," *IEEE Transactions on Smart Grid,* vol. 3, no. 4, pp. 1755-1766, Dec 2012.

[8] M. Geidl and G. Andersson, "Optimal Power Flow of Multiple Energy Carriers," *Power Systems, IEEE Transactions on,* vol. 22, no. 1, pp. 145-155, 2007.

[9] M. R. Almassalkhi and A. Towle, "Enabling City-scale Multi-energy Optimal Dispatch with Energy Hubs," *2016 Power Systems Computation Conference (Pscc),* 2016.

[10] C. C. Shao, X. F. Wang, M. Shahidehpour, X. L. Wang, and B. Y. Wang, "An MILP-Based Optimal Power Flow in Multicarrier Energy Systems," *IEEE Transactions on Sustainable Energy,* vol. 8, no. 1, pp. 239-248, Jan 2017.

[11] M. Moeini-Aghtaie, A. Abbaspour, M. Fotuhi-Firuzabad, and E. Hajipour, "A Decomposed Solution to Multiple-Energy Carriers Optimal Power Flow," *IEEE Transactions on Power Systems,* vol. 29, no. 2, pp. 707-716, Mar 2014.

[12] A. Shabanpour-Haghighi and A. R. Seifi, "Energy Flow Optimization in Multicarrier Systems," *IEEE Transactions on Industrial Informatics,* vol. 11, no. 5, pp. 1067-1077, Oct 2015.

[13] F. Adamek, M. Arnold, and G. Andersson, "On Decisive Storage Parameters for Minimizing Energy Supply Costs in Multicarrier Energy Systems," *Sustainable Energy, IEEE Transactions on,* vol. 5, no. 1, pp. 102-109, 2014.

[14] H. Yu, C. Y. Chung, K. P. Wong, and J. H. Zhang, "A Chance Constrained Transmission Network Expansion Planning Method With Consideration of Load and Wind Farm Uncertainties," *IEEE Transactions on Power Systems,* vol. 24, no. 3, pp. 1568-1576, Aug 2009.

[15] M. C. Bozchalui, C. A. Canizares, and K. Bhattacharya, "Optimal Energy Management of Greenhouses in Smart Grids," *IEEE Transactions on Smart Grid,* vol. 6, no. 2, pp. 827-835, Mar 2015.

[16] S. Chen, Z. N. Wei, G. Q. Sun, K. W. Cheung, and Y. H. Sun, "Multi-Linear Probabilistic Energy Flow Analysis of Integrated Electrical and Natural-Gas

Systems," *IEEE Transactions on Power Systems*, vol. 32, no. 3, pp. 1970-1979, May 2017.

[17]B. M.-i. A. Dolatabadi, M. Abapour and S. Tohidi, "Optimal Stochastic Design of Wind Integrated Energy Hub," *IEEE Transactions on Industrial Informatics*, vol. 13, pp. 2379-2388, 2017.

[18]N. Neyestani, M. Yazdani-Damavandi, M. Shafie-Khah, G. Chicco, and J. P. S. Catalao, "Stochastic Modeling of Multienergy Carriers Dependencies in Smart Local Networks With Distributed Energy Resources," *IEEE Transactions on Smart Grid*, vol. 6, no. 4, pp. 1748-1762, Jul 2015.

[19]M. Rastegar, M. Fotuhi-Firuzabad, H. Zareipour, and M. Moeini-Aghtaie, "A Probabilistic Energy Management Scheme for Renewable-Based Residential Energy Hubs," *IEEE Transactions on Smart Grid*, vol. PP, no. 99, pp. 1-11, 2016.

[20]M. Moeini-Aghtaie, P. Dehghanian, M. Fotuhi-Firuzabad, and A. Abbaspour, "Multiagent Genetic Algorithm: An Online Probabilistic View on Economic Dispatch of Energy Hubs Constrained by Wind Availability," *IEEE Transactions on Sustainable Energy*, vol. 5, no. 2, pp. 699-708, Apr 2014.

[21]M. Alipour, K. Zare, and M. Abapour, "MINLP Probabilistic Scheduling Model for Demand Response Programs Integrated Energy Hubs," *IEEE Transactions on Industrial Informatics*, vol. 14, no. 1, pp. 79-88, Jan 2018.

[22]M. Wendt, P. Li, and G. Wozny, "Nonlinear chance-constrained process optimization under uncertainty," *Industrial & Engineering Chemistry Research*, vol. 41, no. 15, pp. 3621-3629, Jul 24 2002.

[23]G. Dorini, P. Pinson, and H. Madsen, "Chance-Constrained Optimization of Demand Response to Price Signals," *IEEE Transactions on Smart Grid*, vol. 4, no. 4, pp. 2072-2080, Dec 2013.

[24]H. Zhang and P. Li, "Chance Constrained Programming for Optimal Power Flow Under Uncertainty," *IEEE Transactions on Power Systems*, vol. 26, no. 4, pp. 2417-2424, Nov 2011.

[25]Z. Wu, P. L. Zeng, X. P. Zhang, and Q. Y. Zhou, "A Solution to the Chance-Constrained Two-Stage Stochastic Program for Unit Commitment With Wind Energy Integration," *IEEE Transactions on Power Systems*, vol. 31, no. 6, pp. 4185-4196, Nov 2016.

[26]J. Z. Liu, H. Chen, W. Zhang, B. Yurkovich, and G. Rizzoni, "Energy Management Problems Under Uncertainties for Grid-Connected Microgrids: A Chance Constrained Programming Approach," *IEEE Transactions on Smart Grid*, vol. 8, no. 6, pp. 2585-2596, Nov 2017.

[27]Q. F. Wang, Y. P. Guan, and J. H. Wang, "A Chance-Constrained Two-Stage Stochastic Program for Unit Commitment With Uncertain Wind Power Output," *IEEE Transactions on Power Systems*, vol. 27, no. 1, pp. 206-215, Feb 2012.

[28]M. Arnold, R. R. Negenborn, G. Andersson, and B. De Schutter, "Model-Based Predictive Control Applied to Multi-Carrier Energy Systems," *2009 IEEE Power & Energy Society General Meeting, Vols 1-8*, pp. 4592-4599, 2009.

[29]S. W. Xia, X. Luo, K. W. Chan, M. Zhou, and G. Y. Li, "Probabilistic Transient Stability Constrained Optimal Power Flow for Power Systems With Multiple

Correlated Uncertain Wind Generations," *IEEE Transactions on Sustainable Energy*, vol. 7, no. 3, pp. 1133-1144, Jul 2016.

[30]M. Fan, V. Vittal, G. T. Heydt, and R. Ayyanar, "Probabilistic Power Flow Studies for Transmission Systems With Photovoltaic Generation Using Cumulants," *IEEE Transactions on Power Systems*, vol. 27, no. 4, pp. 2251-2261, Nov 2012.

[31]J. R. Birge and F. Louveaux, "Introduction to Stochastic Programming, Second Edition," *Introduction to Stochastic Programming, Second Edition*, pp. 3-+, 2011.

[32]I. Richardson, M. Thomson, D. Infield, and C. Clifford, "Domestic electricity use: A high-resolution energy demand model," *Energy and Buildings*, vol. 42, no. 10, pp. 1878-1887, Oct 2010.

[33]R. M. Yao and K. Steemers, "A method of formulating energy load profile for domestic buildings in the UK," *Energy and Buildings*, vol. 37, no. 6, pp. 663-671, Jun 2005.

[34]S. Paudyal, C. A. Canizares, and K. Bhattacharya, "Optimal Operation of Industrial Energy Hubs in Smart Grids," *IEEE Transactions on Smart Grid*, vol. 6, no. 2, pp. 684-694, Mar 2015.

Chapter 5

[1] M. Geidl and G. Andersson, "Optimal Power Flow of Multiple Energy Carriers," Power Systems, IEEE Transactions on, vol. 22, pp. 145-155, 2007.

[2] M. Geidl, "Integrated Modeling and Optimization of Multi-Carrier Energy Systems," PhD dissertation, Power Systems Laboratory, ETH Zurich, 2007.

[3] F. Adamek, M. Arnold, and G. Andersson, "On Decisive Storage Parameters for Minimizing Energy Supply Costs in Multicarrier Energy Systems," Sustainable Energy, IEEE Transactions on, vol. 5, pp. 102-109, 2014.

[4] M. Alipour, K. Zare, and M. Abapour, "MINLP Probabilistic Scheduling Model for Demand Response Programs Integrated Energy Hubs," IEEE Transactions on Industrial Informatics, vol. 14, pp. 79-88, Jan 2018.

[5] S. Bahrami and A. Sheikhi, "From Demand Response in Smart Grid Toward Integrated Demand Response in Smart Energy Hub," IEEE Transactions on Smart Grid, vol. 7, pp. 650-658, Mar 2016.

[6] S. Althaher, P. Mancarella, and J. Mutale, "Automated Demand Response From Home Energy Management System Under Dynamic Pricing and Power and Comfort Constraints," IEEE Transactions on Smart Grid, vol. 6, pp. 1874-1883, Jul 2015.

[7] N. Neyestani, M. Yazdani-Damavandi, M. Shafie-Khah, G. Chicco, and J. P. S. Catalao, "Stochastic Modeling of Multienergy Carriers Dependencies in Smart Local Networks With Distributed Energy Resources," IEEE Transactions on Smart Grid, vol. 6, pp. 1748-1762, Jul 2015.

[8] H. R. Massrur, T. Niknam, and M. Fotuhi-Firuzabad, "Investigation of Carrier Demand Response Uncertainty on Energy Flow of Renewable-Based Integrated

Electricity-Gas-Heat Systems," IEEE Transactions on Industrial Informatics, pp. 1-1, 2018.

[9] H. Yu, C. Y. Chung, K. P. Wong, and J. H. Zhang, "A Chance Constrained Transmission Network Expansion Planning Method With Consideration of Load and Wind Farm Uncertainties," IEEE Transactions on Power Systems, vol. 24, pp. 1568-1576, Aug 2009.

[10] Y. M. Li, W. Y. Li, W. Yan, J. Yu, and X. Zhao, "Probabilistic Optimal Power Flow Considering Correlations of Wind Speeds Following Different Distributions," IEEE Transactions on Power Systems, vol. 29, pp. 1847-1854, Jul 2014.

[11] M. Fan, V. Vittal, G. T. Heydt, and R. Ayyanar, "Probabilistic Power Flow Studies for Transmission Systems With Photovoltaic Generation Using Cumulants," IEEE Transactions on Power Systems, vol. 27, pp. 2251-2261, Nov 2012.

[12] A. R. Malekpour and A. Pahwa, "Stochastic Networked Microgrid Energy Management With Correlated Wind Generators," IEEE Transactions on Power Systems, vol. 32, pp. 3681-3693, Sep 2017.

[13] F. Kienzle, P. Ahcin, and G. Andersson, "Valuing Investments in Multi-Energy Conversion, Storage, and Demand-Side Management Systems Under Uncertainty," IEEE Transactions on Sustainable Energy, vol. 2, pp. 194-202, Apr 2011.

[14] M. C. Bozchalui, C. A. Canizares, and K. Bhattacharya, "Optimal Energy Management of Greenhouses in Smart Grids," IEEE Transactions on Smart Grid, vol. 6, pp. 827-835, Mar 2015.

[15] M. Moeini-Aghtaie, P. Dehghanian, M. Fotuhi-Firuzabad, and A. Abbaspour, "Multiagent Genetic Algorithm: An Online Probabilistic View on Economic Dispatch of Energy Hubs Constrained by Wind Availability," IEEE Transactions on Sustainable Energy, vol. 5, pp. 699-708, Apr 2014.

[16] M. Rastegar, M. Fotuhi-Firuzabad, H. Zareipour, and M. Moeini-Aghtaie, "A Probabilistic Energy Management Scheme for Renewable-Based Residential Energy Hubs," IEEE Transactions on Smart Grid, vol. PP, pp. 1-11, 2016.

[17] H. Zhang and P. Li, "Chance Constrained Programming for Optimal Power Flow Under Uncertainty," IEEE Transactions on Power Systems, vol. 26, pp. 2417-2424, Nov 2011.

[18] Z. Wu, P. L. Zeng, X. P. Zhang, and Q. Y. Zhou, "A Solution to the Chance-Constrained Two-Stage Stochastic Program for Unit Commitment With Wind Energy Integration," IEEE Transactions on Power Systems, vol. 31, pp. 4185-4196, Nov 2016.

[19] M. Houwing, R. R. Negenborn, and B. De Schutter, "Demand Response With Micro-CHP Systems," Proceedings of the IEEE, vol. 99, pp. 200-213, Jan 2011.

[20] S. W. Xia, X. Luo, K. W. Chan, M. Zhou, and G. Y. Li, "Probabilistic Transient Stability Constrained Optimal Power Flow for Power Systems With Multiple

Correlated Uncertain Wind Generations," IEEE Transactions on Sustainable Energy, vol. 7, pp. 1133-1144, Jul 2016.

[21] H. Z. Huang and C. Y. Chung, "Coordinated Damping Control Design for DFIG-Based Wind Generation Considering Power Output Variation," IEEE Transactions on Power Systems, vol. 27, pp. 1916-1925, Nov 2012.

[22] C. L. Su and D. Kirschen, "Quantifying the Effect of Demand Response on Electricity Markets," IEEE Transactions on Power Systems, vol. 24, pp. 1199-1207, Aug 2009.

[23] C. Y. Zhao, J. H. Wang, J. P. Watson, and Y. P. Guan, "Multi-Stage Robust Unit Commitment Considering Wind and Demand Response Uncertainties," IEEE Transactions on Power Systems, vol. 28, pp. 2708-2717, Aug 2013.

[24] P. R. Thimmapuram, J. Kim, A. Botterud, and Y. Nam, "Modeling and Simulation of Price Elasticity of Demand Using an Agent-Based Model," 2010 Innovative Smart Grid Technologies Conference (Isgt), 2010.

[25] "National Centers for Environmental Information, Available at https://www.ncei.noaa.gov/."

[26] G. Li and X. P. Zhang, "Stochastic optimal power flow approach considering correlated probabilistic load and wind farm generation," in IET Conference on Reliability of Transmission and Distribution Networks (RTDN 2011), 2011, pp. 1-7.

[27] Z. L. Qin, W. Y. Li, and X. F. Xiong, "Generation System Reliability Evaluation Incorporating Correlations of Wind Speeds With Different Distributions," IEEE Transactions on Power Systems, vol. 28, pp. 551-558, Feb 2013.

[28] R. Li, Z. M. Wang, S. Le Blond, and F. R. Li, "Development of Time-of-Use Price by Clustering Techniques," 2014 IEEE Pes General Meeting - Conference & Exposition, 2014.

[29] I. Richardson, M. Thomson, D. Infield, and C. Clifford, "Domestic electricity use: A high-resolution energy demand model," Energy and Buildings, vol. 42, pp. 1878-1887, Oct 2010.

[30] R. M. Yao and K. Steemers, "A method of formulating energy load profile for domestic buildings in the UK," Energy and Buildings, vol. 37, pp. 663-671, Jun 2005.

[31] M. Arnold, R. R. Negenborn, G. Andersson, and B. De Schutter, "Model-Based Predictive Control Applied to Multi-Carrier Energy Systems," 2009 IEEE Power & Energy Society General Meeting, Vols 1-8, pp. 4592-4599, 2009.

Chapter 6

[1] "Exploring how the UK can meet the 2050 emission reduction target using the web-based 2050 Calculator [Online] Available https://www.gov.uk/2050-pathways-analysis."

[2] X. H. Guan, Z. B. Xu, and Q. S. Jia, "Energy-Efficient Buildings Facilitated by Microgrid," IEEE Transactions on Smart Grid, vol. 1, pp. 243-252, Dec 2010.

[3] M. Geidl, "Integrated Modeling and Optimization of Multi-Carrier Energy Systems," PhD dissertation, Power Systems Laboratory, ETH Zurich, 2007.

[4] M. Moeini-Aghtaie, A. Abbaspour, M. Fotuhi-Firuzabad, and E. Hajipour, "A Decomposed Solution to Multiple-Energy Carriers Optimal Power Flow," IEEE Transactions on Power Systems, vol. 29, pp. 707-716, Mar 2014.

[5] A. Shabanpour-Haghighi and A. R. Seifi, "Energy Flow Optimization in Multicarrier Systems," IEEE Transactions on Industrial Informatics, vol. 11, pp. 1067-1077, Oct 2015.

[6] F. Kienzle, P. Ahcin, and G. Andersson, "Valuing Investments in Multi-Energy Conversion, Storage, and Demand-Side Management Systems Under Uncertainty," IEEE Transactions on Sustainable Energy, vol. 2, pp. 194-202, Apr 2011.

[7] M. Geidl and G. Andersson, "Optimal Power Flow of Multiple Energy Carriers," Power Systems, IEEE Transactions on, vol. 22, pp. 145-155, 2007.

[8] H. Da, L. Yinghan, G. Chenghong, and S. L. Blond, "Optimal flow of energy-hub including heat pumps at residential level," in Power Engineering Conference (UPEC), 2015 50th International Universities, 2015, pp. 1-5.

[9] N. Korada and M. K. Mishra, "Grid Adaptive Power Management Strategy for an Integrated Microgrid With Hybrid Energy Storage," IEEE Transactions on Industrial Electronics, vol. 64, pp. 2884-2892, Apr 2017.

[10] Q. Y. Sun, B. N. Huang, D. S. Li, D. Z. Ma, and Y. B. Zhang, "Optimal Placement of Energy Storage Devices in Microgrids via Structure Preserving Energy Function," IEEE Transactions on Industrial Informatics, vol. 12, pp. 1166-1179, Jun 2016.

[11] B. Sanner, C. Karytsas, D. Mendrinos, and L. Rybach, "Current status of ground source heat pumps and underground thermal energy storage in Europe," Geothermics, vol. 32, pp. 579-588, Aug-Dec 2003.

[12] F. Adamek, M. Arnold, and G. Andersson, "On Decisive Storage Parameters for Minimizing Energy Supply Costs in Multicarrier Energy Systems," Sustainable Energy, IEEE Transactions on, vol. 5, pp. 102-109, 2014.

[13] C. C. Shao, X. F. Wang, M. Shahidehpour, X. L. Wang, and B. Y. Wang, "An MILP-Based Optimal Power Flow in Multicarrier Energy Systems," IEEE Transactions on Sustainable Energy, vol. 8, pp. 239-248, Jan 2017.

[14] D. Huo, S. Le Blond, C. Gu, W. Wei, and D. Yu, "Optimal operation of interconnected energy hubs by using decomposed hybrid particle swarm and interior-point approach," International Journal of Electrical Power & Energy Systems, vol. 95, pp. 36-46, 2018/02/01/ 2018.

[15] M. Arnold, R. R. Negenborn, G. Andersson, and B. De Schutter, "Model-Based Predictive Control Applied to Multi-Carrier Energy Systems," 2009 IEEE Power & Energy Society General Meeting, Vols 1-8, pp. 4592-4599, 2009.

[16] M. Moeini-Aghtaie, P. Dehghanian, M. Fotuhi-Firuzabad, and A. Abbaspour, "Multiagent Genetic Algorithm: An Online Probabilistic View on Economic

Dispatch of Energy Hubs Constrained by Wind Availability," IEEE Transactions on Sustainable Energy, vol. 5, pp. 699-708, Apr 2014.

[17] Q. Y. Sun, R. K. Han, H. G. Zhang, J. G. Zhou, and J. M. Guerrero, "A Multiagent-Based Consensus Algorithm for Distributed Coordinated Control of Distributed Generators in the Energy Internet," IEEE Transactions on Smart Grid, vol. 6, pp. 3006-3019, Nov 2015.

[18] C. X. Dou, D. Yue, Q. L. Han, and J. M. Guerrero, "Multi-Agent System-Based Event-Triggered Hybrid Control Scheme for Energy Internet," IEEE Access, vol. 5, pp. 3263-3272, 2017.

[19] A. Sheikhi, M. Rayati, S. Bahrami, and A. M. Ranjbar, "Integrated Demand Side Management Game in Smart Energy Hubs," IEEE Transactions on Smart Grid, vol. 6, pp. 675-683, Mar 2015.

[20] A. Sheikhi, S. Bahrami, and A. M. Ranjbar, "An autonomous demand response program for electricity and natural gas networks in smart energy hubs," Energy, vol. 89, pp. 490-499, Sep 2015.

[21] S. Bahrami and A. Sheikhi, "From Demand Response in Smart Grid Toward Integrated Demand Response in Smart Energy Hub," IEEE Transactions on Smart Grid, vol. 7, pp. 650-658, Mar 2016.

[22] A. Sheikhi, M. Rayati, S. Bahrami, A. M. Ranjbar, and S. Sattari, "A cloud computing framework on demand side management game in smart energy hubs," International Journal of Electrical Power & Energy Systems, vol. 64, pp. 1007-1016, Jan 2015.

[23] J. Kennedy and R. Eberhart, "Particle swarm optimization," in Neural Networks, 1995. Proceedings., IEEE International Conference on, 1995, pp. 1942-1948 vol.4.

[24] M. C. Bozchalui, S. AhsanHashmi, H. Hassen, C. A. Canizares, and K. Bhattacharya, "Optimal Operation of Residential Energy Hubs in Smart Grids," IEEE Transactions on Smart Grid, vol. 3, pp. 1755-1766, Dec 2012.

[25] M. Houwing, R. R. Negenborn, and B. De Schutter, "Demand Response With Micro-CHP Systems," Proceedings of the IEEE, vol. 99, pp. 200-213, Jan 2011.

[26] "About the Domestic Renewable Heat Incentive (RHI), available at https://www.ofgem.gov.uk/environmental-programmes/domestic-rhi/about-domestic-rhi."

[27] "Eunomia, ICAX, the University of Bath, DECC. (2015, 10/04). Owen Square Community Energy project. Available: http://www.cepro.co.uk/2015/04/choices-solar-district-heat-study/."

[28] N. Mendis, K. M. Muttaqi, S. Sayeef, and S. Perera, "Application of a hybrid energy storage in a remote area power supply system," in Energy Conference and Exhibition (EnergyCon), 2010 IEEE International, 2010, pp. 576-581.

[29] S. Ebbesen, P. Kiwitz, and L. Guzzella, "A Generic Particle Swarm Optimization Matlab Function," 2012 American Control Conference (Acc), pp. 1519-1524, 2012.

[30] I. Richardson, M. Thomson, D. Infield, and C. Clifford, "Domestic electricity use: A high-resolution energy demand model," Energy and Buildings, vol. 42, pp. 1878-1887, Oct 2010.

[31] R. M. Yao and K. Steemers, "A method of formulating energy load profile for domestic buildings in the UK," Energy and Buildings, vol. 37, pp. 663-671, Jun 2005.

[32] R. Li, Z. M. Wang, S. Le Blond, and F. R. Li, "Development of Time-of-Use Price by Clustering Techniques," 2014 IEEE Pes General Meeting - Conference & Exposition, 2014